UNIVERSITY OF HERTFORDSHIRE

An investigation of untapered and tapered fibre transmission properties

Author:
Piyamas Choochalerm

Supervised by:
Prof. Hugh R.A. Jones
Prof. William E. Martin

Centre for Astrophysics Research
School of Physics, Astronomy and Mathematics
University of Hertfordshire

Submitted to the University of Hertfordshire in partial fulfilment of the requirements of the degree of Doctor of Philosophy.

December 2022

Abstract

This thesis is about investigation of untapered and tapered fibre transmission properties by experimentation and simulation. Tapered fibre fabricated from commercial products and custom fibre from Bath University was investigated including different fibre type, taper length, and taper ratios. Simulations of untapered and tapered fibre by consideration of geometrical optics using Zemax are presented and compared to electromagnetic waveguide simulations using COMSOL. In addition, the impact of modal noise in tapered fibre is investigated, especially graded-index tapers, by quantifying macro- and micro-bending loss. Moreover, the fabrication of build-in-house connector tapered fibre is introduced as a robust and cost-saving tool for spectrograph link. Lastly, a tapered fibre is tested with a compact EXOplanet high-resolution SPECtrograph (EXOhSPEC) of the University of Hertfordshire using Tungsten and ThAr lamps. Although the cladding light is detected clearly in custom graded-index taper, the light throughput in EXOhSPEC is improved. Overall these results indicate the potential for reasonable fibre-fed spectrograph performance using a 'single tapered fibre'.

Declaration

I declare that no part of this work is being submitted concurrently for another award of the University or any other awarding body or institution. This thesis contains a substantial body of work that has not previously been submitted successfully for an award of the University or any other awarding body or institution.

The following parts of this submission have been published previously:

1. Chapter 1: parts of the discussion in section 1.3 of this chapter have been published as Choochalerm et al., 2021. *Optical Fiber Technology*, **66**, 102632.
2. Chapter 2: parts of discussion on section 2.3 and 2.4 of this chapter has been published as Choochalerm et al., 2021. *Optical Fiber Technology*, **66**, 102632.
3. Chapter 3: parts of discussion on section 3.2 and 3.3 of this chapter has been published as Choochalerm et al., 2021. *Optical Fiber Technology*, **66**, 102632.
4. Chapter 3: parts of discussion on section 3.3 of this chapter have been published as Choochalerm et al., 2023. *Optical Fiber Technology*, **75**, 103140.
5. Chapter 4: parts of discussion on section 4.2 and 4.3 of this chapter has been published as Choochalerm et al., 2021. *Optical Fiber Technology*, **66**, 102632.
6. Chapter 5: parts of discussion on sections 4.2 and 4.3 of this chapter have been published as Choochalerm et al., 2023. *Optical Fiber Technology*, **75**, 103140.
7. Chapter 5: parts of discussion on section 5.5 of this chapter have been published as Choochalerm et al., 2021. *Optical Fiber Technology*, **66**, 102632.

This thesis is part of collaborative project 'EXOhSPEC' between National Research Institute of Thailand (NARIT) and the University of Hertfordshire. There are publications related directly to this project as following:

1. Kawinkij et al., 2019. *SPIE*, **11116**, 443-452.
2. Lhospice et al., 2019. *SPIE*, **11117**, 312-326.
3. Jones et al., 2021. *PASP Publishing* **133**, 025001.

Except where indicated otherwise in the submission, the submission is my own work and has not previously been submitted successfully for any award.

Acknowledgements

I could not have undertaken this journey without the mentoring from my supervisors Prof. William E. Martin and Prof. Hugh R.A. Jones and my previous supervisor and friend Dr. Ronny Errman. I am so honoured to be a part of the EXOhSPEC team and this has been a great research journey. I have been seeing the positive change in myself in many different ways by their mentors not only in academics but also the growth mindset. I have learnt from their excellent examples.

"The best teacher is the one who suggests rather than dogmatizes, and inspires his listener with the wish to teach himself. – Edward Bulwar-Lytton"

I also would like to show gratitude to the examiner who kindly sacrificing valuable time to deliver my Viva exam.

I am very appreciative of very useful discussions, feedback and samples of fibre optics providing from Sarah Usher of Thorlabs, and Stephanos Yerolatsitis and Thomas A. Wright of Bath University.

I am very grateful for my very first optics mentor Dr. Christophe Buisset, who inspired me to persue my career path in this field.

I thank the Thai Royal Government Funding that provided me opportunity to study PhD at the University of Hertfordshire with cost living and tuition fees. Likewise, National Astronomical Research Institute of Thailand (NARIT) the public organization that provided great opportunity in the collaborative project 'EXOhSPEC' between the countries.

I am also grateful for the facilities and support from SPECS and Doctoral College team of the University of Hertfordshire through the years of PhD journey. I thank all PhD students and staff who inspired me on the research.

And also I would like to thank you my friends in the UK who see the potential in me in tough times. Listing names may not be enough but I thank you from all my heart to meet such wonderful people here. You all inspired me to be the better version of myself. Also, my family and friends back home who still keep in touch with big support and love even though we have thousands miles apart.

And I thank you to Herts Sport Village team members, Wednesday Basketball ladies and people from the gym who made life outside of the research more interesting everyday.

Contents

List of Figures

List of Tables

List of Abbreviations

Acronym	**W**hat (it) **S**tands **F**or
GI	**G**raded-**I**ndex
SI	**S**tep-**I**ndex
SM	**S**ingle **M**ode
MM	**M**ulti **M**ode
ESM	**E**ndlessly **S**ingle **M**ode
NA	**N**umerical **A**perture
NA_{eff}	**E**ffective **N**umerical **A**perture
NA_{MOL}	**M**icroscope **O**bjective **L**ens **N**umerical **A**perture
MOL	**M**icroscope **O**bjective **L**ens
TE	**T**ransverse **E**lectric
TM	**T**ransverse **M**agnetic
HE	**H**ybrid **E**lectromagnetic

Chapter 1

Introduction

1.1 Introduction

Optical fibre is renowned for signal transferring with a small amount of loss. The motivation in the early era of fibre optics development was to figure out how to send the information through the thin glass over a long distance with a small loss. The idea was to draw a high-quality glass to a very small size by heating symmetrically and adding another layer with a slightly lower refractive index to obtain 'total internal reflection'(TIR). A collection of stories of the very first fused-silica core low-loss fibre optics was presented by Hecht (2020). Corning in the USA established a research team to study the enhancement of the material and drawing technique of fibre optics in 1970. They focused on fabricating fibre from pure silica glass. The silica glass-made material has a significantly low loss property which led to effective signal transmission especially when the technology merged into the decade of phone, internet and other optics link devices (Winzer et al., 2018). Work by Kapron et al. (1970) shows the first breakthrough reduced the single mode fibre loss from 60-70 dB/km to less than 20 dB/km by improvement of material doping and drawing process as reviewed in Hecht (2020). Singlemode fibre has the property of allowing only the fundamental mode to propagate through the fibre due to the very small core size which is usually less than 10 μm. The improvement on lower attenuation in homogeneous core fibre glass or step-index (SI) multimode fibre down to less than 4 dB/km was successfully (Keck et al., 1973) reported not long after. The rise of telecommunications in 1977 attracted studies on drawing scaled-up waveguides so-called 'multimode' (MM) fibre. Early successful usage of MM fibre was by American Telephone & Telegraph (AT&T) with transmission rate 45 Mb/s as reviewed in the document by Winzer et al. (2018). The core size of multimode fibre typically can

be from 10 μm to up to hundreds μm. Furthermore, the concept of fabricating a gradient profile core was introduced as the radial index allows further improvements of low loss waveguides so called 'graded-index' (GI) multimode fibre optics (Olshansky and Keck, 1976). A preform of layers of glass with different refractive index (n) gradually decreased n from central to the edge of the core which results in a parabolic refractive profile. After the fabrication process, the rays of light can propagate at different speeds and arrive at the other end of the fibre with less time difference than step-index fibre. Hence, less modal dispersion, i.e. loss occurs from different velocities in each mode propagation, occurs in GI than a homogeneous core or SI fibre (Hecht, 2017).

Not so long after the rise of communications applications on typical fibre optics, tapered fibre emerged to challenge the difficulty of light or mode coupling waveguide, especially from one large effective area to a smaller one. If the fibre optics is stretched adiabatically i.e., energy is conserved due to the gradual decrease in the diameter, the light propagation should be contained within the waveguide with small loss (Marcuse, 1987; Birks and Li, 1992) i.e., a mode travelling through the adiabatic tapered fibre should maintain its shape as the fundamental mode (Marcuse, 1987). Theoretical study in transmission properties of MM tapered fibre was done by geometrical optics (Li and Lit, 1985) since 1985. They also introduced the effective numerical aperture of tapered fibre as the ratio of the diameter of the tapered and untapered end which is applied in this work regularly. Though geometrical optics can predict the mode behaviour at a certain level, EM wave or beam propagation in waveguide became very functional tools in the studies (e.g. (Casperson and Kirkwood, 1985; Tovar and Casperson, 1994)). Moreover, to fabricate tapered fibres, the adiabatic criterion was a guide on how steep tapered angle can be (Birks and Li, 1992) but there was no indication of transmission efficiency until spectrogram analysis work introduced by Ravets et al. (2013).

Apart from the use of fibre optics in communication networks, there is a growth of fibre-link systems in astronomical instrumentation for light gathering reviewed by works of Barden (1996); Bland-Hawthorn and Kern (2009); Kryukov (2018). The fibre-fed spectrograph was first introduced named 'MEDUSA' (Hill et al., 1980) with a short large diameter (i.e. 300 μm) fibre optics as light gathering. There has been ongoing use of optical fibres for multiplex gains in multi-object spectrographs. However, there is a rise of interest in extra-solar planet exploration and the use of a fibre link to the spectrograph for stability performance rather than as a means to access fainter targets. For terrestrial-based spectrographs, there is a requirement for achieving higher resolution than before. Instead of classically using a slit for the light aperture entrance

and attaching the spectrograph directly to the telescope mount, a fibre optics link offers flexibility in the placement of the spectrograph. This allows the spectrograph to be located on solid ground and in a stable environment. When the spectrograph is no longer affected by the movement of the telescope, enhancement of the performance can be achieved. The type and size of fibre optics used as the fibre link depend on the optics size of the spectrograph. In order to achieve the high resolution, the optic size of the spectrograph, in general, will be inevitably relatively large and require environmental control such as a vacuum chamber or other complicated supportive optics and these constructions require tremendous space, budget investment and planning and maintaining cost (for example HARPS (Pepe et al., 2000; Lo Curto et al., 2015), CARMENES (Stürmer et al., 2014)).

Another issue of light propagation in the multimode fibre is modal noise that occurs when the waveguide allows a number of modes to propagate and this leads to loss from modes interference (Rawson et al., 1980; Hill et al., 1980; Tremblay et al., 1981; Mickelson and Weierholt, 1983). The loss depends on the mode in the fibre-fed spectrograph and is described as Focal Ratio degradation (FRD) when the incident f-ratio is degraded after the light propagates through the fibre optics (Ramsey, 1988). This specific mode-dependent loss is caused by waveguide scattering and deformation of the structure such as macrobending and microbending. This raised the study of installing mode scrambler to eliminate the impact of signal distortion in some spectrographs (Ishizuka et al., 2018; Halverson et al., 2015; Petersburg et al., 2018). However, the debate whether the modal noise has a significant impact on S/N reduction or mode scrambler is effective was raised in (Oliva, E. et al., 2019). They found this depends on the light illumination into fibre optics.

The application of tapered fibre particularly on fibre-fed spectrograph is studied. This is motivated by the concept that was discussed (Marcel et al., 2006; Haynes et al., 2012) as tapered fibre can be used as the focal reducer or magnification. Hence, this can be a replacement for standard bulky optical apparatus for the unmatched size of the beam from the telescope and the spectrograph. Though early work by Avila (1988) showed briefly poor light coupling efficiency results of tapered fibre for the 3.5m ESO telescope link to the Coude Echelle spectrograph. Geometrical optics of tapered fibre were informatively discussed based on the etendue concept (Marcel et al. (2006); Haynes et al. (2012)). As the tapered fibre can be fabricated from any type such as SM, SI MM, GI MM or even special core arrangement fibre then this comes to the vital question, 'what could possibly be the best candidate for the application in fibre-based spectrograph?'. An example of a special tapered fibre 'Photonic lanterns (PL)', as the link to the spectrograph was

successfully tested in the laboratory (Birks et al., 2012; Jovanovic et al., 2012; Spaleniak et al., 2013). There are now also photonic lanterns employed at observatories in instruments such as PRAXIS (Content et al., 2014). Photonic lanterns (PLs) can be fabricated by adiabatically merging several SM cores into one MM core (Birks et al., 2015). However, PLs can be challenging to fabricate, and tapered single MM fibres have not many studies explored as a platform for fibre feeding. A high-resolution spectrograph prototype was developed at the University of Hertfordshire named EXOhSPEC (EXO-planet High-resolution SPECtrograph) (Jones et al., 2021). This study examines the feasibility of using less complicated fabrication methods to produce graded-index tapers which could be used to link to fibre-fed spectrographs.

1.2 Ray propagation in optical waveguide

The law of refraction or 'Snell's Law' is well-known for light propagation through media that have a different refractive index. The incident ray that is transmitted and bent after passing the two-medium interface is called the 'refracted' ray. If the ray has angle of incidence θ_i and refracted angle θ_r, Snell's law can be written as:

$$n_i sin\theta_i = n_r sin\theta_r \tag{1.1}$$

when n_i and n_r are refractive index of incident and refracted ray. Snell's law can define how the light travels from a less optical dense (less refractive index) or more optical dense (larger refractive index) medium to another medium and how the light is refracted. Figure 1.1 shows the ray travel from medium a to medium b. If a normal line is drawn perpendicular to the medium interface, in (a1), light bends toward the normal when travelling from a less optical dense medium ($n_\mathrm{a} < n_\mathrm{b}$). In contrast, in (a2), if the light travels from the more optical dense to less dense medium ($n_\mathrm{a} > n_\mathrm{b}$), the light will bend away from the normal line.

There is a 'critical angle' θ_c for each medium. The critical angle is when the incident angle allows no light transmitted and refracted through another medium. In other words, the light will be bent 90°from the normal line and travel parallel with the medium interface. Considering light traveling from medium a (n_a) to a medium with refractive index n_b, the critical angle θ_c can be written by using the equation 1.1 as

$$\theta_c = sin^{-1}\frac{n_\mathrm{b}}{n_\mathrm{a}} \tag{1.2}$$

This Snell's law determined how the refractive index of glass has a vital role in a light propagation. The difference of medium's refractive index between core (n_{core}) and cladding (n_{clad}) induces 'Total Internal Reflection (TIR)' (Hecht, 2017) of rays propagated through a waveguide if the core and cladding interface assumed to be symmetry. The lower refractive index of the cladding layer allows light that incident onto the core-cladding interface to reflect back to the core region and continues to propagate through the length of the waveguide until reaching the other end.

Figure 1.1 (b) shows the drawing of the ray is incident with critical angle ($\theta_i = \theta_c$) onto the media interface and refracted with 90°(θ_r=90°) and travels parallel to the media interface.

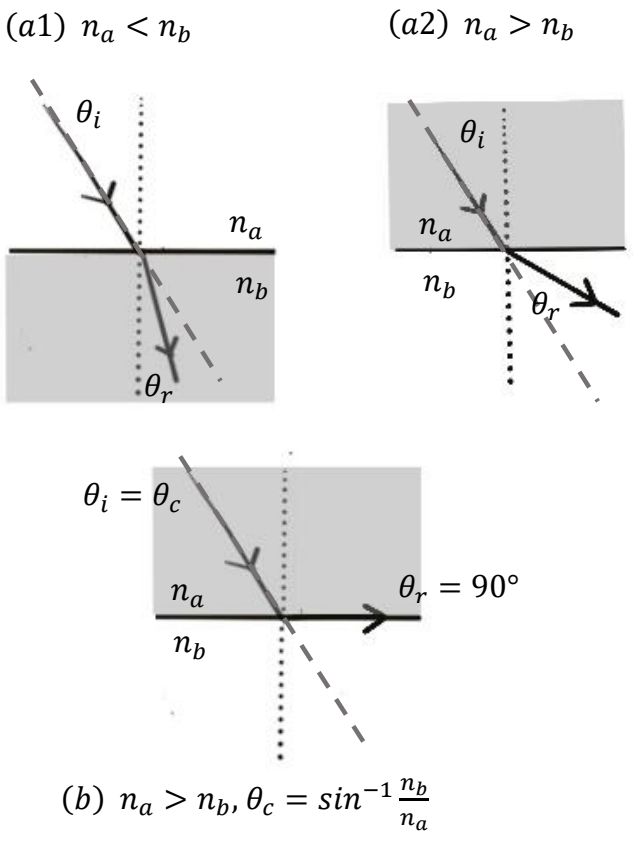

FIGURE 1.1: An illustration of law of refraction. Light travel from medium a to medium b. Medium a and b refractive index are n_a and n_b, respectively. (a1) shows ray bends toward to a normal line due to $n_\mathrm{a} < n_\mathrm{b}$. (a2) shows ray bends away from a normal line due to $n_\mathrm{a} > n_\mathrm{b}$. (b) shows the ray bends 90°travel parallel to medium interface caused by $\theta_i = \theta_c$.

Conventional optical fibre consists of core, cladding and protective layers such as coating, strength layer filament and plastic cover (Snyder and Love, 1983; Nelson, 1988) in a cylindrical shape (showing in Figure 1.2). Though, there are some special shapes such as double cladding, square-core, hexagonal-core, octagonal-core, multi-core or endlessly single mode fibre for a specific application. Most commercial optical fibres today are made from pure silica and doped with chemicals for example, germanium, erbium etc. as a cladding layer.

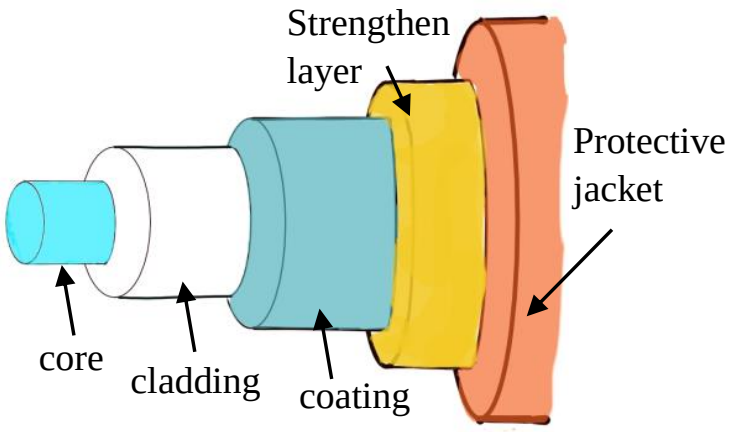

FIGURE 1.2: Drawing of fibre optics construction. The conventional fibre consists protective jacket, strengthen layer, coating, cladding and core.

Though there were some non-silica glass fibres introduced of fluoride glass fibre, plastic optical fibre (polymer fibre) (Gambling, 2000), silica has tremendous advantages of robustness when the glass is properly drawn, polished by flame and protected. It has high-temperature resistance. Silica strength was measured at about 140 000 kg/cm^2 i.e., it can support a weight of 18 kg with a size less than a millimetre (Gambling, 2000). Also, the attenuation is small in Visible (VB) light and starts increasing in Ultraviolet (UV) light (Sums and Cozens, 1992).

1.2.1 Characteristics of optical single mode and multimode fibre

By considering a core size, optical fibre can be classified into two main types: 1) Singlemode (SM) and 2) Multimode fibre (MM). A single mode fibre core diameter is relatively small compared to a multimode fibre to allow one mode propagation which is typically in a range of less than 10 μm. The diameter of a multimode fibre can be up to hundreds of μm depending on the objectives of the application. Multimode fibre in general is characterised into two main types: step-index (SI) and graded-index (GI) fibre. The difference between these two types is how the core material is fabricated. The core of step-index fibre typically has a homogeneous refractive

index while the refractive index of graded-index fibre is gradually decreased from the centre to the edge. This leads to a parabolic profile of refractive index related to the position of the core whereas the refractive profile of step-index fibre related to the position of the core to cladding cross-section looks like a 'step'. Figure 1.3 illustrates the configuration of each fibre type by showing the refractive index profile, fibre end surface and ray propagation.

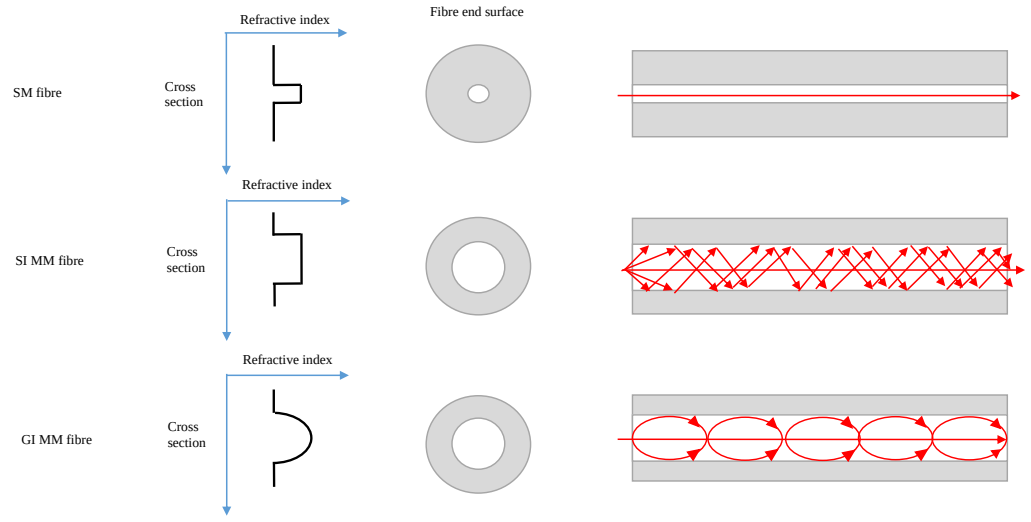

FIGURE 1.3: Illustration of single mode (SM), Step-index multimode (SI MM) and Graded-index multimode fibre (GI MM)

According to TIR, there is a maximum angle of the incident ray to allow light to propagate through the core without exceeding the critical angle (θ_c) between the core and cladding interface i.e., rays are contained within the core region. The Critical Angle from equation 1.2 can also be written as

$$sin\theta_c = \frac{n_{\text{clad}}}{n_{\text{core}}} = sin(90^\circ - \theta_c) = cos\theta_c \tag{1.3}$$

When n_{clad} and n_{core} are the refractive index of cladding and core respectively. Considering that the refracted ray from the air to the core interface has incidence angle $\theta_i = \theta_c$ to the core/cladding interface. Thus

$$\frac{n_{\text{clad}}}{n_{\text{core}}} = (1 - sin^2\theta_c)^{1/2}. \tag{1.4}$$

and rearrange the equation as

$$n_{\text{core}} sin\theta_i = (n_{\text{core}}^2 - n_{clad}^2)^{1/2}. \tag{1.5}$$

If the maximum angle that ray propagates into the fibre core from outside without leaking into core (TIR) is considered as $\theta_i = \theta_{max}$, equation 1.5 can be written as

$$sin\theta_{max} = \frac{1}{n_{core}}(n_{\text{core}}^2 - n_{clad}^2)^{1/2} \tag{1.6}$$

$n_i sin\theta_{max}$ is also known as Numerical aperture (NA). If $n_i = n_{\text{air}}$, NA, in a homogeneous core fibre, is

$$NA_{=}(n_{\text{core}}^2 - n_{\text{clad}}^2)^{1/2}, \tag{1.7}$$

Defining the NA of the step-index profile is straightforward using the difference in the refractive index of the core and cladding. However, the continuous parabolic function of a graded index can be applied to the refractive index profile. The common form is typically written as (Sums and Cozens, 1992)

$$n(r) = n_0\sqrt{1 - (\frac{r}{r_0})^2} \tag{1.8}$$

n(r) is the refractive index considered at radial distance r. n_0 is a core refractive index at the centre of fibre and is a peak value of the profile. r_0 is the physical core radius of the fibre. In order to achieve TIR, n(r) is always smaller than $n_{cladding}$.

1.3 EM waveguide: mode propagation in fibre optics

Although using ray tracing to study light propagation is effective, especially in large-scale optics, electromagnetic analysis using Maxwell's equation is considered the fundamental method for solving waveguide problems. The propagation of light is considered Electromagnetic (EM) field propagation instead of rays. Guided waves electric and magnetic fields with time independence can be expressed in a standard form as

$$E = \mathrm{e}\, e^{(-j\beta \mathrm{z})} \tag{1.9}$$

and

$$H = \mathrm{h}\, e^{(-j\beta \mathrm{z})} \tag{1.10}$$

E and H are electric fields and magnetic fields, respectively. With H$\perp$E and travel (propagating) in the z-direction. e and h are the amplitude of E and H fields and β is the propagation constant. This guided E and H field can also be expressed as a 'mode'. Each mode can also mean each path of light. The light that travels confined in a core region without leaking to cladding and reaches the other end of the fibre is defined as 'bounded mode'. When light travels through the fibre with many paths, they are called 'multimode'. Also, the single mode fibre is when there is only one ray path of light propagated.

In optical waveguides, the mode can be categorised depending on the field and the type of rays. For example, Transverse Electric (TE) and Transverse Magnetic (TM) mode is defined as when there is no E or H field propagating in that considered mode, respectively. In other words, TE mode is defined when E is perpendicular to z (optical axis/ propagation axis) and TM mode is defined when H is perpendicular to z. TE and TM modes are similar to the meridional rays (propagated light passes through the optical axis). However, in fibre optics, considered as cylinder shape, modes are mostly hybrid (Hybrid Electromagnetic (HE or EH) mode), which has a complicated polarization. Hybrid modes are considered as skew rays as the light propagates along the core surrounding the optical axis. The hybrid modes consist of both electric and magnetic fields i.e. e and h are > 0. This complicated polarization combination of fields in both E and H can be expressed by Bessel functions (Sums and Cozens, 1992). In addition, a refractive index of the core typically depends on radial distance but is constrained along the optical/propagation axis (z). In other words, the refractive index is varied along the radius but constant along the length of fibre optics. Each mode has an individual refractive index. Hybrid modes can be simplified by linear combination and expressed in the 'Linear Polarization' (LP) mode. For example, LP_{01} (Fundamental mode) is constructed from HE_{11}, LP_{11} is constructed from HE_{21}, TM_{01} and TE_{01}, LP_{12} is from HE_{22}, TM_{02}, TE_{02} and LP_{22} is from HE_{32} and EH_{12} etc. (Sums and Cozens, 1992).

V-number (V) is a vital parameter used to explain if the fibre is single mode or multimode. This parameter has a direct relationship with the propagation of a number of modes in a fibre, which

also is related to fibre type and size as shown in the following equation. V-number can be written as

$$V - number = \frac{2\pi}{\lambda} rNA, \tag{1.11}$$

where r is waveguide core radius. λ is a wavelength that propagates in the fibre optics. If V-number is less than 2.405, the fibre is single mode support i.e. there is only the fundamental mode propagates along the fibre (Hecht, 2017). As the next higher order mode (LP_{11}) occurs at V-number=2.405, the fibre now supports non-fundamental modes. Moreover, V-number is also used to validate if geometric optics or EM waveguide theory using Maxwell's equations is sufficiently accurate to solve the waveguides problems. Geometrical optics is valid for a case of multimode fibre with V$>>$1 (Snyder and Love, 1983). Also, geometric calculations will have errors of more than 5% for waveguides with V $< \sim$20 (Snyder and Pask, 1973).

In addition, discussions in (Olshansky, 1976; Hill et al., 1980) that number of modes in graded-index fibre is less compared to step-index fibre in comparative size and numerical aperture. The number of modes that GI and SI fibre can support is

$$N_{\mathrm{GI}} = \frac{V^2}{4}, \tag{1.12}$$

$$N_{\mathrm{SI}} = \frac{V^2}{2}, \tag{1.13}$$

respectively. Where N_{GI} is the number of modes that GI fibre can support and N_{SI} is the number of modes that SI fibre can support. V is V-number as mentioned in equation 1.11.

1.4 Fibre transmission

The term 'attenuation' (α) is familiar and commonly used in the fibre optics field. The signal or information or light losses along the length of fibre (L) is determined in units dB/km. Decibel or dB is the fundamental unit used to express measured power on the logarithmic scale. The loss in dB is $dB = -10log_{10}(P_o/P_i)$ (Nelson, 1988; Hecht, 2017), so attenuation can be written as

$$\alpha = -\frac{-10}{L} log_{10}(P_o/P_i). \tag{1.14}$$

While P_i and P_o are input power and output power, respectively. The transmission is also the simplest way to determine the loss by the ratio between radiant flux illuminated on the input surface and measuring at the output surface i.e. P_o/P_i. This is commonly a power measuring in Watts. Transmission can be written in a relationship with attenuation as

$$Transmission = \frac{P_o}{P_i} = 10^{(-\alpha L/10)}. \tag{1.15}$$

Loss in dB can be compared directly to transmission in %. For example, loss in dB=0.01 mean there is 99.8% of transmission per km, 0.2 dB = 95% transmission, 10 dB is 10% etc. (Nelson, 1988).

1.5 Gaussian beam propagation

1.5.1 The shape of Gaussian beam

It is important to understand that when considering highly collimated light (very small divergence), particularly on laser propagation, the Gaussian distribution is used to describe the intensity profile of the beam. This is the so-called 'Gaussian beam'. The Gaussian beam is considered based on the EM wave theory. The shape of the intensity of the Gaussian beam profile can be expressed with the Gaussian function as Figure 1.4. There are two widths categorised for the Gaussian profile. First is Full Width at Half maximum (FWHM), which is the width of the beam defined at half of peak irradiance. The other is $1/e^2$ width which is defined at 13.5% of the peak of the profile.

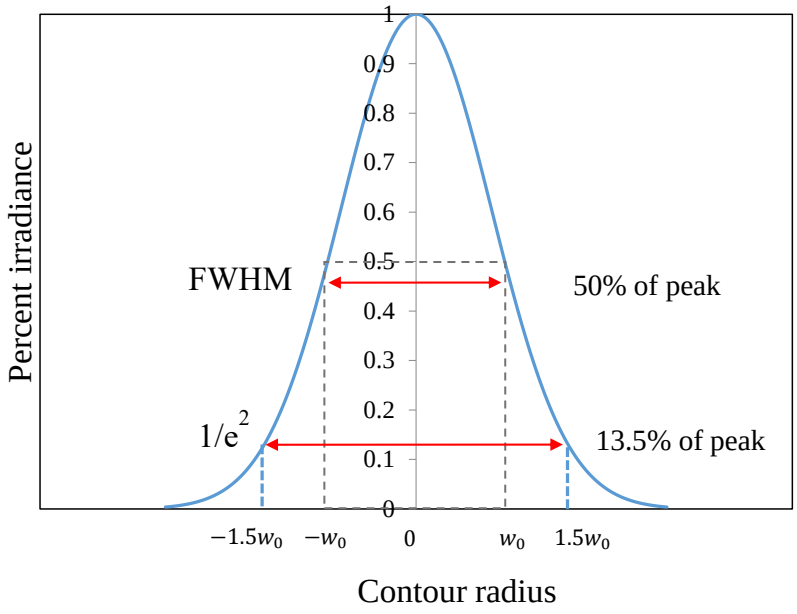

FIGURE 1.4: Irradiance profile of a gaussian beam considering flat wavefront (TEM_{00}) propagation. A width at half of the irradiance peak (50% of peak) is FWHM. A Gaussian width is $1/e^{1/2}$ located at 13.5% of the peak.

Ideally, the perfect collimated light has no divergence and has the shape of perfect Gaussian as shown in Figure 1.4. However, the real-life laser beam is diverged after launching away from the source and if considering light propagation through a finite aperture, the irradiance of the Gaussian beam expressed with Gaussian function can be written as

$$I(r) = I_0 e^{-2r^2/w(\mathrm{z})^2} = \frac{2P}{\pi w(\mathrm{z})^2}. \tag{1.16}$$

I_0 is a peak of the profile. w(z) is a beam radius considering the width of 13.5% of I_0, r is radial distance from the axis, and P is total power. The highly collimated beam has a flat wavefront considered at beginning of light emitting from the laser (z=0) then light eventually spreads after propagation along the distance z, so the flat wavefront slowly transforms into a curvature wavefront, and curvature of the wavefront can be written as

$$R(\mathrm{z}) = \mathrm{z}\left[1 + \left(\frac{\pi \mathrm{w}_0^2}{\lambda \mathrm{z}}\right)^2\right]. \tag{1.17}$$

The R(z) is the curvature of wavefront at the propagation distance z. R(z) is infinity, i.e. no curvature at distance z=0. w_0 is the beam waist when wavefront is flat and not spreading (beam

waist at z=0). Typically this is defined by the diameter size of the laser beam. λ is the coherent light wavelength that is propagating. The beam waist considered at distance z after the light flat wavefront turns to curvature wavefront can be written as

$$w(\mathrm{z}) = \mathrm{w}_0 \left[1 + \left(\frac{\lambda \mathrm{z}}{\pi \mathrm{w}_0^2}\right)^2\right] \tag{1.18}$$

Gaussian beam diverging and increasing of curvature is not linear. Figure 1.5 illustrated the Gaussian beam propagation from the laser along distance z with beam waist w_0. At z=0 the wavefront is flat and spreading over the distance z then returns to be a planar wavefront again at infinity (R(∞)=∞). A beam waist that is spreading and increasing with distance by a factor of $\sqrt{2}$ is called the 'Rayleigh range'. At the Rayleigh range, the wavefront curvature is maximum. This Rayleigh range can be written as

$$Z_\mathrm{R} = \frac{\pi w_0^2}{\lambda}. \tag{1.19}$$

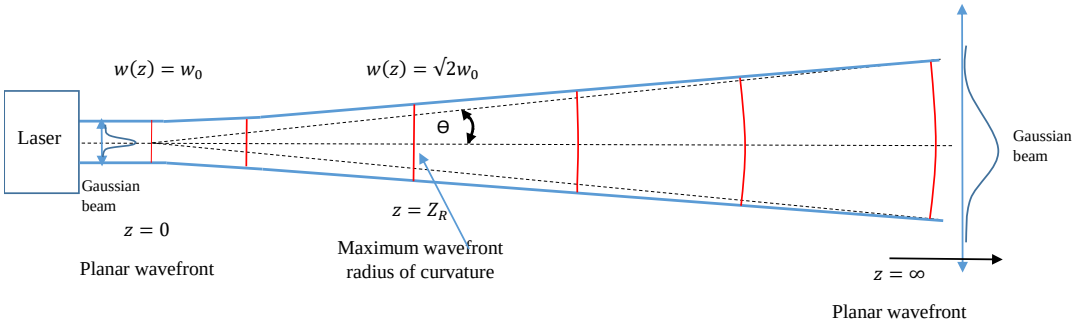

FIGURE 1.5: Illustration of Gaussian beam propagation along distance z

The range of Gaussian beam propagation can be categorised by the Rayleigh range. When curvature can be measured as maximum, these ranges of light propagation are in near-field and mid-field ($\mathrm{z} \leqslant \mathrm{Z_R}$. Far-field divergence is when $\mathrm{z} >> \mathrm{Z_R}$ ($\mathrm{z} > 10\mathrm{Z_R}$). Divergent angle (θ) can be estimated as $w(z)/z$ with large z. Optimum waist size (w_0(optimum)) can be expressed as

$$w_0(\mathrm{optimum}) = \left(\frac{\lambda \mathrm{Z_R}}{\pi}\right)^{1/2} \tag{1.20}$$

1.5.2 Transformation of Gaussian beam by lens and aperture

Gaussian beam waist and magnification can be transformed by passing through lenses and apertures. In geometrical optics, considering the light propagates through lenses, the change of image magnification and distance can be expressed with the Lens-maker's equation as

$$\frac{1}{f} = \frac{1}{s''} + \frac{1}{s} \tag{1.21}$$

when f is the focal length of the lens, s" is the image distance and s is the object distance from the lens. Magnification (m) of the image can be expressed by m=s"/s.

Lens-maker's equation can be written by applying Rayleigh range (Self, 1983) as:

$$\frac{1}{f} = \frac{1}{s''} + \frac{1}{s + Z_{\mathrm{R}}^2/(s-f)} \tag{1.22}$$

Figure 1.6 illustrates the collimated Gaussian beam propagation and focus by a lens. Rayleigh range Z_R is changed to Z_R'' according to a beam passing through a lens as well as magnification of the image spot. The magnification is usually the ratio between the image and object height. For a Gaussian beam, this can be considered as the ratio between the beam waist after and before the light passes through the lens. Applying the Rayleigh range term to the magnification formula and the lens-maker's equation, the magnification of Gaussian beam is

$$m = \frac{w_0''}{w_0} = \frac{1}{\sqrt{[1-(s-f)]^2 + (Z_{\mathrm{R}}/f)^2}}. \tag{1.23}$$

Hence, a transformed Gaussian beam or focus beam Rayleigh range is

$$Z_R'' = m^2 Z_R \tag{1.24}$$

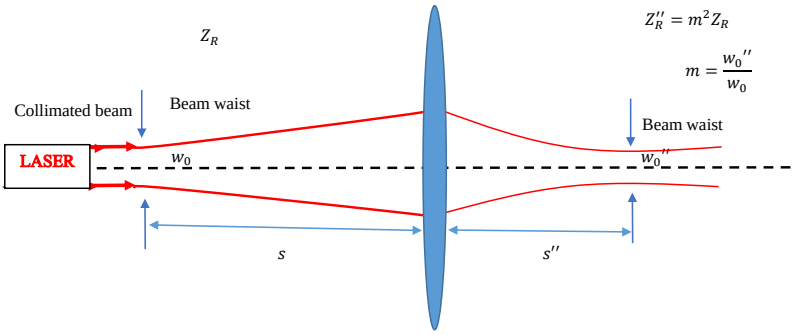

FIGURE 1.6: Illustration of Gaussian beam transformation by a lens. The collimated Gaussian beam with waist w_0 propagates through a lens with focal length f. The focus Gaussian beam has transformed waist w_0''. The focus beam waist magnification m is a ratio between w_0'' and w_0. Rayleigh range of collimated beam R_Z is transformed by focuser lens to Z_R''.

The light, particularly coherent light such as from a laser, diffracted by a circular aperture appears as an 'Airy pattern' or 'Airy disc'. The pattern of the Airy disc is slightly different from the Gaussian beam as the light has a circular bright spot in the middle of alternative bright and dark rings. When intensity drops to the first zero the spot diameter is defined as an 'Airy disc' diameter. This is typically used to show the uniform light image spot illuminated from a uniform circular pupil. Figure 1.7 shows the example of an Airy pattern (image on the top right is from Hecht (2020)) and the profile of an Airy disc. However, when the pupil illumination is not uniform, which happens in the real life, i.e., the intensity at zero can not be defined. The diameter of FWHM and $1/e^2$ becomes alternative ways to determine image spot profile instead.

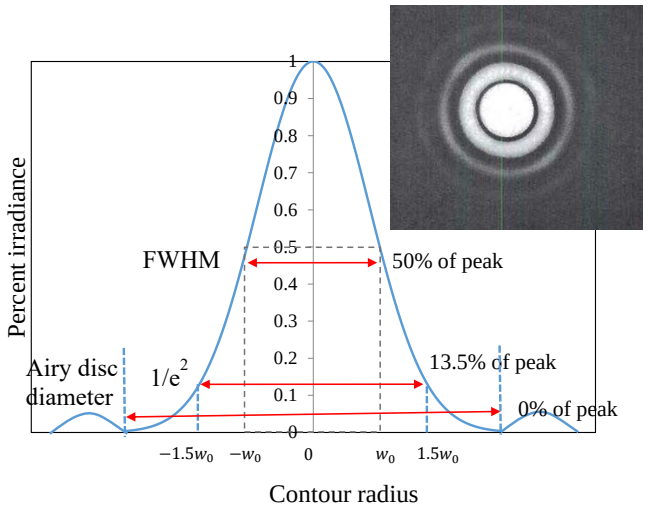

FIGURE 1.7: Irradiance profile of airy disc and an example image of an airy disc. The profile shows the pattern of a bright spot surrounded by alternative dark and bright rings. The Airy disc diameter is defined when the irradiance drops to 0. The top right airy disc image is from Hecht (2020)

Focal spot diameter in a diffraction-limited lens can be expressed as

$$d = K\lambda f/\# \tag{1.25}$$

K is a constant dependent on the truncation ratio. f/# is the f-number of the lens at truncation and can be defined by the ratio of lens pupil diameter to lens focal length in the case of a focusing beam. K of FWHM width and of $1/e^2$ are

$$K_{FWHM} = 1.029 + \frac{0.7125}{(T-0.2161)^{2.179}} - \frac{0.6445}{(T-0.2161)^{2.221}} \tag{1.26}$$

and

$$K_{1/e^2} = 1.6449 + \frac{0.6460}{(T-0.2816)^{1.821}} - \frac{0.5320}{(T-0.2816)^{1.891}} \tag{1.27}$$

Truncation is one vital factor that should not be neglected. Gaussian Beam ($1/e^2$ waist diameter (denoted D_b)) is truncated when the collimated light passes through a limited size aperture (diameter D_t) such as iris diaphragm and lens. For example, Gaussian light is truncated by an iris diaphragm and focused by a lens with focal length f shown in Figure 1.8. The iris diaphragm diameter, which can be adjusted, can affect the spot diameter of the focused beam. The truncation ratio is

$$T = \frac{D_b}{D_t} \tag{1.28}$$

while T>1 approaches the uniform profile, i.e. Airy disc, and T<0.5 approaches Gaussian profile. Note that in this work, $1/e^2$ is considered as the image spot.

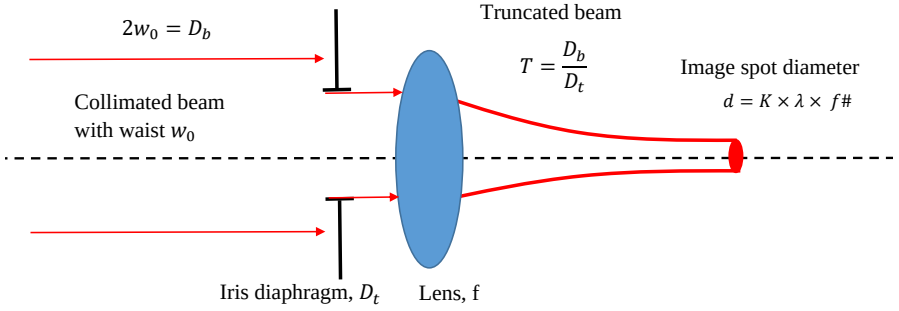

FIGURE 1.8: Truncated Gaussian beam illustration. The Gaussian beam is transformed by propagating through a limited size aperture, which is an iris diaphragm. The spot size is transformed according to the aperture size.

1.6 Tapered fibre background

Over the last decade, tapered optical fibre became known in various applications in optics such as high power laser coupling (e.g. Alder et al. (2000), optical sensors for environmental monitoring (e.g. Korposh et al. (2019)), biosensors (e.g. Tian et al. (2011); Kumar et al. (2019)), astronomical instrumentation such as fibre-fed spectrograph (e.g. early test with ESO telescope Avila (1988) and laboratory test (Marcel et al., 2006; Haynes et al., 2012)). Tapered fibre is one of the most effective optics applications for coupling the light from a large effective area to a smaller one. Tapered fibre is the fibre optics that was stretched symmetrically as a result of uneven size in the stretched region so called 'waist'. Typically, the tapered fibre is fabricated by the adiabatic 'heat and pull' technique (Amitay et al., 1987; Birks and Li, 1992; Marcel et al., 2006; Haynes et al., 2012; Yerolatsitis et al., 2014; Yerolatsitis et al., 2015). Chemical etching techniques were successfully used for taper fabrication in some studies (Alder et al., 2000; Yang et al., 2005). Figure 1.9 shows the structure of tapered fibres with the assumption the fibre is stretched symmetrically. There are three main regions in tapered fibre, which are 1: untapered region 2. taper or transition region, and 3. waist region. Ideally, the pulling is controlled with the pulling rate with stable heating that allows a gradual decrease or increase in core and cladding diameter along the fibre to create two transition regions. In this work transition region is defined by the light propagation direction. Downtaper is considered when the light propagates from untapered end to tapered end and 'uptaper' is when the light propagates from tapered end to the untapered end. The length of transition (L_{down} and L_{up}) can be selected as symmetric for uptaper and downtaper or can be selected with different lengths as will depend on the user needs. Note that in this work, samples of tapered fibre mainly investigated on a half of the two-transition-region as uptaper or downtaper.

'Heat and pull' is one of the most common methods to fabricate adiabatic tapered fibre (Birks and Li, 1992; Yerolatsitis et al., 2015). It is possible to heat and permanently stretch any fibre to narrow it down over a defined short length; thus, single mode (SM) fibres or multimode (MM) fibres can be tapered to meet the needs of a given application. Typical mechanics of a tapering machine has two main elements: 1) highly accurate temperature control heat source and 2) fibre holders with adjustable pulling rate. The conventional fibre is held firmly on the holders and heat is applied while slowly pulling each end of the fibre outward from each other. The parameters of temperature, stress and speed pulling rate are calculated carefully depending on the required specification such as taper length and ratio.

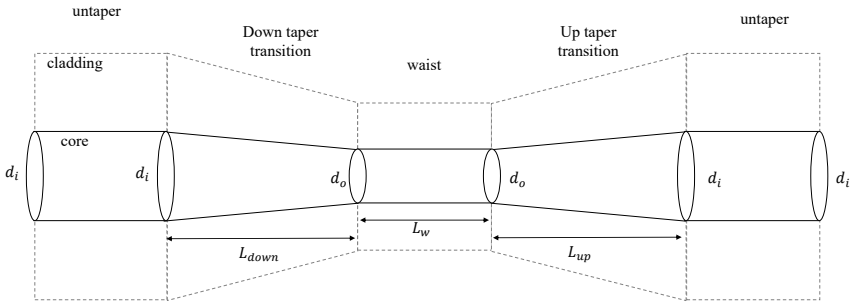

FIGURE 1.9: Illustration of tapered fibre structure. The fibre with original diameter d_i is stretched out from both sides symmetrically and has tapered ends contained in waist region with tapered diameter d_o. The waist length is L_{w}. The transition length of downtaper is L_{down} and uptaper is L_{up}.

The taper length has a vital role in the transmission of the taper. To be able to fabricate an adiabatic taper there is a minimum taper length that depends on the core size and required taper ratio. The criterion of an 'adiabatic' taper is when the transition of taper angle is less than Ω (Snyder and Love, 1983; Musa et al., 2016).

$$\Omega(z) = \frac{r(z)(\beta_1 - \beta_2)}{2\pi} \tag{1.29}$$

where Ω is a maximum transition angle for taper to be adiabatic, r(b) is the core radius at point z where z is the distance along an optical axis of fibre. β_1 and β_2 are the propagation constants of two modes that have the possibility to couple.

1.7 Overview

This thesis is about the study of non-tapered and tapered fibre transmission properties by studying theory, modelling and experimentation on the variety of fibre optics to apply the most effective fibre candidate to fibre-fed EXOhSPEC. Introduction, review theory and related topics in this research are presented in Chapter 1. Explanations about ray propagation in fibre optics and characteristics of single mode and multimode fibre including mode propagation in fibre optics considering EM waveguide are also presented. The transmission of fibres definition was defined. The theory of Gaussian beam propagation is reviewed. Lastly, a background in tapered fibre is presented.

In Chapter 2, the variety of conventional non-tapered fibre transmission properties with coherent light was investigated. Firstly, the comparison between single mode and multimode fibre transmission related to mode number was studied. The preliminary setup designed for transmission measurement and image taking was presented. Test fibres were single mode and multimode fibre with varied core diameters such as 10 μm, 25 μm, 50 μm, and 62.5 μm including plastic fibre, endlessly single mode, and square-core fibre. The results show the rise of mode numbers as the fibre core size increases. Experimental results of an alignment of input beam position impact on transmission are also presented. After that the setup to measure transmission dependence on input beam numerical aperture or effective numerical aperture (NA_{eff}) with an NA matching technique was designed. The technique allows optimal coupling light into test fibre. Due to using a variety of microscope objective lenses for light coupling, an improvement of the setup by a microscope objective lens transmission test was explored. A comparison of 4x and 10x Edmund and Olympus objectives were studied and results confirm Olympus lenses perform better as the beam coupler for the transmission test. In order to verify fibre coupling efficiency, the spot size of the input beam at each varied NA was calculated based on Gaussian beam calculations (Liu et al., 2019) and confirmed with Zemax simulations. The Gaussian beam calculation results identified that the spot size at the small NA_{eff} less than 0.05 will be larger than 10 μm, which is the smallest core diameter of our test fibre. This suggested the light coupling will be performed poorly for the setup at NA_{eff} <0.05 which agreed with the experimental results. Untapered 10μm step-index, 50μm step-index and graded-index fibre were simulated. The models NA were based on Thorlabs SI and GI fibre and custom GI fibre, which are 0.22, 0.20 and 0.30, respectively. Experimental results of transmission versus NA_{eff} of untapered fibres as mentioned are presented and agreed with the simulations.

Tapered fibre transmission properties with coherent light illumination were investigated by both simulations and experimentation in Chapter 3. 5:1 tapered graded-index and step-index Thorlabs fibre were simulated in geometrical optics by Zemax and in EM waveguides by COMSOL. Note that the tapered length of the samples was 100 mm in this chapter but further additional lengths were explored and presented in Chapter 4. The results proved the 5:1 tapered fibre fabricated from the original 50 μm core diameter should be analysed using EM waveguide calculations. Also, the COMSOL simulation results agreed with the experimental results. The difference between tapered fibre samples prepared by Thorlabs and Bath facilities is discussed. The modified transmission versus NA_{eff} experimental setup was described but still used the same method on NA variation and NA matching technique. The impact of cladding light was investigated and

results revealed a small percentage of cladding light contaminated on overall transmission in the case of 100 mm taper length samples. Though taper length impact of cladding light was further studied in Chapter 4 as the shorter length can generate more cladding light contamination. In addition, transmission results showed an unexpected significant loss in step-index tapered fibre and this was confirmed with an additional 'cut back' test that the tapered step-index fibre poorly performed in any case. 'Cut back' test was designed to measure each tapered fibre at different taper ratios after the taper length was cut off from the original 5:1-taper-ratio length to a bigger ratio i.e., the length of tapered fibre was cut off resulting in a bigger diameter at the tapered end. This was suspected as the core-cladding interface of step-index fibres was destroyed by the tapering process.

In Chapter 4, the incoherent and coherent light transmission in tapered graded-index and step-index fibre including untapered multimode fibre was studied. The main focus of this chapter was to explore the best candidate graded-index fibre that performed the best in terms of transmission. At the beginning of the chapter, the optimal setup for coupling incoherent light into test fibre was explored. Then modified coherent light transmission test setup was presented and used for transmission test comparison to the incoherent light results. The evidence from the experimentation shows there is more light loss in general for incoherent light in the same test taper compared to the coherent light coupling. Moreover, the impact of the taper length on transmission properties was investigated. The results from both COMSOL simulations and experimentation indicated shorter tapers allow more light transmitted with lower loss than longer tapers although the cladding light rises accordingly. Then the modal noise of tapered fibre was studied by coupling beam misalignment and bending impact on transmission. There were two bending techniques presented which are the macro-bending and micro-bending methods. The main focus of fibre for the modal noise test is graded-index Thorlabs and custom fibre.

The application of the tapered fibre concept and tests on high-resolution spectrograph EXOhSPEC were presented in Chapter 5. The fabrication of tapered fibre was explained further including a preparation method for built-in-house connectors with trifurcated fibres and customised packaging of spliced tapers. The trifurcated fibre prototype comprises tapered fibre, 10 μm step-index fibre and 50 μm graded-index fibre. The tapered fibre was originally either from a Thorlabs GI commercial product or a custom GI from Bath University. The methods of feeding light to EXOhSPEC were described including the EXOhSPEC throughput test. After that, the results of tapered fibre feeding by EXOhSPEC from a Tungsten lamp and ThAr lamp were shown. The tungsten lamp indicated that the tapered Thorlabs GI taper does not improve

the spectrograph performance but custom GI results are promising. The ThAr lamp results were mainly used to measure the fullwidth of half maximum of output spots. The focus on 690 nm wavelength is to simplify the experimentation and was discussed. The results indicated that ThAr spots of 690 nm obtained by the EXOhSPEC with Thorlabs taper are smaller than 10 µm SI fibre. Although the light throughput is better in custom GI taper compared to 10 µm SI fibre and Thorlabs GI taper, the cladding light was detected and the spots diameter is larger than the other two. Lastly, the research conclusions are presented including future work in Chapter 6.

Chapter 2

Transmission properties and modes in conventional optical fibre

2.1 Introduction

This chapter is about studying transmission properties and modes in conventional fibre optics i.e. 'untapered' fibre, both single mode and multimode type. In section 2.2, the preliminary setup for transmission tests related to mode number and the input light illuminating position are presented. The impact of misalignment is also discussed as this can cause a significant light loss in fibre optics. After that in section 2.3, setups for transmission test were explored and optimised by selecting the most compatible microscope objective lenses (Edmund and Olympus). An NA matching technique that allows optimal light coupling into a test fibre is presented in section 2.3.1. Relative transmission definition for the experimentation is described in section 2.3.2. The Gaussian beam theory on fibre coupling on the transmission test setup by Zemax simulations is explained in section 2.3.3. This is used to calculate spot size from the variable NA beam setup to couple into the fibre optics.

Moreover, untapered fibre was simulated based on Thorlabs and Bath custom fibre specifications by Zemax calculations of geometric optics in section 2.3.4. Models are step-index and multimode fibre with a core size of 10 μm and 50 μm with varied NA: 0.1, 0.2, 0.22 and 0.3. Fibres that were simulated are custom graded-index fibre, Thorlabs step-index and Thorlabs graded-index fibre. Lastly, the transmission dependence on NA_{eff} experimental results are presented from both early and improved version of the setup here.

2.2 Mode number and transmission property impacts on light illumination in single mode and multimode fibre

Generally, the number of modes propagation through the fibre optics depends on the size and type according to equation 1.11. Multimode and larger core diameter fibre should allow more modes to propagate. In this preliminary work, images of the spot pattern from fibre output were taken. The setup was designed to take a far-field image with a ZWO ASI178MM camera by using a 635 nm red laser diode. SharpCap 3.0 was used to record the images. The setup drawing is shown in Figure 2.1. The fibre input was held on a 3-axis translation stage. The power output was measured in a relation to the input beam position i.e., transmission variation, while the far-field images were taken. Selected exposure time for each image was based on the output image that was not saturated. As the mode number was counted manually, the likely error from estimation can be higher than 20% for multimode fibre that supports hundreds of modes. While the error is small (less than 5%) when the single mode or small size ($<$10 µm core diameter) fibre was tested.

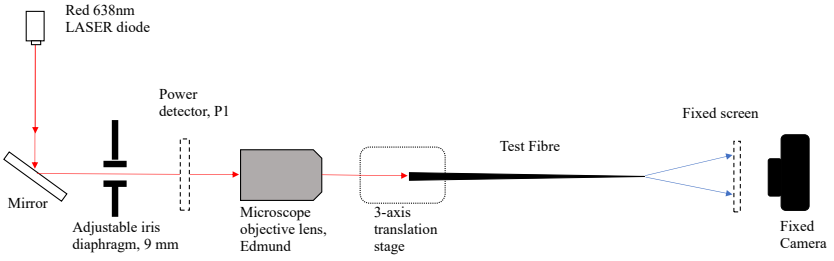

FIGURE 2.1: Drawing of far-field image taking setup. The setup is designed to take a far-field image of fibre output and be able to record the transmission of fibre.

Test fibres were single mode, 10 µm multimode step-index, 25 µm multimode step-index and 62.5 µm multimode graded-index fibre. All were tested for mode number and transmission influenced by the input light illumination. All test fibres have jackets and FC/PC connectors. In this work, the mode was defined by the bright spot shown on the far-field image of fibre output as there is a simple concept for the understanding of mode variations from the change of spots pattern. Thus, the number of modes in this work is a bright spot shown in the output image. Images of fibre output or mode number variation were manually counted as this is considered to be related to mode number propagation in fibre. Results of four fibres were presented in a

relationship between transmission or mode number and input beam position in three axes (x, y, z).

25 μm core diameter step-index multimode fibre output images are shown in Figure 2.2. The position at x = 0 μm (or y = 0 μm, or z = 0 μm) is defined as a position when light propagates into the centre of the fibre's core. Experimentally, the centre of the fibre core was defined when the maximum power output/ transmission was measured. Transmission is a ratio of output power to input power. After a fibre centre position was defined, the input beam was slightly misaligned by adjusting a three-axis translation stage in either axis (vertical, horizontal or optical axis) then the power output was measured at each displaced position. Figure 2.3 shows the mode numbers increasing by off-centre alignment in each direction. Note that the z-axis is defined as the focal plane axis, the x-axis is the horizontal plane and y-axis is the vertical plane. Results show that changes in mode number are less sensitive in the focal plane or z-axis compared to x- and y-axis. This is also related to the power output measured in Figure 2.4. Transmission measured is decreased at each off-centre position and reaches zero when the beam input is completely off the fibre core region. Mode numbers or spots were increased with the off-centre position. Due to the light was not in the most optimal condition. i.e., light is not incident on the centre of the core. The mode pattern appeared as lots of speckle patterns as non-fundamental mode instead of the fundamental mode. This suggests that losses of the fibre waveguide are related to the mode number propagation.

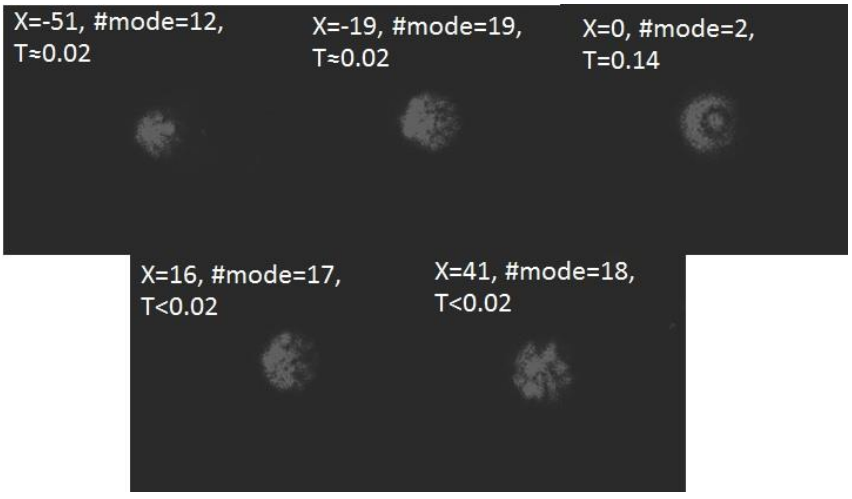

FIGURE 2.2: The output spot images of 25 μm core diameter step-index multimode fibre. The maximum transmission is defined at x = 0 μm. T is the transmission of the fibre. Mode number is increased with more off-centre beam distance.

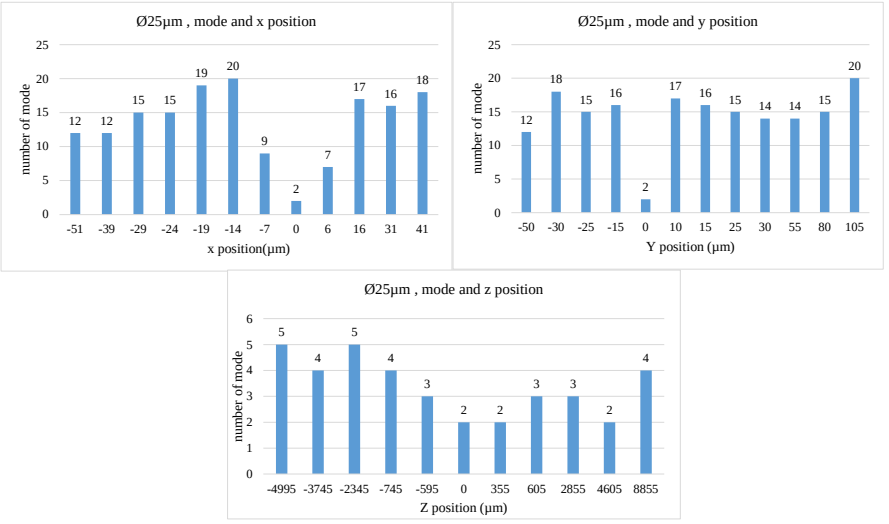

FIGURE 2.3: The graphic columns demonstrate a number of modes depending on the position of input beam for a 25 µm core diameter step-index multimode fibre. There is an increase in mode numbers for each decentered position. Mode number is lowest at the centre position.

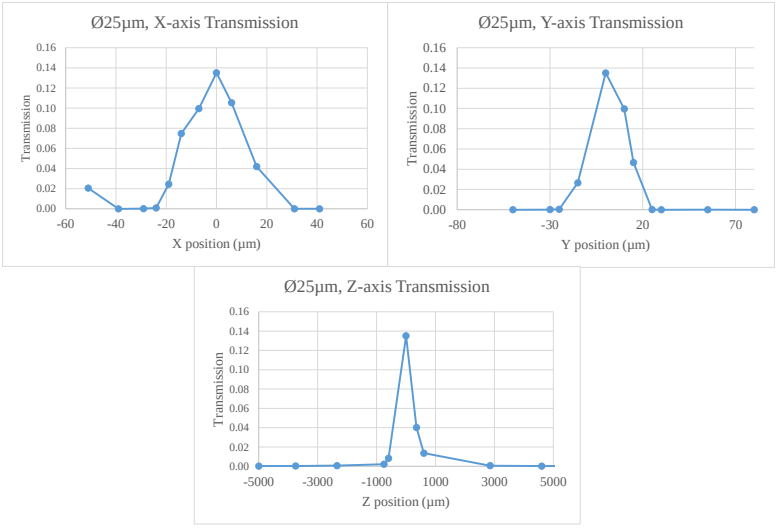

FIGURE 2.4: The output transmission versus beam input position in each axis results of 25 µm core diameter step-index multimode fibre. The maximum transmission is defined at x = 0 µm. Graphs show a drop of transmission as soon as the beam input is slightly off the centre and reach zero when the beam is completely off the fibre input centre.

10 µm core diameter step-index multimode fibre output mode numbers are related to input beam position is shown in Figure 2.5 and transmission variation results are shown in Figure 2.6. The core size is smaller than 25 µm core diameter step-index multimode fibre, hence there are fewer mode numbers that this fibre can support. For 635 nm wavelength, this 10 µm core diameter step-index multimode fibre has V-number 4.95 and can support about 13 modes. Compared to 25 µm core diameter fibre, the transmission dropped more rapidly when the beam input position was moved further from the core if considering the same scale change. This is because of a

smaller diameter. Maximum transmission of 10 µm SI fibre is similar to 25 µm SI fibre (∼0.14).

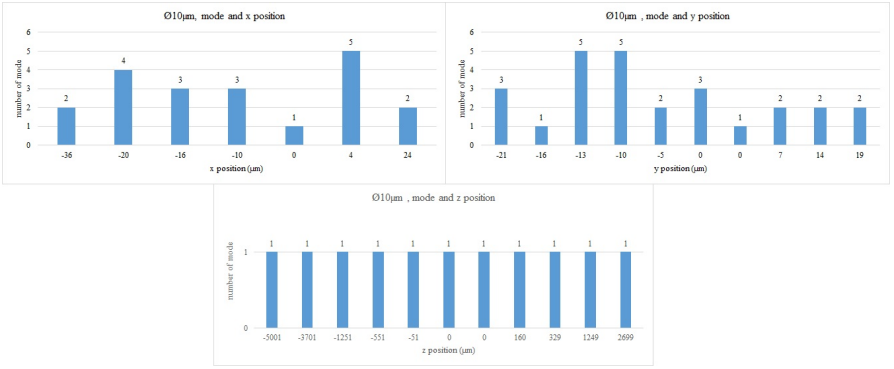

FIGURE 2.5: Results of mode number dependence on the beam input position in each axis of 10 µm core diameter step-index multimode fibre.

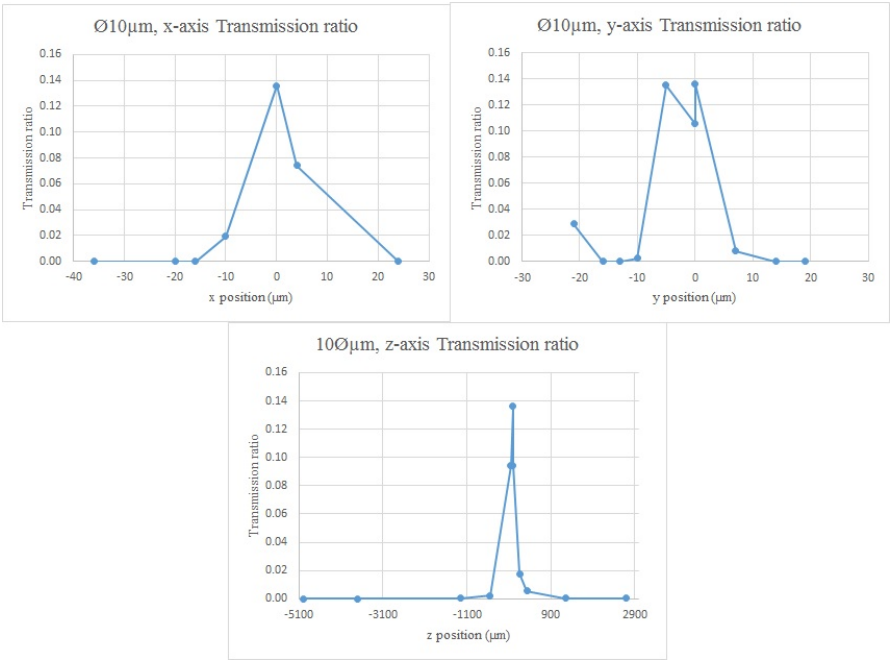

FIGURE 2.6: Results of transmission variation dependence on the beam input position in each axis of 10 µm core diameter step-index multimode fibre.

Lastly, 62.5 µm core diameter graded-index multimode fibre output mode number related to input beam position is shown in Figure 2.7 and transmission variation results are shown in Figure 2.8. The core size is bigger than 25 µm and 10 µm core diameter step-index multimode fibre, hence there are more mode numbers at the fibre output and more transmission (∼0.55).

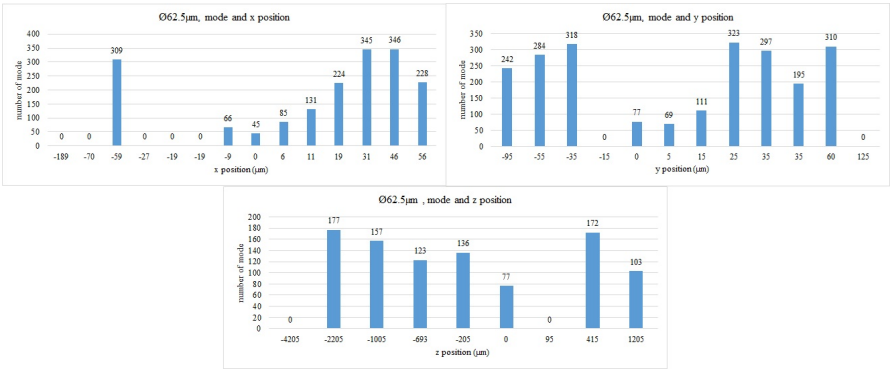

FIGURE 2.7: Results of mode number variation dependence on the beam input position in each axis of 62.5 µm core diameter graded-index multimode fibre.

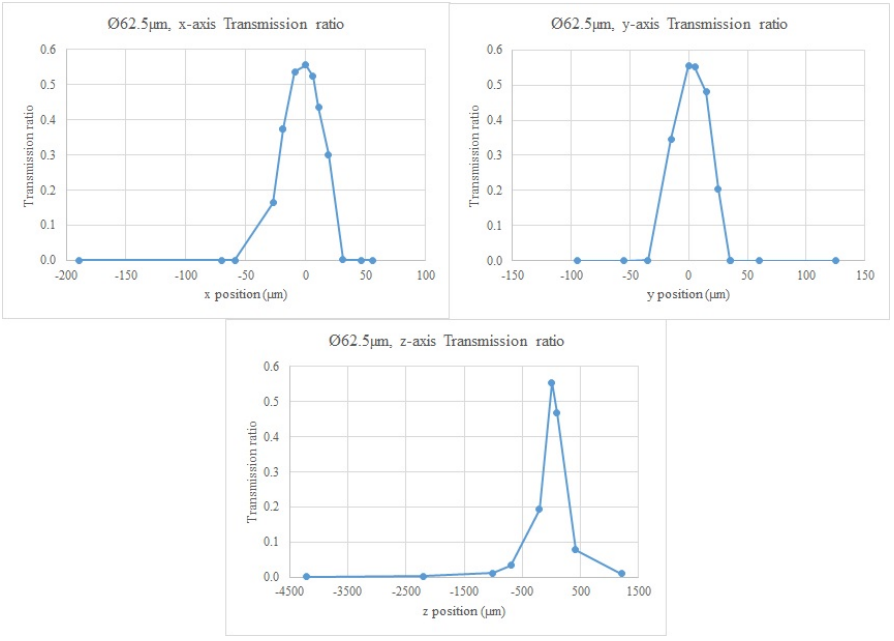

FIGURE 2.8: Results of transmission variation dependence on the beam input position in each axis of 62.5 µm core diameter graded-index multimode fibre.

2.3 Transmission and effective numerical aperture of single mode and multimode fibres

This section describes details of the experimentation, the fibre test setups for coherent light illumination, the principle of the numerical aperture matching technique applied, and the relative transmission definition. Test fibres was obtained from Thorlabs[1], Chromis Fiberoptics [2] and custom fibre from the University of Bath.

[1] `https://www.thorlabs.com/`
[2] `https://chromistechnologies.com/`

Figure 2.9 shows a drawing of the early setup. This setup was designed for transmission measurement and far-field image recording. Relative transmission in this first setup is a ratio between output power and input power ($T = \frac{P_{out}}{P_{in}}$). An Edmund microscope objective lens (MOL) was attached to a three-axis translation stage and used to focus the laser (638 nm) beam onto the fibre input end. The iris diaphragm diameter was fixed at 9 mm in order to select a rectangular beam into a circle to match the objective lens entrance pupil size. A rectangular beam was used for the source. The beam has a width and height larger than 9 mm (maximum iris diameter) as there was a limitation of source supplies on a circular laser. There were two three-axis translation stages used which have different precision: course and fine precision. The first one has 500 µm fine adjustment at 50 µm per revolution and the second has more precision which is 300 µm fine adjustment at 50 µm per revolution. The Edmund microscope objective lenses (10x and 20x) specification in this setup is shown in Table 2.1.

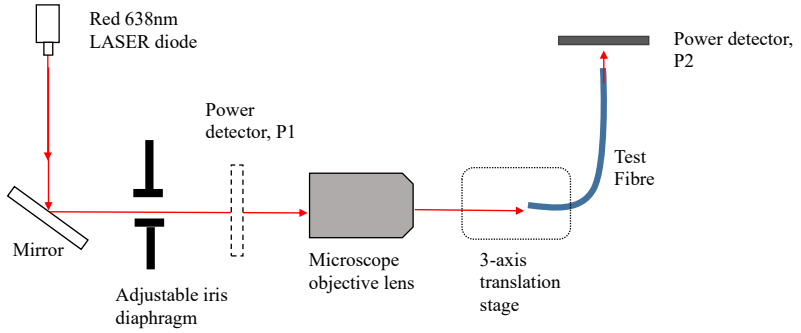

FIGURE 2.9: A diagram of an early stage of the transmission measurement setup. The source is 638 nm laser diode. The iris diaphragm is fixed at 9 mm. A microscope objective lens is used to focus the collimated light into test fibre. The 3-axis translation stage is used to adjust the fibre position for light coupling and the detector is placed after the test fibre.

TABLE 2.1: Microscope objective lens (MOL) specification

MOL	focal length (mm)	NA_{MOL}	Exit pupil diameter(mm)
4x	29.27	0.10	5.85
10x	17.02	0.25	8.51
20x	8.33	0.40	6.66

NA_{MOL} is the Numerical Aperture of a microscope objective lens. Entrance pupil diameter (Φ_{MOL}) is calculated by using the equation $NA = \frac{n\Phi_{MOL}}{2f}$, where n is a refractive index which is 1 for air and f is the focal length of microscope objectives lens.

Apart from the conventional fibre such as single mode and multimode fibre, there were the special types of fibre studied such as a square core, double cladding layers, and endlessly single mode fibres. All tested untapered fibre specifications for this research are shown in Table 2.2.

Note that test fibres were with and without protective jackets. 'Bared' fibre is used for the fibre without connectors and protective layers and 'Connectorised' fibre is used for the fibre with a jacket and FC/PC connectors. The preliminary tests of transmission with this first setup and results are shown in Table 2.3.

TABLE 2.2: Untapered fibre specification comprises of type, geometrical core size, manufacturer's NU (NA†), and Part number. Note that the core specification of single mode fibre is mode field diameter. *POF-62SR is Chromis Fiberoptics product.

Type	Core (μm)	NA†	Part number
SM	2.8-4.1 at 488 nm	0.10-0.14	SM450
SM	3.6-5.3 at 633 nm	0.10-0.14	SM600
SM	4.0 ± 0.5 at 630 nm	0.13	630HP
ESM	12.2	0.09 ± 0.02 at 1064 nm	ESM-12B
Double-clad	9 (1st)/ 105 (2nd)	0.12/ 0.2	DCF13
SI MM	10	0.10	FG010LDA
GI MM	25	0.10	FG025LJA
SI MM	50	0.22	FG050LGA
GI MM	50	0.20	GIF50E
GI MM	62.5	0.275	GIF625
GI MM plastic	62.5	0.185	POF-62SR*
Custom GI MM	50	0.30	custom fibre
SI MM	105	0.39	FP150QMT

TABLE 2.3: Transmission results of untapered fibre without NA matching technique applied. 10x Edmund objective lens was used as a focuser.

Fibre	$NA^{\dagger}$	Transmission
single-mode	0.10	0.12
ϕ10 μm Step-index	0.10-0.14	0.14
ϕ25 μm step-index	0.10	0.14
ϕ62.5 μm graded-index	0.275	0.55

2.3.1 Numerical Aperture matching technique and the improved transmission test setup

A primary characteristic determining the transmission of an optical system is the Numerical Aperture (NA). If the numerical aperture and image size of the optical system matches the fibre's numerical aperture and core size then maximum coupling to the fibre core is possible. In other words, if the beam is incident at a suitable convergence angle on the fibre it can propagate along the core without leaking into the cladding. The collimated beam and focusing lens combination can vary the NA of the focused beam on the fibre core depending on the aperture stop. This is the typical technique used in experimental works (Marcel et al., 2006; Haynes et al., 2012; Jovanovic et al., 2012; Spaleniak et al., 2013). In the test apparatus, the numerical aperture of the focused beam from the collimated source to a fibre is varied by adjusting an iris stop

diameter at a fixed distance from the microscope objective lens. Thorlabs presented a beam profile measurement setup which is very similar to the setup[3]

Figure 2.10 shows the matching setup drawing. There is an iris diaphragm with an adjustable diameter d_{iris}, and a microscope objective lens of either 10x or 20x with entrance pupil d_{MOL}. Collimated light from Laser diode is used as a source.

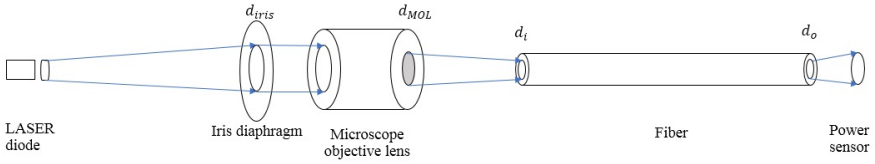

FIGURE 2.10: Drawing of NA matching setup.

The effective numerical aperture (NA_{eff}) of this optical system is calculated by the following equation:

$$NA_{\text{eff}} = NA_{\text{MOL}} \frac{d_{\text{iris}}}{d_{\text{MOL}}}, \tag{2.1}$$

where NA_{eff} is an effective numerical aperture. NA_{MOL} is the full numerical aperture of a microscope objective lens (MOL). The diameter of the iris diaphragm and the internal stop diameter of the microscope objective lens is d_{iris} and d_{MOL} respectively.

Edmund 10x and 20x magnified objective lenses were used in the early stage of the setup (Figure 2.1). The proper magnification objectives were chosen for each fibre, e.g., 10x is matched with an up to 0.25NA fibre such as single mode, ϕ10 µm, ϕ25 µm and ϕ50 µm fibre while 20x is matched with ϕ150 µm square-core fibre.

There are example results of a relationship between transmission and fibre input position after applying NA matching technique. The graphs present the transmission varies according to the fibre input position along the x- and y-axis. Results of test fibres shown here are single mode (Figure 2.11 and Figure 2.12) and multimode fibre with varied core sizes. Multimode fibres results are 10 µm step-index fibre (Figure 2.13), 25 µm step-index fibre (Figure 2.14), 50 µm 5m-length graded-index fibre (Figure 2.15), 62.5 µm 3m-length graded-index fibre (Figure 2.16) and 150 µm square-core step-index fibre (Figure 2.17).

[3] `https://www.thorlabs.com/images/TabImages/Multimode_Fiber_Beam_Lab_Fact.pdf`

TABLE 2.4: Transmission results of untapered fibre with NA matching technique applied. Transmission results were measured by the setup in Figure 2.9. The test fibre has FC/PC connectors and jacket protective layers.

Fibre	matched MOL	NA_{eff}	Transmission
488-633 nm, single-mode	Edmund 10x	0.09	0.6
633-780 nm, single-mode	Edmund 10x	0.07	0.6
ϕ10 µm 1m-length step-index	Edmund 10x	0.10	0.6
ϕ25 µm 2m-length step-index	Edmund 10x	0.03	0.6
ϕ50 µm 1m-length step-index	Edmund 10x	0.15	0.7
ϕ50 µm 2m-length step-index	Edmund 10x	0.10	0.7
ϕ50 µm 5m-length step-index	Edmund 10x	0.10	0.7
ϕ50 µm 5m-length graded-index	Edmund 10x	0.15	0.8
ϕ150 µm square-core step-index	Edmund 20x	0.15	0.7
ϕ62.5 µm 3m-length graded-index	Edmund 10x	0.10	0.8

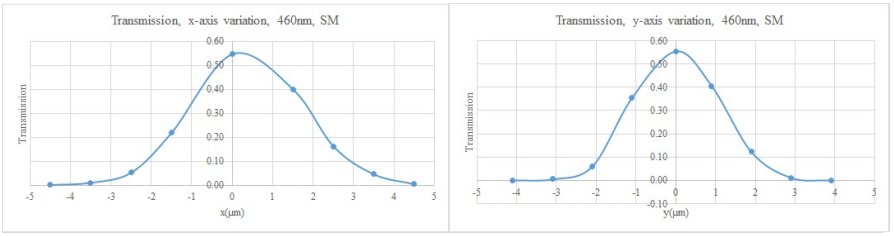

FIGURE 2.11: A relationship between transmission and beam-input position on the fibre input end of 488-633 nm operating wavelength range single-mode fibre (Thorlabs: P1-460B-FC-5). Maximum transmission is about 0.55.

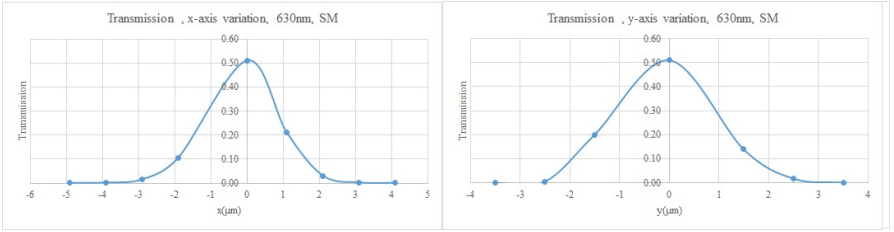

FIGURE 2.12: A relationship between transmission and beam-input position on the fibre input end of 633-780 nm operating wavelength range single-mode fibre (Thorlabs: P1-630A-FC-2). Maximum transmission is about 0.50.

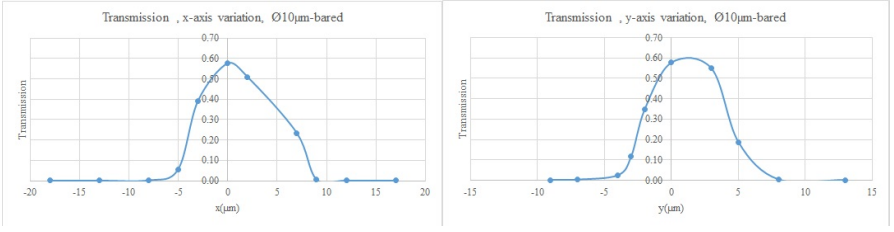

FIGURE 2.13: A relationship between transmission and beam-input position on the fibre input end of 10 µm step-index fibre (Thorlabs: FG010LDA). Maximum transmission is about 0.60.

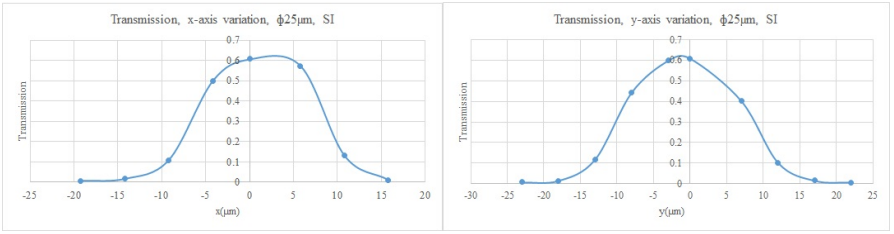

FIGURE 2.14: A relationship between transmission and beam-input position on the fibre input end of 25 μm step-index fibre (Thorlabs: M67L01). Maximum transmission is about 0.60.

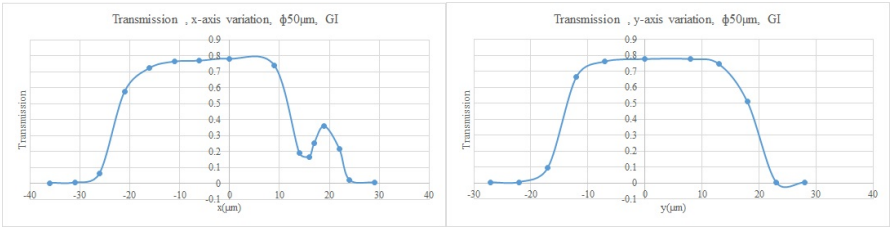

FIGURE 2.15: A relationship between transmission and beam-input position on the fibre input end of 50 μm 5m-length graded-index fibre (Thorlabs: M116L05). Maximum transmission is about 0.80.

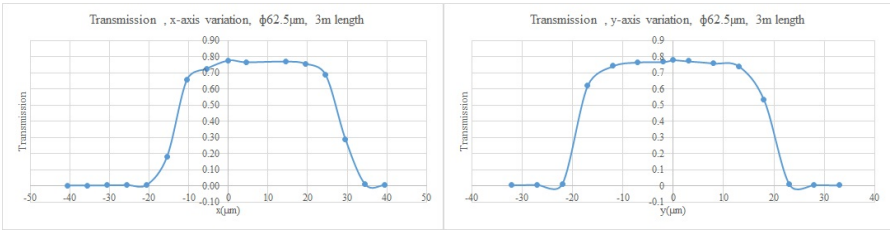

FIGURE 2.16: A relationship between transmission and beam-input position on the fibre input end of 62.5 μm 3m-length graded-index fibre (Thorlabs: M116L05). Maximum transmission is about 0.80.

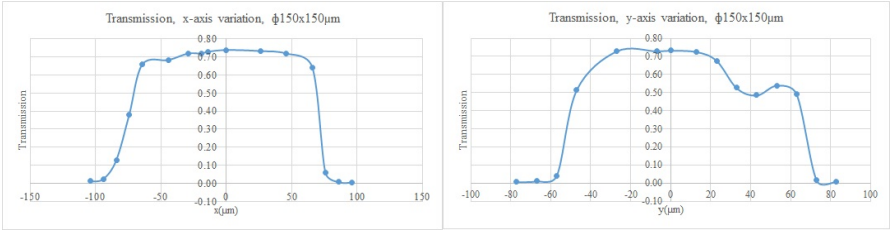

FIGURE 2.17: A relationship between transmission and beam-input position on the fibre input end of 150 μm square-core step-index fibre (Thorlabs: M101L02). Maximum transmission is about 0.72.

This technique was also continued to be used for the improved version of the setup with better quality objectives Olympus with 4x and 10x magnifications. This is due to an improvement in transmission results from the trial test by Edmund lenses. Two microscope objective lenses were used: 4x (NA_{MOL}= 0.10) and 10x (NA_{MOL}= 0.25) in order to take wide-ranging NA_{eff} data related to transmission ratio. The microscope objectives were carefully measured to confirm the manufacturer's NA_{MOL} specification by measuring the exit pupil diameter and the focal length. Edmund and Olympus objective lens transmission comparison is presented in Figure 2.18. The 10x Olympus lens transmission is slightly better than Edmund objectives and light coupling is significantly better at $NA_{\mathrm{eff}} > 0.17$ due to the exit pupil diameter being bigger than Edmund's even though the manufacturer's NA is the same. There is no significant transmission difference for the 4x objectives. The experimentation was repeated 5 times within the same condition without changing the alignment and the microscope objective was left on the holder without any disturbing. For the reproducing measurement such as repeating the same test with the same objective lens but the alignment of test fibre was repeated, the systematic error is contained within 5-10 %. This is also applied to the fibre transmission test in the later sections. Error of the experimentation was explained further in section 3.3.3.

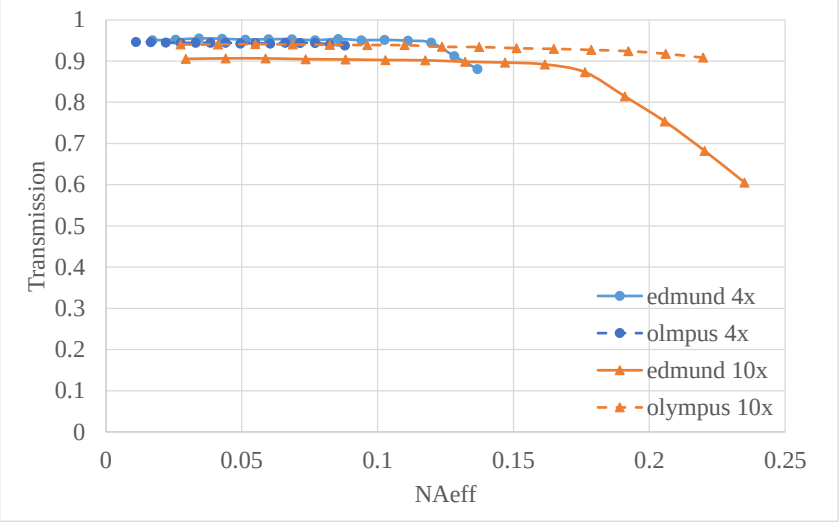

FIGURE 2.18: Comparison of transmission of Edmund and Olympus objective lens. A relationship between transmission and effective numerical aperture is presented for 4x and 10x objective lenses. One sigma errors of transmission are contained within the plotting symbol.

Then transmission setup was modified (shown in Figure 2.19). The position of a detector for input power measurement was fixed in one place. This is for same-time recording with output power. This eliminates time-consuming input and output power measuring that was done

separately in the previous setup. Beam expansion was added to the setup to match the input beam to the entrance pupil size of the microscope objective lens (∼9 mm). Previously, the beam shape was rectangular. The new setup has a round shape beam. The setup drawing shown in Figure 2.19 comprises a 635 nm laser diode source (Thorlabs: CPS635R), a beam expansion telescope, an adjustable iris diaphragm, a three-axis adjustable translation stage and 4x or 10x Edmund/Olympus microscope objective lenses. A 2° uncoated deviation prism was used to sample the input beam power and standard optical power sensors with digital outputs (Thorlabs: SN120B and Thorlabs: SN120UV) were used for the input and output measurements. The output from the beam expansion telescope was a 9.7 mm diameter collimated beam. One important change here is an adjustable iris diaphragm that allows the beam input numerical to be adjusted. This leads to the discovery of how to optimally couple light into the fibre in this research. NA matching technique is explained further in section 2.3.1. Also, the change of setup shows slight improvement on the $NA_{\text{eff}} > 0.17$ as example results of 50 µm step-index untapered and tapered fibres in Figure 2.20.

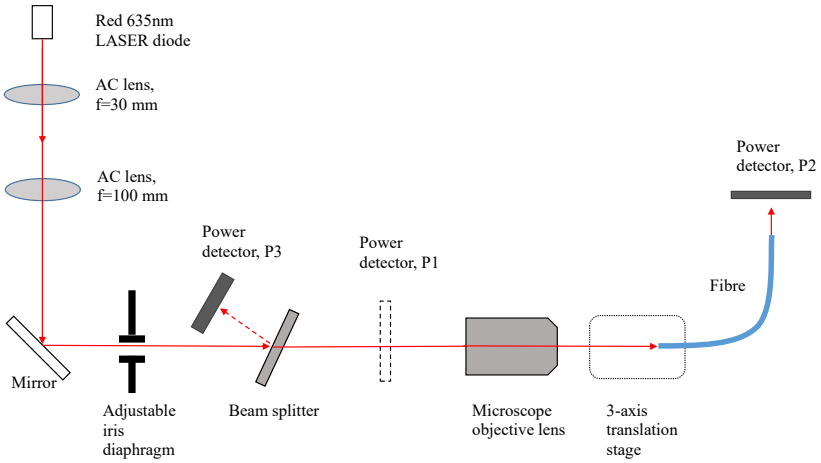

FIGURE 2.19: An illustration of an improved version of fibre transmission test setup. The fibre test setup comprises a 635 nm red diode laser, a collimated-beam expander consisting of a two lens-telescope using achromatic doublets, an adjustable iris diaphragm, a beam splitter, a microscope objective lens (4x or 10x magnification), a three-axis translation calibrated stage and two power detectors.

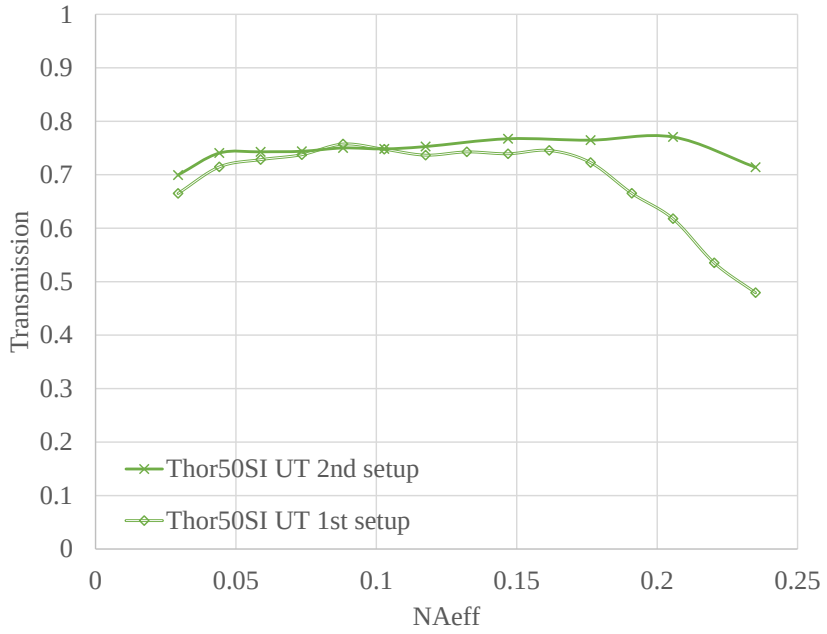

FIGURE 2.20: A comparison of transmission versus NA_{eff} between early setup (Figure 2.9) and the improved setup (Figure 2.19). Test fibre used for comparison are Thorlabs 50 µm SI untapered (UT) fibre. one sigma errors of transmission are contained within the plotting symbol. Systematic error is about 5%.

2.3.2 Relative transmission

According to the setup in Figure 2.19. The power at the fibre end was measured and sampled the input beam with the beam splitter. The power at the position after the beam splitter is defined as P_1. P_2 is the power output after the fibre end and P_3 is the power output of the reflected beam from the beam splitter. The intensity of the beam after the beam splitter P_1 is directly proportional to the intensity P_3 with proportionality constant α. The parameter α is determined from the measured beam with the two detectors at different positions and is written as $\alpha P_3 = P_1$. The transmission is the ratio of power output to input, which is

$$T = \frac{P_2}{P_1} = \frac{P_2}{\alpha P_3}. \tag{2.2}$$

The transmission measurement includes all input and output losses and fibre absorption losses. The latter are very small with the one metre lengths used for testing. The measurements are done repeatedly each time the iris is adjusted. The power output of P_2 and P_3 are recorded five times for each measurement. The mean and standard deviation of each recorded data point are

calculated. The same apparatus and procedure were used for all fibres. All untapered fibres were measured with one metre lengths of fibre and cleaved ends unless otherwise noted.

2.3.3 Gaussian beam fibre coupling

Coupling light into the fibre cores requires care to achieve consistent results with multimode fibres. A truncated Gaussian beam propagation calculation was used to estimate input coupling variations. Useful explanation on the truncated beam is referred from the document provided by CVI Melles Griot[4]. Our setup calculations specifically can be found in Github[5]. The Gaussian beam waist transformation by lens and truncation problems for the setup of a coherent light transmission test setup in this work can be calculated to identify the final image spot. Figure 2.21 shows the drawing of Gaussian beam propagation in the transmission test. The 635 nm laser diameter is 2.9 mm so the beam waist w_o is 1.45 mm. There are three lenses in this setup denoted as L1, L2 and L3. The first two lenses with separated distances L=130 mm are used to magnify the overall beam size 3.3 times with focal lengths L1=30 mm and L2=100 mm. An iris diaphragm with a variable diameter range 1-9 mm is placed after the second lens and located before the third lens. The third lens is the microscope objective 4x or 10x with focal length L3= 45 mm or 18 mm, respectively. Considering the collimated beam focused by the first lens L1, the Rayleigh range Z_R can be obtained by 1.19 and is 10401.89 mm. The distance between the laser and the first lens (s) is 55 mm. Image distance of L1 (s") obtained by equation 1.22 is 30 mm. The magnification of the beam after the L1 is 0.0029 (calculated from equation 1.23). Hence, the transformed Gaussian beam from L1 has a transformed waist (w_0'') 4.18 µm and Rayleigh range after the first lens is Z_R'' 0.09 mm, which is calculated from 1.24. After that, the beam is collimated by the second lens L2 (f2=100 mm). A similar approach with the lens L1 was applied. As S_2 = 100 mm according to telescope optics (L=f1+f2). The magnification is 1155.77, Z_R''' is 115576.53 mm and w_0''' is 4833.33 µm.

The collimated beam now has waist diameter $2w_0'''$ = 96.666 mm. Truncation factor of the beam is calculated from equation 1.28 for 4x and 10x objective lenses. The spot diameter is calculated by equation 1.25, considering K from $1/e^2$ in equation 1.27.

[4] https://www.physics.utoronto.ca/~phy326/hene/Gaussian-Beam-Optics.pdf

[5] https://github.com/Piyamas-Ch/Tapered-and-untapered-fibre-investigation/blob/master/Zemax/Gaussian-spot_calculations.JPG

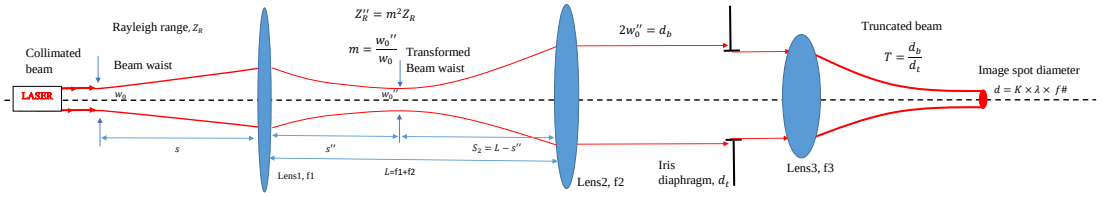

FIGURE 2.21: Gaussian beam transformation and truncation of the coherent light test setup. The coherent light λ is 635 nm. The setup comprises three lens L1, L2 and L3 with focal lengths f1, f2 and f3. f1=30 mm, f2=100 mm and f3, which can be selected from either f3=18 mm for 10x objectives or 45mm for 4x objectives. The iris diaphragm has an adjustable diameter (d_t) from 1-9 mm.

The setup will produce the largest spot size with a Gaussian ($1/e^2$) waist of 47 µm and with the iris diaphragm set at 1 mm using the 4x microscope objective lens. The 4x measurements will thus have some coupling losses at this setting for fibres with smaller core diameters than 50 µm. The focal spot sizes for the 10x objective were less than 20 µm for all iris settings.

Zemax 19.8 is used to model comparative setups in order to calculate the focal spot of a 635 nm Gaussian beam. The setup Zemax model shows in Figure 2.22 The file is also located in Github[6]. The non-sequential mode was selected. The beam original waist was 1.45 mm and M^2 is defined as 1. A pair of lenses in the telescope were selected as paraxial lenses with focal lengths 30 and 100 mm, respectively. The stop Circular Obscuration aperture type was defined to imitate iris aperture and the size of the iris aperture can be adjusted at the minimum radius box. The stop aperture location is after a pair of AC doublet lenses with 30 mm and 100 mm focal lengths. The focuser located after the aperture stop is either a 45 or 18 mm focal length paraxial lens for the 4x and 10x microscope objective lens, respectively. The calculations by Zemax agree with Gaussian beam calculations and there was no significant difference.

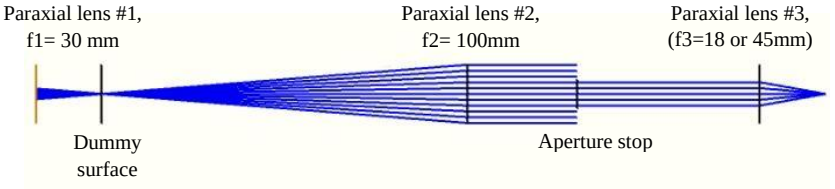

FIGURE 2.22: A 2D images of Zemax model of the transmission dependence on NA_{eff} setup. All three lenses in the model are paraxial. A pair of lenses #1 and #2 magnified beam input x3.3 and the adjustable aperture stop is located before the focuser lens. the focal length of the focuser can be selected either 45 or 18 mm in order to imitate 4x and 10x objectives, respectively.)

[6] `https://github.com/Piyamas-Ch/Tapered-and-untapered-fibre-investigation/tree/master/Zemax` (paraxial_fibre_setup_ZMX)

The focal spot sizes were also measured directly by scanning a small core fibre through them and these agreed with the calculations. Note there is no attempt to exactly match the fibre core diameters with the Gaussian waists from the two focusing objectives so that transmission measurements in this research will be smaller than the absolute maximums that could be theoretically achieved for the lowest order modes in multimode fibres and in single mode fibres. Our principal objective was to achieve consistency across a large range of fibre and taper geometries.

The experimental results at very low NA_{eff} ($NA_{\text{eff}}<0.05$ for untapered fibre and $NA_{\text{eff}}<0.02$ for SI taper and <0.05 for GI taper reveal a significant drop in transmission due to inefficient mode coupling to low order modes, i.e. the mode profile that is not matched at all diameters of the iris diaphragm. To couple the same mode into the fibre for each iris diameter (NA_{eff}) is extremely time consuming. Since, the principal interest is in $NA_{\text{eff}}>0.05$, the setup is valid to identify the best performing tapers for the EXOhSPEC. The spectrograph has a 0.16NA acceptance so a method used to measure light is for different numerical aperture outputs at 0.24 NA and 0.12 NA by variation of the detector distance. The output detector used for fibre characterisation has 9.5 mm diameter and the detector was fixed at two distances 20 mm and 40 mm. At 20 mm from the output fibre end, the light was detected at 0.24 numerical aperture (denoted as 0.24NAO). At 40 mm from the fibre end, the light was collected at 0.12 numerical aperture (denoted as 0.12NAO). This emulates the transmission of the taper into the EXOhSPEC spectrograph NA limitation (0.12NAO) compared to the entire output of the taper (0.24NAO).

2.3.4 Untapered fibre transmission: simulations and experimentation

The untapered fibre was simulated by the non-sequential mode of Zemax version 19.8. The scaled up dimensions of the fibre optics configuration is used as to approach geometrical optics rather than EM waveguide, so mode propagation is not considered. The composite optical model had a 0.5 mm rod with a cylinder of 0.5 mm inner diameter and 1.25 mm outer diameter with 1 m lengths. For 0.22 NA step-index fibre, the core is selected as silica and the cladding index is defined as 1.4419 to imitate the 0.22 NA fibre. The graded-index simulations use a typical parabolic profile for the core refractive profile to imitate the 0.20 NA and 0.30 NA of graded-index fibre. The design of custom graded-index fibre has 6.25 mm outer diameter with the same inner diameter as Thorlabs fibre. A wavelength of 635 nm was used with 100000 rays to perform

the calculations for tapered geometries. Details of the model calculations and the Zemax model files are found in Github[7].

Figure 2.23 presents Zemax simulations of 10 SI (0.10NA), 50 SI (0.22NA), 50 GI (0.20NA), and 50 custom GI fibre in a relationship between transmission and NA_{eff}. The detector in the simulation collected light from both the core and cladding. The trends of each fibre were gradually decreased at $NA_{\text{eff}} > \text{NA}^{\dagger}$ except for custom GI fibre results. The transmission of the custom GI fibre is constant over the range of NA_{eff} because the cladding diameter (620 µm) is relatively big compared to the other three fibres (125 µm). When the input NA exceeds the fibre's NA, the light that leaked to the cladding propagates through the cladding region and reached the other end. This was collected at the detector. Whereas, smaller cladding fibre such as 10 SI (0.10NA), 50 SI (0.22NA) and 50 GI (0.20NA) has no light leak to cladding and propagates to the other end of fibre when NA_{eff} exceeded $\text{NA}^{\dagger}$.

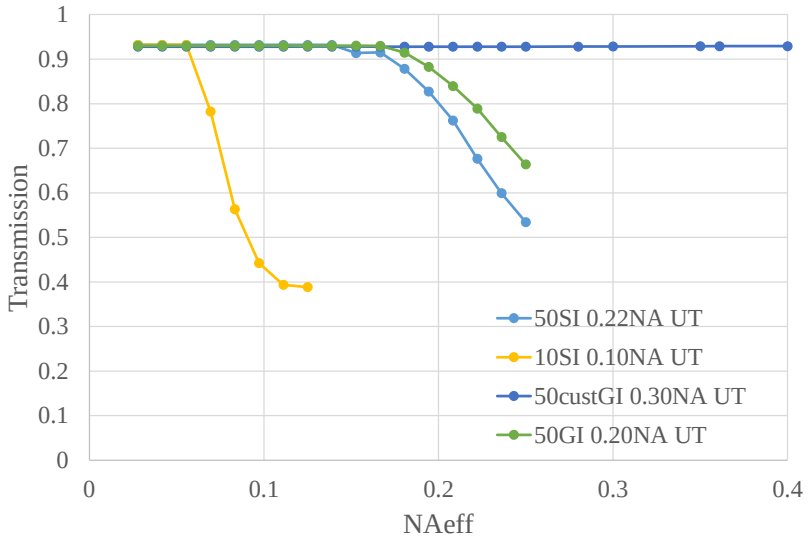

FIGURE 2.23: Results of Zemax model of untapered fibre. There were 50 µm SI (0.22NA), 10 µm SI (0.10NA), 50 µm custom GI (0.30NA) and 50 µm GI (0.20NA) fibre presented.

For the transmission experimentation, test fibres are listed in Table 2.2. Untapered fibre results were tested with the improved setup (Figure 2.19). Some results were tested with Edmund objective lenses. Conventional and endlessly single mode fibre results show in Figure 2.24 and 2.25. Comparison between the 488-633 nm and 633-780 nm operating wavelength range for single mode fibre results are presented. Note that single mode fibres have a jacket and FC/PC connectors and all light from fibre output was collected into a detector in both 0.12NAO and

[7] `https://github.com/Piyamas-Ch/Tapered-and-untapered-fibre-investigation/tree/master/Zemax`

0.24NAO setup. Later ESM fibre was tested (Figure 2.25) including MM fibre. For the multi-mode fibre, results are divided into two sets from 1)early setup and 2)improved setup. The early MM fibre results were connectorised fibre while the later results were bared fibre.

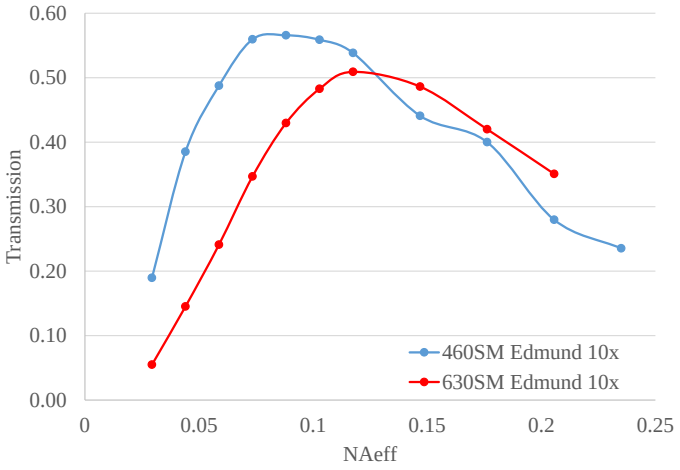

FIGURE 2.24: Transmission versus NA_{eff} results of two different operating wavelength ranges single mode fibres (Thorlabs: SM450 (488-633 nm) and SM600 (633-780 nm). These results were measured with 10x Edmund objective lens with the improved setup with 635 nm coherent light.

Figure 2.25 shows the results of Endlessly single mode (ESM) photonic crystal fibre. This fibre was tested with Edmund lenses with an improved setup. Light collected to the detector at 0.24NAO.

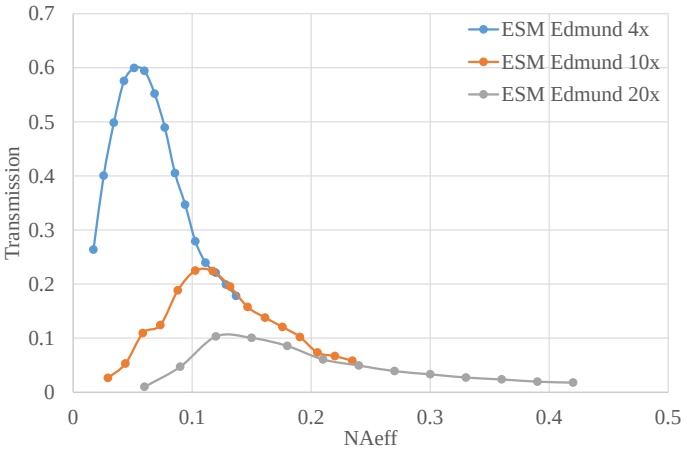

FIGURE 2.25: Transmission versus NA_{eff} results of Endlessly single mode (ESM) photonic crystal fibre. These results were measured with Edmund objective lenses with a magnification of 4x, 10x and 20x.

Untapered multimode step- and graded-index fibre transmission versus NA_{eff} results with the early setup presented in Figure 2.26. All light of the fibre output was collected. There are various core diameter sizes presented: 10 µm, 25 µm, 50 µm, 62.5 µm and 150 µm. Note that the core of 150 µm step-index fibre is a square shape. The 50 µm step-index multimode fibre has similar overall transmission compared to 62.5 µm graded-index fibre.

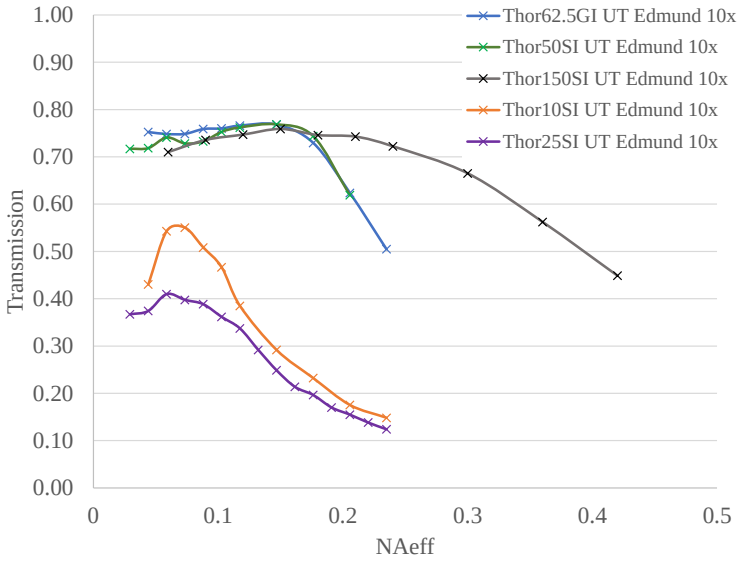

FIGURE 2.26: Transmission versus NA_{eff} results of untapered SM and MM fibre. Test fibres core diameter sizes are 10, 25, 50, 62.5 and 150 µm. These results were measured with Edmund objective lenses with the early setup without an accurate translation stage for light coupling into a fibre. All light is collected at the output. All fibres are connectorised fibre.

After the more accurate model three-axis translation stage was applied with the modified transmission test setup (Figure 2.19). There is combination results from both Olympus and Edmund objective lenses. This setup improves light coupling into a test fibre. There is $< 5\%$ change on repeating the same test and $< 10\%$ change with a new setup to repeat the experimentation. Note that this time 'bared' fibres were tested instead of FC/PC connectors with jacket layer fibres. Figure 2.27 shows transmission results from the improved setup test. Light collected at 0.24NA (0.24NAO) and 0.12NA (0.12NAO). Tested fibres are 62.5 µm Plastic optical fibre, 62.5 µm GI Thorlabs fibre, 50 µm GI Thorlabs fibre, 50 µm SI Thorlabs fibre and 10 µm SI Thorlabs fibre.

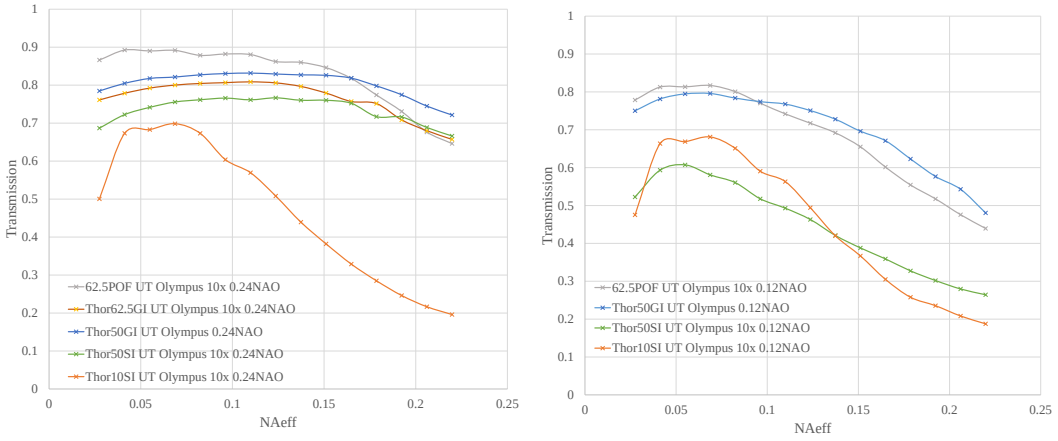

FIGURE 2.27: Transmission versus NA_{eff} results of untapered MM fibre. Test fibre's diameter sizes are 10, 50, and 62.5 µm. Olympus's objective lens was used to improve the setup. Light was collected at the output on 0.24NAO (left) and 0.12NAO(right). All fibres are bared fibres.

Typically, there is more overall transmission in the bigger core fibre because the light can propagate more per area unit if considering the same type (SI or GI fibre) and core shape fibre (e.g. circular, square etc.). For example, from experimental results, transmission in general of 62.5 µm GI is higher than 50 µm GI fibre but the square core fibre with 150 µmx150 µm core size has less transmission than the other two mentioned. This is because the light coupling has better efficiency from the circular beam to circular core fibre than the square core fibre.

The transmission trends of MM 50 µm and 62.5 µm were relatively flat and slowly decreased when the NA_{eff} exceed manufacturer NA i.e., NA $>$ 0.27 for 62.5 µm MM Thorlabs GI fibre, $>$ 0.185 for 62.5 µm Plastic Optical MM fibre, $>$ 0.22 for 50 µm MM SI fibre, $>$ 0.20 for 50 µm MM GI fibre and $>$ 0.10 for 10 µm MM SI fibre. The transmission trends of 10,µm MM SI fibre has a small area of the peak due to the smallest of manufacturer NA. There was also a significant drop of transmission at small NA_{eff} for all test fibre because the coupling on small NA_{eff} was not optimal as the Gaussian input beam (discussed in section 2.3.3 spot exceeded the fibre diameter). Moreover, the results of different NAO show less light measured or transmission for 0.12NAO of 50 and 62.5 µm MM fibre of which NA 0.185, 0.20, 0.22 and 0.275. The part of the output light was not included on the measurement for 0.12NAO. 10 µm SI fibre with 0.10NA has similar transmission trends in both 0.12NAO and 0.24NAO due to output beam NA is 0.1 and can be all collected to the detector at both NAO.

2.4 Summary

In this chapter, the early stage of the transmission test on the conventional untapered fibre is presented including mode properties in SM and MM fibre studies. The preliminary test on the impact of mode number and transmission by the light coupling was investigated. The commercial product fibres are the main interest in this chapter. Results of mode number and fibre input alignment showed that there is a vital role for optimum coupling light into the centre of the fibre core otherwise loss will increase as well as mode numbers, especially in multimode fibre. Then the improvement of the transmission test was discussed. The adjustable effective numerical aperture (NA_{eff}) is required in order to improve light coupling into the test fibre i.e., NA matching technique. Optimal light coupling is when NA of beam input i.e., NA_{eff} matches the fibre's NA. In other words, transmission is optimal when the $NA_{\text{eff}} \sim$ manufacturer NA. Also, lens quality can improve the light coupling into fibre optics from the evidence of transmission comparison between Edmund and Olympus lenses. In addition, the theoretical Gaussian beam calculations by Zemax were discussed and used to model the spot size coupling into the test fibre as there is significant transmission reduction at small NA_{eff} ($<$0.05). Moreover, some of the untapered fibres were successfully modelled (10 SI with 0.1NA, 50 SI with 0.22NA, 50 GI with 0.20NA and 50GI with 0.30NA) with Zemax based on a geometrical optics scale to imitate the experimentation.

Chapter 3

Tapered fibre and transmission properties with coherent light illumination

3.1 Introduction

This chapter is about the investigation of transmission properties of tapered fibre with coherent light sources with both experimentation and simulations. Tapered fibre is the fibre optics that were stretched symmetrically between the input and output interface. The tapered end has a smaller diameter (see section 1.6). The tapered fibres in this study mainly focus on 5:1 taper ratios with varied lengths from 15, 25, 50 and 100 mm. Commercial products based from Thorlabs were used as well as custom graded-index fibre provided by Bath University. The main interesting fibres are 50 μm step-index and graded-index fibre. This is due to the main application focus on applying a 10 μm core size to our high-resolution spectrograph prototype EXOhSPEC fibre feeding.

The concept of an adiabatically tapered fibre is presented by consideration of geometrical optics and EM waveguide in section 3.2. 5:1 tapered fibre is simulated in geometric optics by Zemax in section 3.2.1.2 and EM waveguide by COMSOL in section 3.2.2.1. The parameters such as the diameter of core and cladding and refractive index were based on Thorlabs and custom fibre specification.

In order to investigate the performance of tapered fibre, a continuing study in the transmission dependent on NA_{eff} test with tapered step-index and graded-index fibre is presented in section 3.3. A coherent source (635 nm) was used for the light illumination. Test fibres were 'connectorised' tapered and 'bared' tapered fibre. Also, the preparation of the samples is described in 3.3.1. Cladding light of 100 mm tapered fibre results is discussed in section 3.3.2. The experimental error of the transmission test is explained in section 3.3.3. Discussion of the transmission dependence on NA_{eff} of tapered fibre results of two separated set of samples are in section 3.3.4.1 (connectorised taper) and in section 3.3.4.2 (bared taper). Additional 'cut back' experimentation is presented to investigate the impact of taper ratios on transmission and confirmed the poor performance of tapered SI taper.

3.2 Geometrical optics and EM waveguide considerations in tapered fibres

3.2.1 Geometrical optics of tapered fibre

3.2.1.1 Etendue and tapered fibre

The definition of a tapered fibre is a fibre which has different diameter sizes between input and output ends. The etendue principle is applied to describe the optical geometry of taper (Marcel et al., 2006; Haynes et al., 2012). The energy is assumed to be conserved among the ideal tapered fibre. In other words, the etendue is used to describe light cone characteristics in terms of its size, and angle in the optical system. The light travelling along the optical system required two factors to characterise itself, which are angular space and light transmitted area. In this work, etendue is defined as G. Then G = AΩ, when Ω is light cone solid angle and A is light transmitted area. If considering 3-D geometry optics, the etendue in differential form is:

$$\int dG = n^2 \int dA \int \int \cos\theta d\Omega \tag{3.1}$$

with

$$d\Omega = \sin\theta d\theta d\phi.$$

If considering the maximum concentration case in an area A, the etendue can be written as:

$$G = n^2 A \int_0^{2\pi} \int_0^{\theta} \cos\theta \sin\theta d\Omega \tag{3.2}$$

$$G = A n^2 \sin^2\theta, \tag{3.3}$$

or

$$G = A(NA^2) \tag{3.4}$$

when

$$NA = n \sin\theta$$

Figure 3.1 illustrates the geometry of a tapered fibre. Light travels from the left and is incident on the bigger surface area with NA_{i}. The light propagates from the wider core to the narrowed part until it reaches the tapered end with the numerical aperture NA_{taper}. In this case, which is light propagating from the untapered end toward to tapered end, energy conservation applies when light propagation in both core and cladding are considered together. The light propagates along the space or material with a refractive n. NA is the numerical aperture of the optical system. Then, the energy conservation of etendue can be written as:

$$G_i = G_o \tag{3.5}$$

when $\mathrm{G_i}$ is an input etendue and $\mathrm{G_o}$ is an output etendue. Yield to

$$A_i n_i^2 \sin^2\theta_i = A_o n_o^2 \sin^2\theta_o \tag{3.6}$$

$\mathrm{A_i}$ and $\mathrm{A_o}$ are effective areas on input and output sides, respectively θ_{i} is the acceptance angle of light incident onto fibre core and θ_{o} is the angle that light can propagate outward the fibre core.

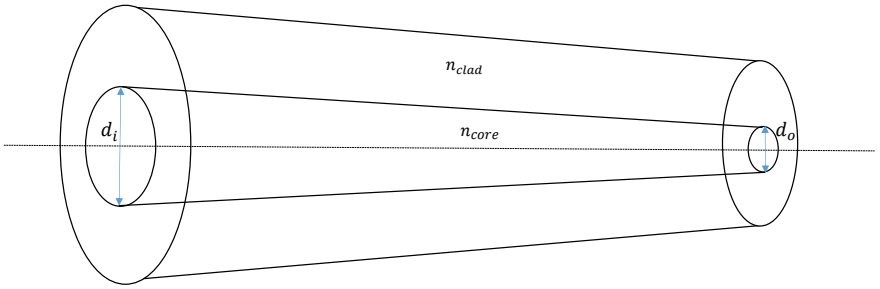

FIGURE 3.1: A diagram to illustrate a tapered fibre. This illustration shows the light is incident from the untapered end with diameter d_i toward to tapered end with diameter d_o. core and cladding refractive index are labelled as n_{core} and n_{cladd}, respectively.

If the tapering process does not change the core and the cladding indices, then NA_{i} is the manufacturer's numerical aperture. Considering the effective tapered numerical aperture when the light is injected into the untapered end, NA_{taper} can be expressed using the taper ratio R as

$$NA_{\mathrm{taper}} = R\,NA_{\mathrm{i}} = \frac{d_{\mathrm{o}}}{d_{\mathrm{i}}}\,NA_{\mathrm{i}}. \tag{3.7}$$

Where d_{i} and d_{o} are the respective untapered and tapered fibre diameters. Note that this effective numerical aperture is smaller than expected from an untapered fibre. NA_{taper} in this work defines the input beam NA that has optimal light coupling. If the light is incident on the untapered end at a numerical aperture greater than NA_{taper} it appears in the cladding at the tapered end, not in the core. An estimate of the maximum geometric optics transmission of tapered fibres can be obtained from the Etendue. For uptapered fibres the maximum transmission will be the same as an untapered fibre with the same core diameter and numerical aperture since energy is conserved and the light is emitted at a numerical aperture that is R times smaller than the input. For downtapered fibres the maximum transmission of the tapered core will be $1/R^2$ times the maximum transmission of an untapered fibre core and will have an output numerical aperture scaled from the untapered fibre based on the equation 3.7. Hence, the tapered numerical aperture of 5:1 Thorlabs step-index (originally 0.22 NA) and graded-index (originally 0.2 NA) tapers in this work are 0.044 and 0.040 respectively.

3.2.1.2 Zemax models

The non-sequential mode of Zemax version 19.8 was used to simulate a scaled-up version of the fibre optics configuration similar to the setup in the experiment. The non-sequential mode

in Zemax is used when the ray tracing order is not defined from one surface to the next surface. The ray will be traced and incident into surfaces randomly. With an approach of scaling up the fibre dimensions, waveguide mode propagation is not considered and the simulation can exclude small-scale effects such as diffraction. The non-sequential mode was chosen because multiple 'standard 3D components' are available such as the cylinder and rod which can be used to model the fibre as well as a variety of sources, and detectors. In addition, 3D objects model with Gradient material profiles is a criteria factor for fibre simulation and can be adjusted by using the non-sequential mode. Hence, the transmission of light through the fibre model with a variety of core types and sizes can be studied by the function of the Detector viewer. The composite optical model had a 0.5 mm rod with a cylinder of 0.5 mm inner radius and 1.25 mm outer radius with 1 m lengths. The refractive index of the core and cladding were chosen to imitate the 0.22 NA of step-index fibres. The graded-index simulations use a typical parabolic profile for the core refractive profile to imitate the 0.20 NA of graded-index fibre. A wavelength of 635 nm was used with 100000 rays to perform the calculations for tapered geometries. Details of the model calculations and the Zemax model files are found in Github[1]. The Zemax results of step- and graded-index 5:1 tapered fibre are shown in Figure 3.2 along with the COMSOL EM waveguide simulations considered in the next section.

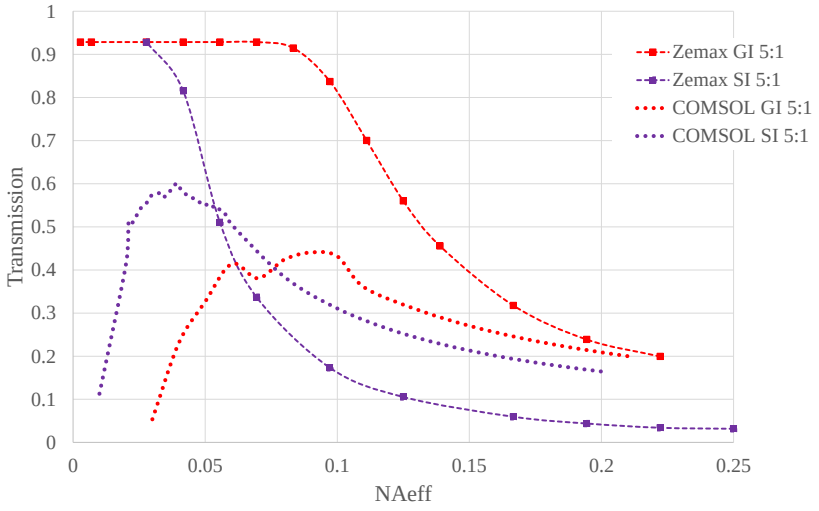

FIGURE 3.2: The Zemax and COMSOL simulations of transmission and NA_{eff} of the 50 µm step- and graded-index 5:1 tapered fibre. Both simulations agree on the drop-off transmission of step-index taper is about 0.04 NA_{eff} whereas the drop of transmission of graded-index taper is about 0.08 NA_{eff}. Zemax results show no transmission loss and reach maximum transmission of nearly 95% while the COMSOL results considered coupling loss by a taper itself and resulted in lower transmission overall compared to the Zemax results.

[1] `https://github.com/Piyamas-Ch/Tapered-and-untapered-fibre-investigation/tree/master/Zemax`

3.2.2 EM waveguide of tapered fibre

The Etendue principle applies to highly multimode optical fibre systems in general. However, some care is needed when considering optical fibre tapers with small dimensions and in particular electromagnetic wave optics modelling should be considered. The well-known V parameter ($V = \frac{2\pi}{\lambda} rNA$, where r is waveguide core radius) (Snyder et al., 1973) is used to determine number of modes propagated along the fibre by its physical geometry: core size, numerical aperture and the wavelength in free space. Geometric optics calculations will have errors of more than 5% for waveguides with $V < 20$ (Snyder and Pask, 1973), i.e., single mode or small number (<100) of modes waveguides (Snyder et al., 1973). Our work is investigating the 10 μm taper core custom grade-index, Thorlabs graded-index and Thorlabs step-index tapers with 0.10 NA_{taper}, 0.04 NA_{taper} and 0.044 NA_{taper}, respectively. Thus, V of our custom graded-index, graded-index and step-index tapered fibre is 4.9, 9.9 and 10.9, respectively, i.e., $V<20$ for our tested tapers and wave optics solutions will be required.

3.2.2.1 COMSOL models

The COMSOL 5.6 wave optics module was used to model the tapers in 3D and the results are shown in Figure 3.2. The model inputs were based on 50 μm core and 125 μm cladding diameter step and graded index profiles of NA 0.20 with a total taper length of 50 mm. The shorter length was chosen to reduce computing time and in separate calculations results in only small changes ($\sim$2%) with these long adiabatic taper lengths. A wavelength of 635 nm was used. Details of the model parameters and the COMSOL model files are found in Github[2]. The model produces input and output modal patterns and transmission for each mode with an effective index n_{i} propagating in the fibre structure where i is the mode number. The individual mode results were converted into transmission versus numerical aperture as follows:

The effective numerical aperture for an individual mode is found from the effective index n_{i} (effective refractive index of mode i) as $NA_{\text{i}} = \sqrt{n_{core}^2 - n_i^2}$ with a transmission or coupling efficiency of t_{i}. n_{core} is fibre core refractive index. The overall transmission for the fibre structure at a given numerical aperture NA is then determined by summing over all the modes that can be excited $0 \leq NA \leq NA_{\text{eff}}$. Thus

[2] `https://github.com/Piyamas-Ch/Tapered-and-untapered-fibre-investigation/tree/master/COMSOL`

$$T(NA) = \sum_{0}^{NA} t_{\mathrm{i}} * C_{\mathrm{i}}(NA) * \Delta NA_{\mathrm{i}}, \tag{3.8}$$

where $C_{\mathrm{i}}(NA)$ is a slowly varying function expressing the variation in coupling efficiency with mode number when exciting multiple modes simultaneously in measurements with a fixed optical configuration. The 3D COMSOL models are shown with $C_{\mathrm{i}}(NA)$=1, i.e. no corrections for mode coupling efficiency. In Figure 3.2 it can be seen that the consideration of wave optics makes a very significant difference with the COMSOL modelling predicting a lower and different shaped transmission as a function of numerical aperture. The details of individual mode transmission are important in low mode number regime being considered. The calculations included all modes that propagated through the taper with transmission $t > 1\%$. The summation of overall transmission is small at $NA_{\mathrm{eff}} < NA_{\mathrm{taper}}$ as a result in significant drop transmission in this range shown in Figure 3.2. The Figure also indicates that the difference between step- and graded- index should be relatively small.

3.3 Tapered fibre experimentation

Tapered fibres were characterised with the same setup used for the untapered fibre transmission test explained in Chapter 2. The characterisation work of fibres/tapers in this project has never been published by Thorlabs and the University of Bath. All tapered fibre lengths were varied from 25, 50 and 100 mm with 5:1 taper ratio. There are two main types of fibre focused on in this chapter: step-index and graded-index tapered fibres which are Thorlabs products and custom from Bath University.

3.3.1 Tapered fibre sample preparation

Table 3.1 shows all studied tapered fibres in this research including 'cut back' taper length of the additional test shown in the second part of the Table 3.1. The 'Cut back' technique is used to vary the taper ratio. This is explained in detail in section 3.3.4.3.

TABLE 3.1: Tapered fibre descriptions. The SI MM and GI MM fibres are from Thorlabs and are based on a 50 μm core with 125 μm cladding. The custom GI MM is based on tapering a custom 50 μm core graded-index fibre with 600 μm cladding. Cut back tapered fibres have the original 100 mm taper transition length. All fibres have a 50 μm core diameter and are tapered by the adiabatic heating process by the University of Bath machine and Thorlabs Vytran machine.

Type	NA†	Part number	Taper ratio	Final core (μm)
Tapered fibre				
SI MM	0.22	FG050LGA	5:1	10
GI MM	0.20	GIF50E	5:1	10
Custom GI MM	0.30	custom fibre	5:1	10
Type	NA†	Part number	Taper ratio	Final cladding (μm)
Cut back tapered fibre				
SI MM	0.22	FG050LGA	3.1:1	40
SI MM	0.22	FG050LGA	2.5:1	50
SI MM	0.22	FG050LGA	1.25:1	100
GI MM	0.20	GIF50E	3.79:1	33
GI MM	0.20	GIF50E	1.47:1	85
Custom GI MM	0.30	custom fibre	4.4:1	135
Custom GI MM	0.30	custom fibre	3:1	199
Custom GI MM	0.30	custom fibre	2.4:1	250
Custom GI MM	0.30	custom fibre	1.6:1	370

Bath University and Thorlabs machine Vytran Automated glass processing workstation (GPX3400) provided tapered fibres for this study. In principle, there is no significant difference in the performance of waveguide properties from either machine. One main difference is the limitation of the fibre holder's distance and space for the tapering process. Thus, Thorlabs machine has limitations on fabrication taper length at maximum $\sim$90 mm while Bath's machine has the ability to produce 100 mm taper length fibre.

The first samples of tapered fibres were purchased from Thorlabs and were tapered by Bath University tapering facility. Connectorised 50 μm step-index ((Thorlabs: M42L02) and 62.5 μm graded-index (M31L02/GIF625) fibre were the selected fibre for tapering. Note that the term 'connectorised' fibre is for the fibre that has FC/PC connectors and jackets on. In order to prepare a fibre for tapering, a jacket and one FC/PC end of these tapers were removed. Test tapers were 25 mm and 50 mm taper length with 5:1 taper ratio.

The next set of samples was prepared from bared fibres i.e., fibre without jackets and connectors. There is only a coating layer on the cladding of the fibre. Fibres were purchased from Thorlabs and custom graded-index fibres were provided by Bath University. For the bared fibre preparation, the fibre coat was stripped off by a fibre stripper tool (Thorlabs: FTS4). For custom GI fibre Acetone was used for coating removal because of the thickness and stiffness of the coating

layer are difficult to be removed by fibre stripper. The fibre ends were carefully cleaved by a ruby fibre scribe (Thorlabs: S90R). To check the consistency of sample preparation, the output spot shape was checked after the cleaving and cleaning with isopropyl alcohol if it is round and symmetric. With the cleaving on the different samples but the same type and size fibres, the variation of results can change up to 5% for good cleaving.

3.3.2 Cladding light in 100 mm-taper-length tapered fibre

A key element of fibre construction is to ensure that light remains in the fibre core and is not significant in the cladding. This is particularly the case for a high-resolution spectrograph where cladding light will degrade the resolution. Figure 3.3 presents a number of images chosen to represent our measurements of cladding light. The top row of 'typical' images presents the impact of cladding light of a tapered fibre taken 'face-on' (i) and in a prototype EXOhSPEC spectrograph image appearing as 'blurred' orders of tungsten light in (a1). The green 'line out' trace from (a1) is displayed in (a2) showing very significant 'wings'. These images can be contrasted with those in the row below where cladding light is relatively absent. In the left-hand example, images of the cladding light from a 5:1 Thorlabs graded-index taper fibre with no index matching gel around the cladding are presented (i) and with index matching gel (ii). Based on (i) and (ii), the Maxlm DL6[3] aperture analysis function can be used to compare the intensity of the core and cladding area. With the $0.1NA_{\text{eff}}$ input setup, the cladding light in this example (considering outer ring area in (i) and (ii)) is decreased to 1.8% from 4.3%. For the 'worse' case of a 5:1 step-index taper, there is about 9% cladding light contamination before applying the index matching gel. So, although the impact of a cladding light can be ameliorated and measured it remains a key factor to consider in the tapered fibres.

[3] `https://diffractionlimited.com/maxim-dl/`

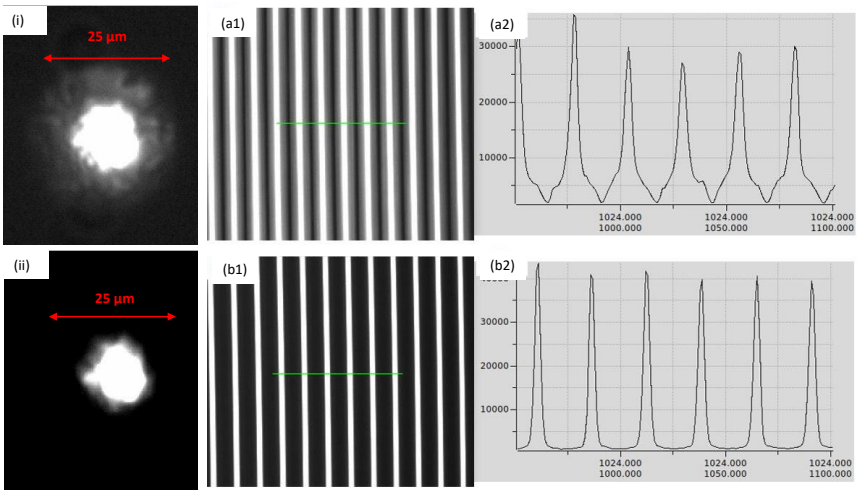

FIGURE 3.3: Visualising the impact of cladding light: Output light distribution at the end of the tapered region for a Thorlabs graded-index 5:1 tapered fibre without (i) and with (ii) index matching gel applied to the transition to suppress the cladding light. The image of cross dispersed spectral orders of Tungsten for a tapered 5:1 graded-index fibre and for an untapered 10 µm core fibre as shown in (a1) and (b1), respectively. "Line out" traces along the green lines shown in (a1) and (b1) are plotted in (a2) and (b2), respectively. In these spectra, there is the cladding light present in the tapered fibre output broadens the spectral lines, causing 'wings'.

3.3.3 Experimental error

There are two major factors that give rise to uncertainty in the experiment: (1) the influence of the physical optics and (2) the environmental conditions. In the early staged setup, measured transmission varied by approximately 5-10 per cent according to the environment change from background light and the fibre-light coupling alignment was not accurate due to the lack of fine adjustment apparatus.

For the improved setup, the measured transmission can be varied by approximately three per cent in repeat measurements on the same fibre. The initial alignment of the fibre was performed by maximising the output to the detector by varying the focus (z) and position (x,y) of the input fibre with respect to the microscope objective. This position was then fixed during the measurements and optimised when the iris diameter was changed. The NA_{eff} of the beam launched into the fibre is then changed by varying the diameter of the iris diaphragm. The numerical aperture at the maximum transmission is called NA_{max}. The setup will not give absolute maximum transmissions for core diameters smaller than 50 µm at NA_{eff} less than 0.02. Small core ($\sim$10 µm) fibres can be accurately tested at NA_{eff}¿0.05 with both 4x and 10x objectives. Also, as presented in section 3.3.2 the impact of cladding light in 100-mm-tapered-length taper will influence the measurements. In the worst case, it increases the measured transmission values by less than 5% for tapered fibres with the index matching gel.

In addition, the fibres were contained or installed in very clean and stable grips. The lab environment was temperature stable to ± 2 degrees Celsius with a filtered air supply. The setup allowed only relatively small impacts from any external mechanical factors on the fibre such as touching or bending. A standard cleaning process was used to ensure the fibres remained clean since dust on the fibre face produces fluctuating results. Reproducibility for each fibre transmission measurement is less than 5% error (systematic error). The error of each repeated measurement is mainly due to external physical movement of the fibre from touching, bending and slight misalignment. Note that the errors presented in the results of Transmission versus NA_{eff} based on the repetition of the experiments with no change of alignment of optics and a certain test fibre (or taper) was rested on the fibre holder after the maximum coupling position was adjusted. Then the power output and input were recorded 5 times in order to find the error propagation of transmission. This was also mentioned earlier in the discussion of Figure 2.18 in Chapter 2.

The error for the 'cut back' measurement is larger than our other measurements and can reach about 5% error in transmission measurement because the cleaving procedure is difficult to perform consistently. The manual cleave does not guarantee an ideal perpendicular flat end.

3.3.4 Transmission and NA_{eff} with coherent light experimental and simulation results

NA matching technique is used to investigate transmission dependent on effective NA (NA_{eff}). Results are divided into two stages, which are from early setup (Figure 2.9) and from improved setup (Figure 2.19). The early setup results used Edmund objective lenses and the improved setup used Olympus lenses.

3.3.4.1 Transmission and NA_{eff} of the connectorised step-index and graded-index taper

Firstly, the transmission of the first generation tapered fibres, which are 50 µm step-index and 62.5 µm graded-index with 5:1 tapered ratios, were investigated. These tapers have 25 mm and 50 mm tapered lengths with the same tapered ratio. The transmission test was done by an early setup with a coherent light source (635 nm). Figure 3.4 shows the results of the first generation of tapered fibre as mentioned.

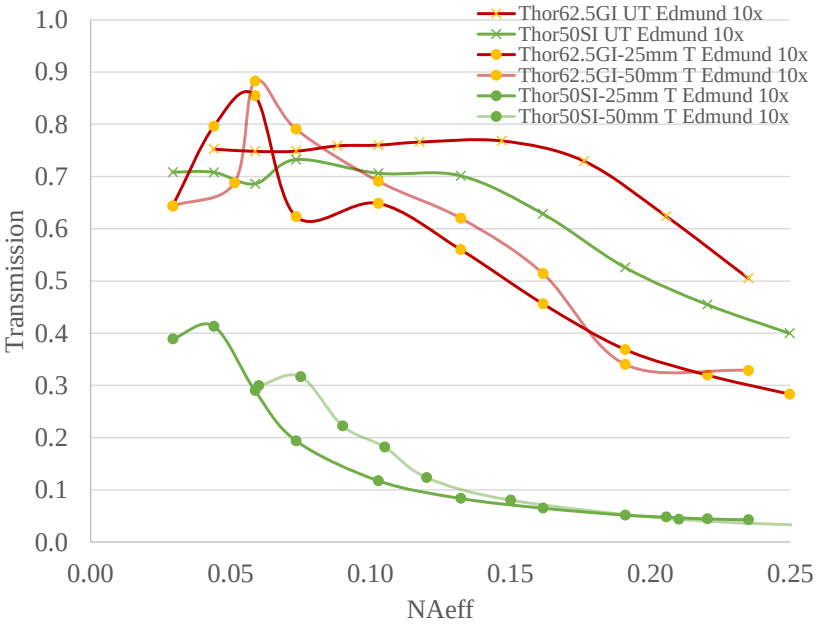

FIGURE 3.4: Transmission and NA_{eff} results of 50 µm step-index and 62.5 µm graded-index untapered (UT) and tapered (T) fibre. The early setup used 10x Edmund lens for light coupling. All tapers have 5:1 taper ratio with 25 mm or 50 mm taper length. One sigma error bars are smaller than the data symbol for results at $NA_{\text{eff}} > 0.05$.

The results suggested two important points. Firstly, the step-index tapered fibre has a significantly high loss compared to a graded-index tapered fibre. This disagreed with the simulations and our hypothesis. The adiabatic step-index taper should have overall transmission higher than 30% when the light does not exceed NA_{taper} i.e., $NA_{\text{eff}} < 0.10$ according to COMSOL results (shown in Figure 3.2). At the ideal optimal coupling, light propagation in 50 µm step-index taper should reach ∼60 %, however, the experimental results suggested otherwise. The maximum transmission of 25 mm-taper-length SI taper is about 30% and is about 40% for 50 mm-taper-length SI taper. For 62.5 µm graded-index taper, transmission can reach about 85% and 89% for 25 and 50 mm taper length tapered fibre. Note that coupling light into small NA_{eff} (<0.05) was highly uncertain. That is why GI tapered fibre light coupling has higher transmission than untapered GI results. The second point is that a shorter length taper has a better overall transmission for SI taper but it was not clear for the GI taper due to the early stage of the test apparatus has a higher %error compared to the improved setup. Moreover, the early test results have more handling errors from the observer due to the learning curve of experimentation skill development. However, the results suggested that there are undesired transmission results from step-index tapered fibre, most likely from the tapering process destroying the adiabatic shape of the taper. This was further investigated in the next section.

3.3.4.2 Transmission and NA_{eff} of the bared step-index and graded-index taper

The results of the simulations and measurements of fibre transmission related to NA_{eff} are presented in Figure 3.5. The untapered fibre measurements provide a firm basis for the more difficult tapered fibre measurements and are also useful in comparing the relative performance of the fibres with a fixed setup and consistent test methodology. Note that all values of NA_{max} are smaller than the manufacturer quoted NA† in Table 3.2 and so NA^*, which is based on 80% of maximum measured transmission of the fibre, is included. Using 80% allows us to approximately match the quoted numerical aperture of fibres from manufacturers. Since there were only two different input coupling lenses used for testing it is likely that our peak transmission numbers are not optimum for all fibres because of non-optimum mode matching. The measurements should, however, allow a fair comparison between the various fibre types. The NA_{max} are presented as maximum transmission for each tapered fibre and are shown in Table 3.2.

TABLE 3.2: The result of tapered fibre transmission dependent to NA_{eff} characterisation. All tapers are fabricated from 50µm core diameter fibre. NA† is the manufactured numerical aperture. NA_{taper} is the taper numerical aperture defined in equation 3.7. NA_{max} is the measured numerical aperture at T_{max}. T_{max} is the maximum measured transmission at NA_{max}. NA^* is the measured NA at 80% of T_{max}.

Type	NA†	NA_{taper}	NA_{max}	NA^*	T_{max}
Tapered fibre					
SI, 5:1	0.22	0.044	0.03	0.050	0.17
GI, 5:1	0.20	0.040	0.05	0.088	0.44
Custom GI, 5:1	0.30	0.060	0.05	0.096	0.66
Cut back tapered fibre					
SI, 3.13:1	0.22	0.070	0.04	0.069	0.19
SI, 2.5:1	0.22	0.088	0.03	0.077	0.35
SI, 1.25:1	0.22	0.176	0.06	0.20	0.30
GI, 3.79:1	0.20	0.07	0.07	0.16	0.79
GI, 1.47:1	0.20	0.05	0.06	0.016	0.79
Custom GI, 4.4:1	0.30	0.07	0.09	0.16	0.48
Custom GI, 3:1	0.30	0.10	0.06	0.14	0.69
Custom GI, 2.4:1	0.30	0.12	0.05	0.12	0.69
Custom GI, 1.6:1	0.30	0.18	0.06	0.18	0.72

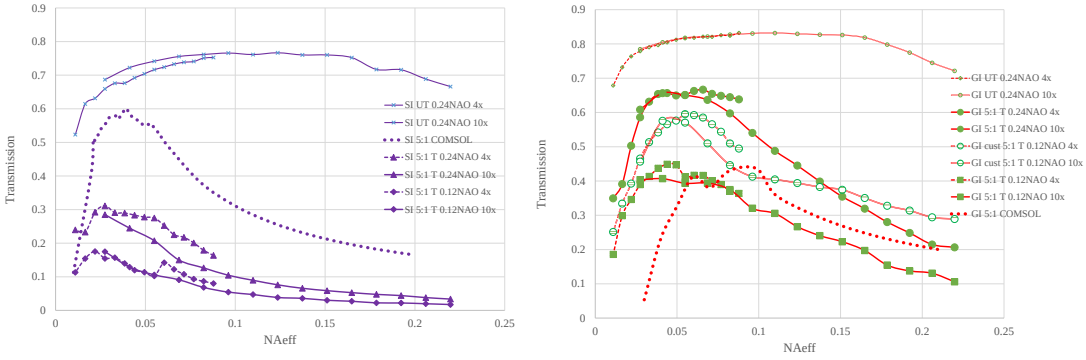

FIGURE 3.5: The transmission and NA_{eff} results of untapered and tapered fibres. Step-index and graded-index fibre results show in the left and right graphs, respectively. Both untapered fibres have 50 µm core diameter and all tapered fibres presented in both graphs are 5:1 tapers. UT and T denote untapered fibre and tapered fibre, respectively. 'GI cust' abbreviates a 5:1 custom graded-index tapered fibre. The COMSOL graded-index and step-index 5:1 taper simulation results are shown as dotted lines. 4x and 10x are the microscope objective lenses used. One sigma error bars are smaller than the data symbol.

3.3.4.3 Cut Back measurement

An additional set of measurements was performed on three 'bared' tapered fibres to look at how the transmission characteristics change with the taper ratio. The configuration of the tapers was a lead-in of untapered fibre of length 400-500 mm followed by the 100 mm taper. All samples have 50 µm core diameter and were tapered to 5:1 taper ratio. Each sample was cut back and carefully cleaved to decrease the taper ratio from the original taper ratio 5:1 to 1:1 (until all the 100 mm tapered length was cut off). For each 'cut back' the transmission is measured as well as the fibre size (and thus the new taper ratio is determined). The beam inputs for the cut back measurements were 0.10 and 0.15 NA_{eff}. The 'cut back' results are shown in Table 3.2 and the transmission of different fibres were quantified with tapers and supplemented these with 'cut back measurements' and effective numerical aperture in Figure 3.6.

The 'cut back' result reveals clearly that the tapered step-index fibre performs poorly with any taper. For example, the 5:1 tapered step-index fibre measurements revealed a peak transmission of 17% compared to 35% for the cut off 2.5:1 taper (see in Table 3.2 and Figure 3.6). The Thorlabs graded-index fibre tapers and the custom graded-index fibre taper showed high transmissions at all taper ratios.

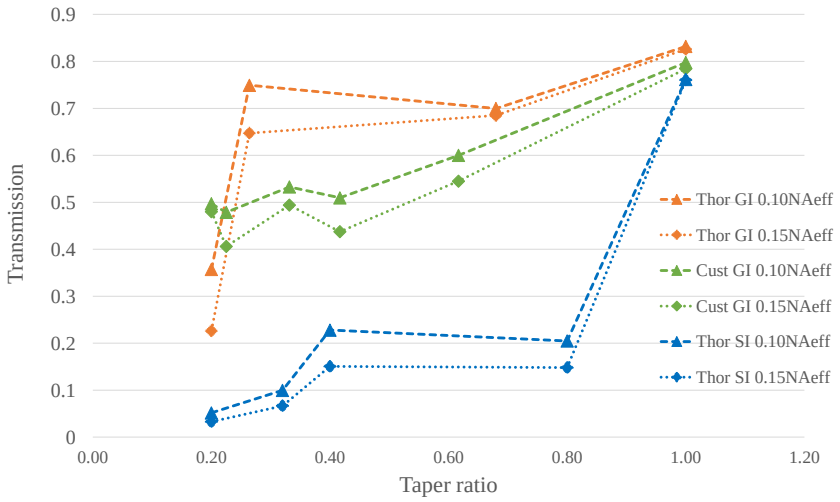

FIGURE 3.6: Transmission of the cut back tapers versus the taper ratio expressed as a fraction, e.g. 5:1 is 0.20, 1:1 is 1.0, etc. The presented result is by 0.12NAO setup. The taper ratio in this graph is the ratio between the untapered end and tapered end diameter. Cut back measurements are shown for the custom graded-index fibre, Thorlabs step-index and graded-index fibre at the $0.1NA_{\text{eff}}$ and $0.15NA_{\text{eff}}$. All tapered fibres have 50 µm untapered core diameter.

3.3.4.4 Taper length impact on transmission by COMSOL simulations and experimentation

Ideally, the tapered fibre with a longer taper length should contain the mode propagation with a small amount of loss as long as it was fabricated under adiabatic criteria. Taper length impact was studied with a ray-tracing method Arrue et al. (2008) of tapered simulations of graded-index polymer optical tapered fibre and shows the shorter taper has less loss than a longer taper but this is considered between 2 mm and 10 mm taper lengths. A similar conclusion was presented in Musa et al. (2016) as they explored the optimum profile for tapered single mode fibre. Their results claimed that if the tapers have the same tapered ratio and core diameter, longer tapered lengths (smaller taper angle) introduce less transmission loss, as well as less modes escaping to cladding. However, this statement is not always applicable because the transmission loss starts increasing again at a certain taper length as this is discovered by the COMSOL simulation.

COMSOL version 6.1 was used to model a taper ratio of 5:1 in graded-index and step-index tapers with taper lengths of 10, 25, 50, 75 and 100 mm. The COMSOL simulations and parameter descriptions can be found in Github[4]. COMSOL is well-known for EM waveguide problems. The simulation of beam input in COMSOL has a direct relationship with the number of modes

[4] `https://github.com/Piyamas-Ch/Tapered-and-untapered-fibre-investigation/tree/master/COMSOL`

selected to propagate through the waveguide, in this case, fibre optics. Each mode that propagates through fibre has an individual refractive index (n_i). The COMSOL transmission results are calculated from a summation of the power in the first 20 modes propagating in graded-index and step-index tapers with a source illumination of 635 nm. In order to imitate the experimentation of defining NA_{eff}, the number of modes launching into taper is selected to define NA_{eff}. The effective NA for an individual mode i (NA_i) can be defined as

$$NA_i = \sqrt{n_{\text{core}}^2 - n_i^2} \tag{3.9}$$

where n_{core} is the core refractive index and n_i is the effective refractive index of an individual mode i. For example, the 20th mode (i=20) for GI Thorlabs taper with n_{core}=1.4708. The calculated $n_{i=20}$ by COMSOL is 1.4699, so NA_{20}= 0.050. In other words, NA_{eff} is 0.050 by defining 20 modes for input beam with the core refractive index = 1.4708. n_{core}=1.4708 was selected based on the silica refractive index that can give NA fibre = 0.2 with the parabolic refractive index profile used in COMSOL parameters explained in Github[5]. The same n_{core} was used for step-index fibre simulation but with the step-index refractive index profile for the core and NA of fibre is 0.22. Thorlabs SI and custom GI, results of NA_{eff} of the 20th mode are 0.027 and 0.085, respectively. The reason to select 20 modes was the relative lack of importance of higher order modes and the practical consideration that each calculation time was 10 minutes per mode using a Dell PowerEdge R740 Server.

The results in Figure 3.7 show the relationship between transmission and tapered length. In both step-index and graded-index cases, the tapered fibre transmission increases with shorter taper length. In contrast, the graded-index taper has transmissions less than those of the step-index for all taper lengths modelled. Also, the trend for the GI tapers shows a generally steeper decrease in transmission than the step index tapers as the taper length increases.

Experimental results of 5:1 taper ratio graded-index and step-index Thorlabs are presented along with the COMSOL results. A red laser 635 nm was used as a source. 25, 50 and 100 mm taper lengths tapered fibres were tested. The experimental results shown in Figure 3.7 were with 0.12 NA light collection at the detector. The COMSOL results agree reasonably well with the experimental results of graded-index tapers. COMSOL predicts slightly less transmission but

[5] `https://github.com/Piyamas-Ch/Tapered-and-untapered-fibre-investigation/blob/master/COMSOL/ComsolPara.txt`

the overall trends of transmission dependence on taper length are similar. The transmission improves as taper length reduces especially from 100 mm to 50 mm and with a small improvement from 50 mm to 25 mm. The GI model results suggested that at 15 mm the transmission can improve further with an increase in transmission by a factor of 2.4 compared to the 100 mm taper length. However, the handling becomes a significant challenge for the 15 mm taper length fibre.

For the step-index tapered fibre, the COMSOL results suggest that for all lengths investigated the overall transmission should be greater than graded-index tapered fibres with comparable geometry. The experimental results, however, do not agree with the COMSOL calculations as much lower transmission than GI tapers was seen. This is consistent with previous results shown in Figure 3.2. The higher losses in the step-index tapers are probably due to the destruction of the core/cladding interface during the tapering process for these fibres. This leads to the consideration for future work that step-index which is made of different core doping materials may be able to perform successfully.

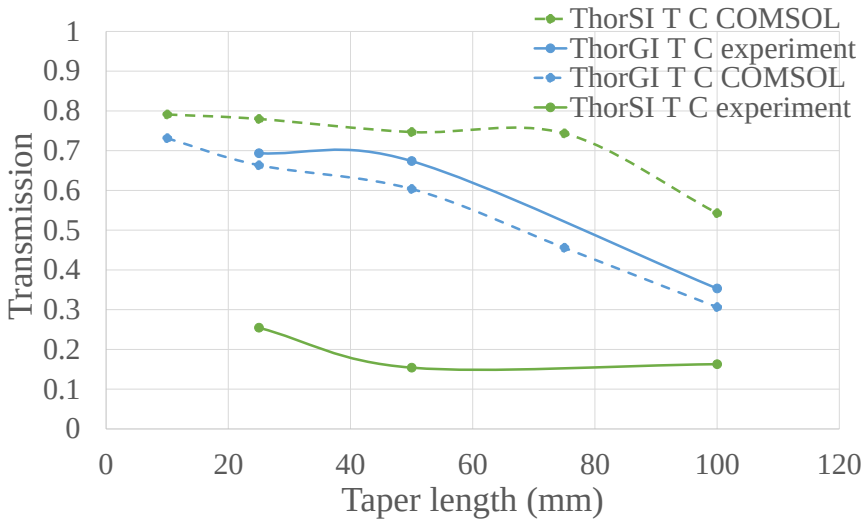

FIGURE 3.7: COMSOL and experimental results of transmission in relation to taper length. COMSOL simulations (dash lines) of 5:1 graded-index and step-index taper have 15, 25, 50, 75 and 100 mm taper lengths. The original size of the core before taper is 50 µm. Experimental results (solid lines) of tapers have 25, 50 and 100 mm taper lengths. The results are for coherent light (635 nm) illumination (denoted 'C'). NA output of experimental results was 0.12 in order to compare core light collection from COMSOL simulations. Experimental errors are contained within the plotting symbol.

3.4 Summary

Transmission properties of tapered fibres with coherent light source illumination were investigated by the relationship between transmission and NA_{eff} by both simulations and experimentation. Main interest tapered fibres investigated in this chapter are 50 μm core fibres and tapers from 50 μm to 10 μm i.e., 5:1 tapered ratio. The comparison of fibre types that are tapered are step-index and graded-index type is the main interest in this chapter. The samples were Thorlabs step-index and graded-index and also custom GI fibre including some other tapered fibre such as 62.5 μm GI Thorlabs fibre. Also, the concept of tapered fibre considering both geometrical optics and EM was investigated by using two different software Zemax and COMSOL. Simulations by Zemax were considered for the geometrical optics and COMSOL for EM waveguide.

While Zemax calculations are not accurate because of geometrical optics scale was considered, COMSOL calculations, which considered EM waveguide show more accurate results of transmission dependence on effective NA. Experiments and COMSOL simulations show agreement on the graded-index tapered fibre for our interest taper ratio 5:1 of 50 μm core diameter fibre. However, the transmission in step-index taper COMSOL simulations is very high. This contradicts experimental results that overall loss in step-index tapered fibre was higher than graded-index tapered fibre.

For the experimental results, a variety of fibres and tapers were measured for transmission with a numerical aperture matching technique. Graded-index tapers show a more consistent and higher transmission versus numerical aperture than do equivalent step-index tapered fibres. The Thorlabs graded-index tapers and custom graded-index tapers give transmissions of over 40% and 60% into a numerical aperture $<$0.10 for 0.12NAO, respectively.

Based on the COMSOL simulations, the 5:1 step-index tapered fibre should have transmission greater than 50% for the 0.05 NA_{eff} or at the drop-off numerical aperture. The simulations and the Cut Back measurements suggest that our step-index tapers are undergoing some deterioration in the tapering process which is disturbing the core/cladding boundary at high taper ratios. In addition, the results of taper length impact on the transmission both simulations and experimentation suggested that the shortest taper length, in this case, 15 mm for COMSOL simulation, is the optimal length for transmission property.

Chapter 4

Incoherent light and the optical untapered and tapered fibre transmission property

4.1 Introduction

This chapter follows the experimental results of the untapered and tapered fibre with coherent light from Chapter 2 and Chapter 3. Transmission dependence on NA_{eff} is a main focus on the tapered fibre performance. The optimal setup for the incoherent light coupling to fibre optics was explored with a variety of paired objective lenses in section 4.2.1 by the test of untapered and tapered fibre transmission. The coherent light transmission test was modified in this chapter but the setup is still similar to the previous one in Chapter 2 and there is an additional imaging setup to investigate mode pattern impact on transmission by misalignment. Section 4.2.2 focuses on the transmission test of GI tapered fibre both Thorlabs 50 μm and custom fibre. An addition cladding light investigations by using index matching gel are presented in section 4.2.3. This work investigated more variety of taper lengths: 15, 25, 50, 75 and 100 mm. Only 25, 50 and 100 mm tapers were used in experimentation as the results confirmed the shorter taper length tapered fibre has more cladding light than the longer taper length.

After that, modal noise impact on transmission properties was investigated in untapered and tapered fibre in section 4.3. The setup of the modal noise test is explained in section 4.3.1. Modal noise was measured by: 1. output power change affected by input beam misalignment

(see section 4.3.2.1) 2. transmission drop from macro-bending (see in section 4.3.2.2) and 3. percentage of power change from micro-bending (also see in section 4.3.2.2). Moreover, the throughput concept in this research is presented in section 4.4. Throughput tests were especially used to quantify light transmitted from the source fed to 50 μm GI untapered fibre to the end of the test fibre. The throughput was measured by the 'butt coupling' method and the incoherent light transmission test setup method was applied in order to explore the most optimal way to gather the light from the source to the test fibre as well as the spectrograph. Results were presented for each fibre both untapered and tapered and suggested that 'butt coupling' is the most optimal method for light gathering from light illumination from 50 μm GI untapered fibre.

4.2 Incoherent light transmission test

Coherent light transmission results (Choochalerm et al., 2021) (and in Chapter 3) indicate that graded-index tapered fibre is an effective candidate for transferring light into a spectrograph instead of using more complicated fabrication processes for example Photonic Lanterns (Birks et al., 2015; Kryukov, 2018) or multicore fibre (Kerttula et al., 2012). A new setup was designed in order to investigate incoherent light illumination on fibre. Transmission dependence on NA_{eff} is the main focus for fibre characterisation. Also, an investigation further of how cladding light varied with taper length is presented in this chapter.

4.2.1 Incoherent source coupling setup

In general, the difficulty of coupling incoherent light spatially into a fibre arises because the radiance of the source cannot be changed according to the laws of thermodynamics (Hudson, 1974; McMahon, 1975; Stokes, 1994). In contrast, light coupling into fibre is relatively easy with the coherent light sources as used successfully in the previous chapter 3. Only a single objective lens was used as the focuser for the 635 nm light source coupling. The focal length and NA of this lens determine the coupling. More optics are required in order to couple light optimally into the fibre core with incoherent light.

Firstly, the setup with applying different pairs of different objectives: 4x and 4x, 4x and 10x and 10x and 10x was investigated. The objective is to find the most optimum setup that allows optimal transmission readout for a test fibre. The results show that applying the 4x for the beam

collimation and 10x objectives as the focuser is the best pairing for our transmission measurement. Note that the fibre feeding from a lamp has 0.20 NA and the 4x objectives has 0.10 NA, there will be an inevitable light loss from the unmatched NA or effective area portion from the fibre-fed source to the 4x microscope objectives. However, proportioning the beam size down from 0.20 NA fibre to 0.10 NA with the first collimation objectives (0.1 NA, 4x) means relatively collimated light from the objectives will be spread less per distance compared to using bigger aperture objectives such as 0.25 NA, 10x). The main sample fibres that were tested including 5:1 tapered fibres have relatively small to medium size core diameters (<50 µm) and NA (<0.22NA). This is the reason that incoherent beam light will couple to test fibres best with the original smaller NA. Figure 4.1. Test fibres were 50 µm graded-index untapered fibre, custom 5:1 graded-index tapered fibre, 10 µm step-index fibre and endlessly single mode fibre. The output beam was collected at 0.24NAO. Figure 4.1 clearly shows that transmission measurement setup with the pairing of 4x and 10x objectives is best for the fibre that has numerical aperture from 0.1 to 0.2.

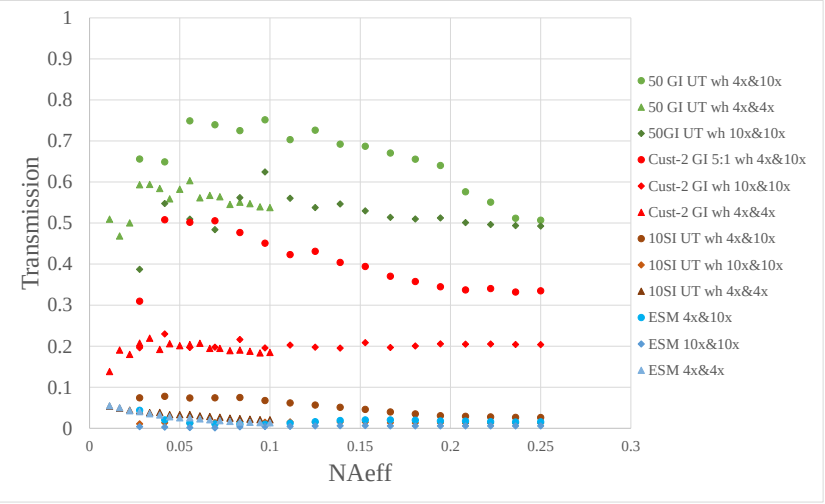

FIGURE 4.1: Example transmission versus NA_{eff} results from different pair of microscope objective lens: 4x and 4x, 10x and 10x and 4x and 10x illuminating with incoherent light. Selected test fibre are 50 µm GI untapered fibre, 100mm-taper length custom GI tapered fibre, 10 µm SI untapered fibre and endlessly single mode fibre.

Finally, the test setup for characterising the incoherent light transmission in tapers is presented (illustrated in Figure 4.2). A High-Intensity Fibre-Coupled Light sourced (Thorlabs: OSL2) was used to couple light directly to a 50 µm graded-index multimode fibre (Thorlabs: GIF50E). Tungsten Halogen lamp emits across the wavelength range of 400-1600 nm with typical coherence properties of these sources. Two microscope objective lenses (4x and 10x) were used as the collimator and focuser for the incoherent light coupling into the test fibre. An iris diaphragm

was placed between the two objectives to vary the collimated beam size and therefore the numerical aperture. The effective numerical aperture (NA_{eff}) of this optical system is calculated using the equation 2.1. Input power was measured after the second objective (position P1). The output power was measured at the exit point of the test fibre (position P2) at fixed distances of either 20 mm or 40 mm. The diameter of the detector's active aperture is 9.5 mm. Therefore when the output power at P2 is measured at a distance of 20 mm from the test fibre, this results in an output beam numerical aperture of 0.24 (denoted '0.24NAO'). When the output power at P2 is measured at a distance of 40 mm, this gives an output beam numerical aperture of 0.12 ('denoted 0.12NAO').

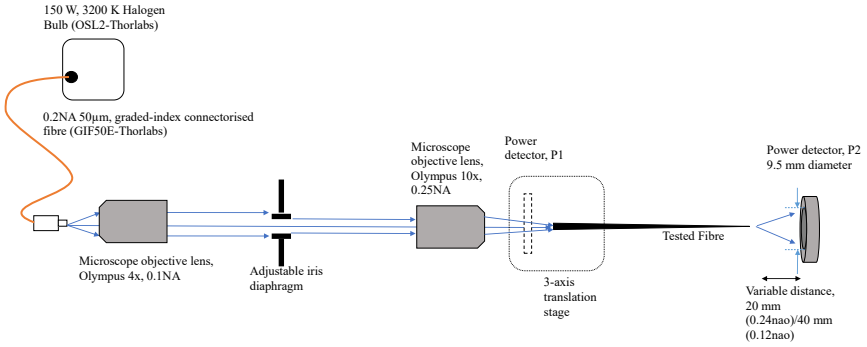

FIGURE 4.2: The setup for incoherent light measurements of fibre transmission dependence on effective numerical aperture. The light source is coupled directly to 50 µm graded-index fibre with 0.2NA. The first objective lens (4x, 0.1NA) is used to collimate the light. The waist of collimated light can be varied by an adjustable iris diaphragm that is located before the second objective (10x, 0.25NA). The NA_{eff} of beam is defined by the second lens (10x, 0,25NA) and transmission is a ratio of power measured at P2 and P1.

In this section, transmission tests comparison between with coherent and incoherent light is presented. This is for proving if the setup is valid. The coherent light setup is shown in Figure 4.3. A 635 nm red laser source was used. The light beam was magnified 3.3x by a pair of achromatic (AC) doublet lenses with focal lengths 100 mm and 30 mm. The beam NA_{eff} can be changed with an adjustable iris diaphragm and was focused into the tapered test fibre input end by an Olympus microscope objective of 10x. Power input of the coherent light setup is located after the 10x objective lens. By changing optics after test fibre position, this setup can be modified for two purposes: (a) transmission related to NA_{eff} test, which is discussed in this section, and (b) near-field image taking, which is used for the misalignment impact test discussed in section 4.3. In (a), light is collected from the fibre end using a 9.5 mm-diameter detector. This was placed at two different distances to vary the collection NA when at 20 mm the NA was 0.24 (denoted

‘0.24NAO) and when at 40 mm the NA was 0.12 (denoted ‘0.12NAO). In (b), the near-field image of fibre output is taken by a combination of collimator: 10x objectives, focuser: AC doublet lens with 200 mm focal length, and ZWO ASI178MM CMOS camera.

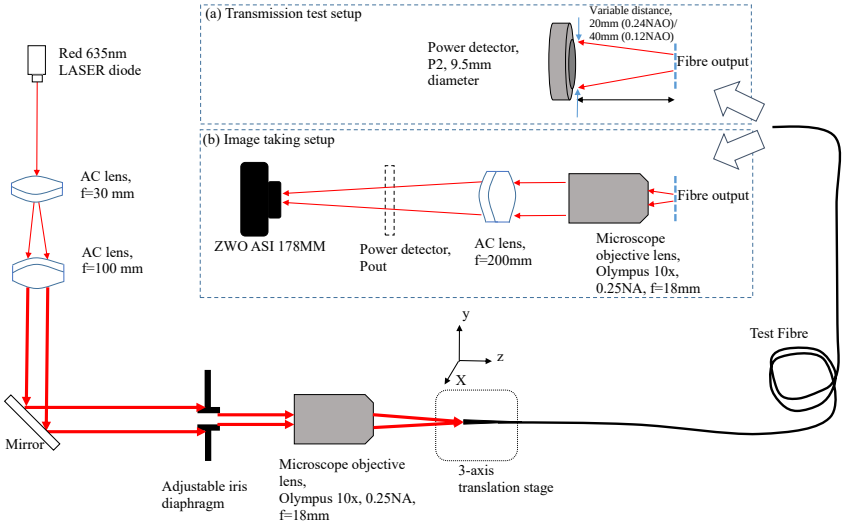

FIGURE 4.3: A drawing of a coherent light fibre coupling setup for (a) transmission dependence on NA_{eff} test and (b) near-field image taking for the misalignment impact test. The 3.3x magnified collimated beam from a pair of AC doublet lenses (30 and 100 mm focal length) is focused into the test taper with a 10x Olympus objective lens. An adjustable iris diaphragm varies the input beam numerical aperture (NA_{eff}). The input end of the fibre is mounted onto a 3-axis translation stage.

A setup in (a) was used to test both untapered and tapered fibre with the same dimensions, 50 µm core diameter for untapered fibre and tapers with 5:1 taper ratio and 25 mm down taper length. The NA of tapered fibre (NA_{taper}) can be defined as in the equation 3.7. Thus, NA_{taper} of Thorlabs SI, Thorlabs GI and custom GI tapered fibre are 0.044, 0.040 and 0.060, respectively. The transmission of light through an untapered fibre is expected to start to decrease when the NA of the input light, in this case, NA_{eff} is greater than the NA of the fibre. Similarly, taking a geometric optics approach, for light entering a step-index fibre that has been tapered, it is expected that the transmission will start to fall if NA_{eff} (the NA of the input light) exceeds NA_{taper}. This trend was indeed seen in COMSOL models in Figure 3.2.

Figure 4.4 extends the results obtained previously and presents results of transmission dependence on NA_{eff} for both coherent light (635 nm red laser diode, denoted ‘C’) and incoherent light (denoted ‘IC’) for a Thorlabs GI taper. For untapered fibre, the trend is relatively flat due to the manufactured NA being relatively large ($NA^{\dagger}$=0.2) for both coherent and incoherent light illumination. When the input beam exceeds the manufactured NA (beyond 0.2 NA_{eff}) a gradual reduction in transmission is seen as expected. When the same GI fibre is tapered, and

the fibre diameter and core gradually decrease, there is a slow decrease in transmission after $\sim 0.1 NA_{\text{eff}}$, which is larger than $NA_{\text{taper}} = 0.04$. This is because the graded-index fibre has a parabolic rather than step refractive index core profile and so has less intermodal dispersion and a smaller number of modes compared to a step-index fibre with similar attributes such as core radius and NA (Olshansky, 1976; Hecht, 2017). Hence, when GI fibre is tapered, the drop of transmission is seen at $NA_{\text{eff}} > NA_{\text{taper}}$. This was also seen in COMSOL simulations which used EM waveguide calculations that are presented in 3.2.2.1. In addition, the overall transmission of incoherent light for both untapered and tapered fibre is less than the coherent light results. This is due to the smaller coupling efficiency of incoherent light into the fibre. Note that the small experimental errors in this Figure are defined from the results of the power input that were recorded repeatedly 5 times with no change of the alignment of the setup and the fibre sample was rested at the fibre holder after the alignment was done. This was explained in section 3.3.3.

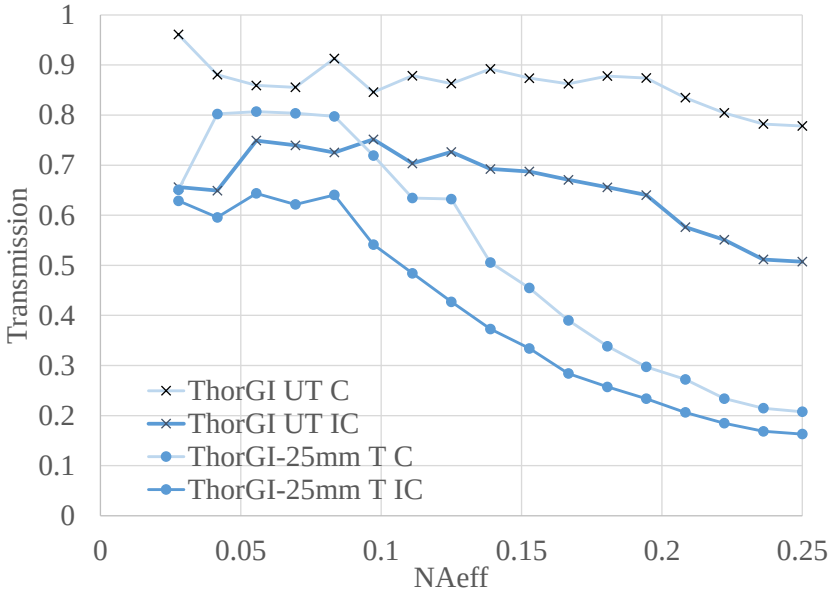

FIGURE 4.4: Comparison of transmission related to effective numerical aperture results with coherent (C) and incoherent (IC) light. Test fibres are 50 µm Thorlabs GI untapered (UT) and 5:1 taper (T) from 50 µm Thorlabs GI fibre. Results with coherent light are in light blue thin lines and with incoherent light are in solid blue thick lines. Crosses are used to denote untapered experimental values. Filled circles are used to denote tapered experimental values. All results were collected with 0.24NAO. Experimental errors are contained within the plotting symbol.

4.2.2 Experimental results of transmission dependence on NA_{eff} in optical tapered fibre with incoherent light

This section discusses the experimental results of incoherent light transmission tests of tapered and untapered SI and GI fibre. Table 4.1 shows all test fibres in this Chapter. 100 mm length tapers were fabricated by the University of Bath's adiabatic taper machine and others were fabricated using a Thorlabs Vytran Automated glass processing workstation (GPX3400). There are additional special tapers: Mode Field Adapters (MFA[1]) and Spliced Taper (SP) customised by Thorlabs. SP fibre was customised from 10 μm SI spliced to Thorlabs GI taper (specification explanation shown in section 5.4). Figure 4.5 shows transmission results using incoherent light illumination of graded- and step-index tapered fibres including 10 μm step-index, 50 μm graded-index and custom graded-index untapered (UT) fibre. The light is collected at 0.24NA. There were two different GI tapers tested: a custom fibre from Bath University (denoted 'CustGI') and Thorlabs product GIF50E (denoted 'ThorGI'). The original NA and cladding sizes of the Bath custom GI and the Thorlabs GI fibre is 0.30NA/ 600 μm, and 0.20NA/125 μm, respectively. The step-index tapered fibre tested is a Thorlabs FG050LGA product (denoted 'ThorSI'). The untapered length of these test tapers was relatively short (from 50 to 150 mm). Results are shown here for 25, 50 and 100 mm tapered (length) fibre. Error propagation of transmission in experimentation in each NA_{eff} was very small ($<0.01\%$). Thus error bars are insignificant compared to the trends seen in the data and so are omitted from the graph. Note that with reproducibility, i.e., repeat the same measurement from the beginning, the error can be up to 5-10%.

The experimental results are shown in Figure 4.5. There is a find that for both the custom GI fibre and also Thorlabs GI fibre the shorter taper lengths allow more light transmission through the fibre. These results indicate that shorter taper lengths allow more transmitted light. This also agrees with the COMSOL simulations of tapered fibres shown in Figure 3.7 even though the models only simulated for coherent light illumination. For a custom GI with NA_{eff}=NA_{taper}=0.06 the transmission of the 25 mm taper is roughly 15% more than the transmission for the 100 mm taper. The Thorlabs GI fibres also show increased transmission at NA_{eff}=NA_{taper}=0.04. Transmission in the 25 mm length taper is 30% more than the 100 mm length taper. Over the full range of NA the transmission of the 25 mm taper is higher than that of the 100 mm taper in the range 10-40% for Thor GI tapers and 12-30% for custom GI tapers. A fibre-fed high-resolution

[1] `https://www.thorlabs.com/newgrouppage9.cfm?objectgroup_id=12063`

spectrograph EXOhSPEC (Jones et al., 2021) is under development and it has 0.16NA acceptance. Therefore if the transmission at $NA_{\text{eff}} = 0.1$ is compared, for the custom GI 25 mm taper it is about 75% and for the Thorlabs GI it is 55%.

TABLE 4.1: The list of test fibre in this work. NA† states for a manufacturer numerical aperture. MFA is Mode Field Adapters fibre and SP is spliced taper customised by Thorlabs. Taper length, ratio and final core are physical dimensions specified from Thorlabs and Bath machine.

Type	NA†	Part number	Taper ratio	Taper length (mm)	Final core (µm)
Untapered fibre					
SI MM	0.10	FG010LDA	-	-	10
SI MM	0.22	FG050LGA	-	-	50
GI MM	0.20	GIF50E	-	-	50
Cust GI MM	0.30	custom fibre	-	-	50
Tapered fibre					
SI MM	0.22	FG050LGA	5:1	25	10
SI MM	0.22	FG050LGA	5:1	50	10
SI MM	0.22	FG050LGA	5:1	100	10
GI MM	0.20	GIF50E	5:1	25	10
GI MM	0.20	GIF50E	5:1	50	10
GI MM	0.20	GIF50E	5:1	100	10
Cust GI MM	0.30	custom fibre	5:1	25	10
Cust GI MM	0.30	custom fibre	5:1	50	10
Cust GI MM	0.30	custom fibre	5:1	100	10
MFA	0.08 & 0.11	MFA4A	proprietary	proprietary	10
SP	0.20	spliced taper	5:1	25	10

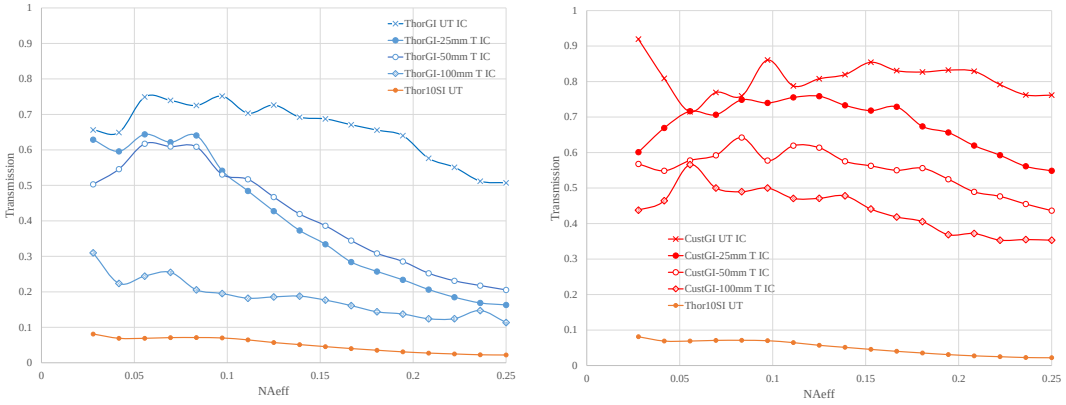

FIGURE 4.5: Transmission versus NA_{eff} results by incoherent light (IC) source illumination. Comparison results between (left) Thorlabs GI taper ('ThorGI-') and (right) Custom GI taper (CustGI-) in 25 mm, 50 mm and 100 mm taper length are presented including 10 µm step-index (Thor10SI UT), 50 µm graded-index (ThorGI UT) and custom GI (CustGI UT) untapered fibre. All results have the light collection at a detector at 0.24NA. Experimental errors are contained within the plotting symbol.

The trends of the transmission of custom GI tapers are flatter than Thorlabs GI taper and gradually drop as NA_{eff} increases over the range investigated. There is some trend rises in transmission when NA_{eff} increases for instance at $NA_{\text{eff}} \sim 0.06$. This is due to poor coupling when $NA_{\text{eff}} \leqslant$

0.05 as explained in Chapter 2 section 2.3.3. The spot size of input beam at each NA_{eff} was calculated (also in Github[2]) and shows that the spot size will be larger than 10 µm when $NA_{\text{eff}} \leqslant 0.05$. Results of spot size are shown in Figure 4.6. In other words, coupling beam efficiency can significantly reduce at $NA_{\text{eff}} \leqslant 0.05$ as the taper core diameter is smaller than the spot size. The Thorlabs taper transmission trends drop more sharply as NA_{eff} increases compared to custom GI fibre. This is due to the original NA of the custom GI fibre (0.3 NA) being larger than Thorlabs GI taper (0.2 NA). It was observed by eye that the cladding light increased in custom GI fibre as the taper length got shorter. Thorlabs tapers however had slightly less light in the cladding. This motivated the investigation of whether the flatter curve in the custom GI taper was due to cladding rather than core light increasing the transmission. This investigation is discussed in section 4.2.3.

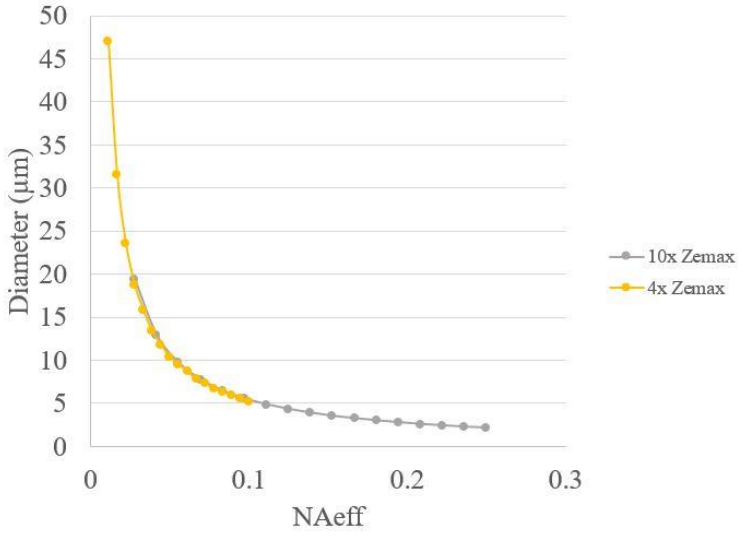

FIGURE 4.6: Calculation results of spot sizes versus the NA_{eff} by the coherent light transmission test setup. This graph includes the calculations of using 4x and 10x microscope objective lens from Zemax software (denoted '10x Zemax' and '4x Zemax', respectively).

4.2.3 Cladding light in short tapered lengths

In section 3.3.2 in chapter 3, results show that the cladding light in 100 mm 5:1 graded-index taper fibre is not significant. Now that light can be seen leaking into the cladding with shorter taper lengths of 25 mm and 50 mm, this needs to be reconsidered. The 100 mm taper length

[2]https://github.com/Piyamas-Ch/Tapered-and-untapered-fibre-investigation/blob/master/Zemax/Gaussian-spot_calculations.JPG

should now be considered as relatively long. Also, the measurement of cladding light in section 3.3.2 was for only at a single NA_{eff} ($0.10\,NA_{\text{eff}}$) and these conditions would have excluded cladding light to some degree. Therefore investigation of cladding light was extended to include shorter tapers at various NA_{eff}, measuring the output light at 0.12 and 0.24NA.

The effect of cladding light was measured on taper output by comparing transmission both with and without the use of an index matching gel. The results for outputs of 0.12NAO and 0.24NAO are shown in Figure 4.7. Thorlabs GI and Custom GI tapers with 25 mm taper length and 5:1 taper ratio were test fibre. The original core diameter for both is 50 µm. The manufacturer's NA of the Thorlabs GI and custom fibre are 0.20 and 0.30, respectively. The gel was applied to the fibre taper but left the tip of taper gel free ($\sim$1 mm) in order to not contaminate the output surface. The index matching gel has a higher refractive index than the cladding. This means the gel diverts any light that leaks into the cladding out of the taper, so it will not be measured at the taper output. The results shown in Figure 4.7 indicate higher transmission in the custom GI taper compared to the Thorlabs GI fibre. It is clear that cladding light increases transmission through the taper at both 0.12NAO and 0.24NAO. For custom GI taper, the larger NA_{eff} contributed more light leaked into the cladding. For the Thorlabs GI taper results with and without gel show less transmission difference as NA_{eff} increases. The graphs with/without gel follow the same general trend as NA_{eff} increases. The results show that cladding light can increase the transmission through the taper in the range of 15-30% as NA_{eff} varies. However, the custom GI fibre also generally has more cladding light than the Thorlabs fibre, especially as NA_{eff} increases.

Cladding light can raise the measured transmission according to the increase of NA_{eff}. For the Custom GI taper, consider at 0.24NAO, the measured transmission rose in a range of a factor of 1.3-2.7 for the whole range of test NA_{eff} from 0.03-0.25. There is an increase in a factor of 1.3-1.4 for $NA_{\text{eff}} < NA_{taper}$ (0.06) and can achieve to a factor of 1.7-2.7 at 0.07-0.25NA_{eff}. Considering a similar way for 0.12NAO of custom GI taper results, the rise of transmission is 1.5-2.9 for 0.03-0.25NA_{eff}. Factor of 1.4-1.7 for $NA_{\text{eff}} < NA_{taper}$ (0.06) and 1.9-2.9 for 0.07-0.25NA_{eff}.

For Thorlabs GI taper, cladding light can raise the measured transmission in a range of factors of 1.6-2.4 for 0.24NAO and 1.8-3.0 for 0.12NAO. Considering 0.24NAO results, transmission increasing in a factor of 1.6-1.7 for $NA_{\text{eff}} < NA_{taper}$ (0.04) and 1.9-2.4 for 0.05-0.25 NA_{eff}. Considering 0.12NAO results, transmission increasing in a factor of 1.8-2.2 for $NA_{\text{eff}} < NA_{taper}$ (0.04) and 2.4-3.0 for 0.05-0.25 NA_{eff}.

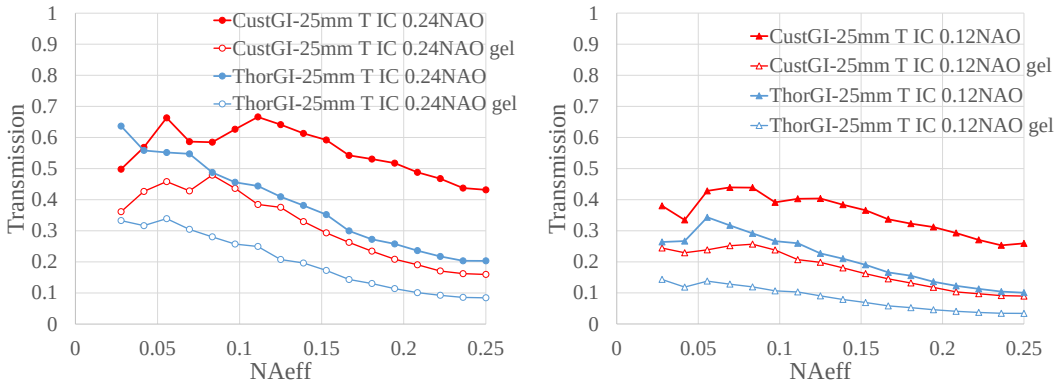

FIGURE 4.7: Investigation of cladding light by difference transmission versus NA_{eff} with an incoherent light source illumination. Comparison results between Custom GI (CustGI) and Thorlabs GI (ThorGI) taper with 25 mm taper length are presented. 0.24NAO results are presented in the left graph with circle marks. 0.12NAO results are presented in the right graph with triangle marks. Open circles ("o") and open triangles ("△") with thin lines are used to distinguish experimental values obtained using gel for 0.24NAO and 0.12NAO, respectively. Experimental errors are contained within the plotting symbol.

4.3 Modal noise in optical fibre

Mode patterns present at the output plane of a multimode waveguide can fluctuate giving rise to instability (Rawson et al., 1980; Tremblay et al., 1981; Mickelson and Weierholt, 1983) as a modal noise in optical signals which impact optical systems using fibre optics. Modal noise is time dependence and usually can be found in a multimode fibre. The mode interference as a result of the degraded signal as Signal to Noise Ratio (S/R) is decreased. Another concern of transferred signal quality degradation via fibre optics, the Focal Ratio Degradation (FRD) is one of the most well-known phenomena studied. Consider particularly on the fibre-fed spectrograph, when using fibre as the link, the light f-number is degraded from the input beam f-number effects on the Signal to Noise Ratio (S/R) and can reduce spectrograph resolution (Ramsey, 1988; Avila, 1988, 1998). This can be induced by mechanical changes such as bending, movement, stress or change in temperature of the fibre (Tremblay et al., 1981; Mickelson and Weierholt, 1983; Oliva, E. et al., 2019). Another main cause is non-ideal illumination such as misaligned coupling between input beam to fibre or between two fibres (Matsuura et al., 2014) or the fibre output mismatched with a detector (Mickelson and Weierholt, 1983).

In this work, the modal noise is defined by the impact of bending and light illumination. As there is a correlation between modal noise and FRD. The modal noise investigation in this work is divided into two parts. First, the impact of the input source illumination was tested on the tapered fibre output. This was done by misaligning the coupling of the coherent light source

into the taper and observing the effect this had on the mode patterns travelling through the taper as well as how the transmission power varied. Second, the effect of bending the tapered fibre was measured with both incoherent and coherent sources.

4.3.1 Modal noise test setup

In Figure 4.3 dashed box (b) the setup designed for near-field imaging of the tapered fibre output end with coherent light is shown. The 635 nm laser coupling system is the same as used for the transmission dependence on NA_{eff} experiments described in section 4.2.1. A 10x objective lens and AC doublet with a focal length 200 mm were used to collect the near-field images onto a ZWO ASI178MM camera. In this arrangement, the power output is also measured at the position after the AC lens before the camera. Power input is measured before the fibre input (after the first 10x objectives lens). For the modal noise test with incoherent light the setup as shown in Figure 4.2 was used, and this was used for the transmission tests described in section 4.2.1 but added fibre holders and posts with a translation stage for the fibre bending test.

4.3.2 Modal noise experimental results

4.3.2.1 Source illumination impact on transmission

The mode patterns changed accordingly to the power output was studied including the mode patterns dependence on a misalignment of the illumination by the coherent (635 nm red laser diode) source. The test fibre was a 25 mm-taper-length Thorlabs GI tapered fibre. Figure 4.8 shows the relationship between power output and input beam misalignment position (X-offset). The image magnification is x11 resulting from the pair of 10x objectives and the 200 mm focal length AC doublet. The beam launched into the fibre was misaligned in the lateral plane (x-axis). Each image shows the mode pattern at the taper output for each beam input position. At an X-offset = 0 μm there is the optimal coupling with the highest output power and smallest number of modes. At this position there is a very bright spot in the middle as the light propagates mostly in the centre of the core of taper. As the X-offset is increased or decreased, the mode pattern appears as a combination of bright spots and light distributed into other weaker spots. This corresponds to progressively higher order modes being able to propagate along the fibre which also reduces the overall transmission. The results clearly show the effect that beam alignment has on the amount of modal noise and hence transmission through the taper.

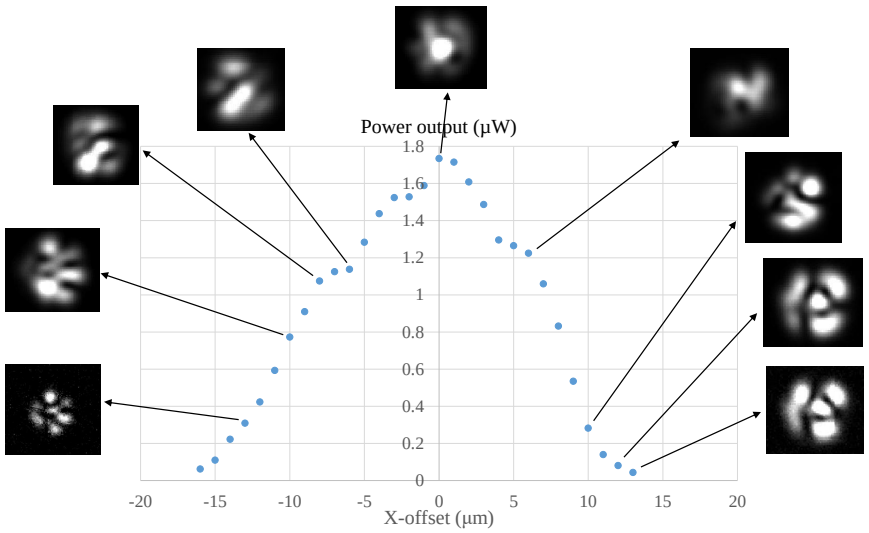

FIGURE 4.8: Results of power output variation as the position of beam input at the fibre input end (X-offset). The test fibre is a 25 mm Thorlabs graded-index 5:1 tapered fibre. Near-field images of taper mode pattern taken by ZWO178MM CMOS.

Proper beam launch condition can optimise coupling efficiency. Results are categorised by the beam input as under-filled, filled and overfilled in Table 4.2. There is an additional test on the misalignment test on 10 µm step-index untapered, 50 µm GI untapered, Thorlabs GI tapered, and custom GI tapered fibre. Three launching conditions were selected for each fibre; under-filled, filled and over-filled.

TABLE 4.2: Description of beam launch conditions for light coupling into fibre classified by a relationship of launched beam NA and NA of fibre. $NA^{\dagger}$ is manufacturer NA and NA_{taper} is taper NA as define by equation 3.7.

	Beam Input		
	under-fill	fill	over-fill
untapered fibres	$<95\%NA^{\dagger}$	95-100%$NA^{\dagger}$	$>100\%NA^{\dagger}$
tapered fibres	$<95\%NA_{\text{taper}}$	95-100%NA^{taper}	$>100\%NA^{\text{taper}}$

Figure 4.9 shows results of transmission related to the decentre distance of the mentioned fibres. With different beam launch conditions, the shape of profiles is different and the transmission reaches at higher value can be found with under-filled or filled condition. The shape of the beam appeared to be sharper and reaches optimal coupling when the beam is in filled condition. Then the transmission drops and the beam shape is broader with the over-filled condition.

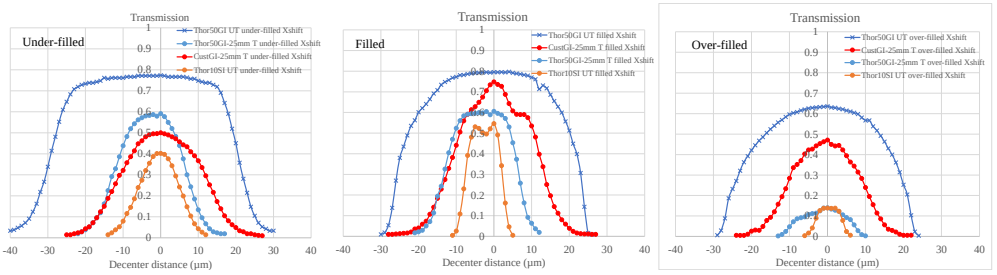

FIGURE 4.9: Results of misalignment impact on transmission of untapered and tapered fibre. Test fibres are 10 μm SI untaper, 50 μm GI untaper, Thorlabs 50 μm GI taper and custom GI taper. There were three launched conditions presented for each test fibre: under-filled, filled and over-filled.

4.3.2.2 Fibre bending impact on transmission

Another factor that can cause signal distortion is mechanical displacement such as bending. The effect of bending on tapered fibre transmission was measured using two different methods, a single bend radius and multiple micro bends. In the single bend experiments the tapered fibre was prepared differently. Test samples have a 25 mm down taper, a 20 mm waist, and a 25 mm up taper. This is different to the transmission versus NA_{eff} tests described in the previous section where only a downtaper with ∼10 mm waist was tested. For the single bend radius experiment the untapered input fibre is held firmly in two secured fibre rigs and a small post attached to a translation stage is lightly touched to the untapered fibre. The post (Thorlabs:PM4) was then moved with a micrometer (Thorlabs: PT1/M) in the lateral plane to bend the fibre (illustrated in Figure 4.10). Power output was measured at each 0.5 mm lateral move. The whole range of translation was from 0 to 5 mm (0°-14.3°), which is the minimum fibre bend radius which limits transmission. Transmission starts significant drops more than 50% from maximum at around 10°for $0.25NA_{\text{eff}}$ and 12°for $0.055NA_{\text{eff}}$ results of custom GI taper. Figure 4.10 shows from the top view that the fibre was held firmly with a distance of 85 mm between two the holders. Assuming the post travels in a direction perpendicular to the test fibre, this will create a bending angle, a. The total translation distance is B+b. B is a distance of lateral move from non-bending position to bending position in mm by the translation stage and b is a radius of post used for bending. The diameter of the post was 6.6 mm so b is 3.3 mm. Thus, fibre's bending angle can be defined as

$$a = \tan^{-1}\left(\frac{B+b}{L/2}\right) \tag{4.1}$$

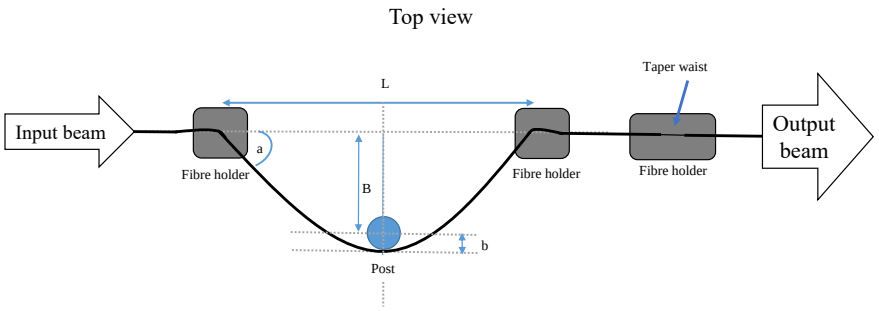

FIGURE 4.10: Illustration of fibre bending technique from top view. Test fibre is held firmly on the holders. Taper waist is supported on the holder on the right of the second fibre holder. The post was attached to a 1-axis translation stage and was adjusted to a certain mm distance to create an angle a. The post radius, b is 3.3 mm. Total translation distance is B+b and L is 85 mm. Then the angle a can be $\sim \tan^{-1}\left(\frac{B+b}{L/2}\right)$.

Figure 4.11 shows results of transmission variation dependent to a bending angle (a) of the Custom graded-index taper. The incoherent white light source was collected at 0.12 NA (0.12NAO). The taper's effective numerical aperture is calculated based on the equation 3.7 for custom and Thorlabs graded-index taper and are 0.06 and 0.04, respectively. Two NA_{eff} were selected: 0.055 and 0.25 in order to compare different beam inputs which generate mode propagation conditions in multimode fibre differently. In other words, the $0.055NA_{\text{eff}}$ beam is under-filled for Custom GI taper and slightly over-filled for Thorlabs GI tapered fibre. There was no significant change in Thorlabs GI taper with the macro bending so the focus of test fibre is only on under-filled beam impact on bending for custom GI taper.

The results show that bending effects are more significant in custom graded-index tapers and cause transmission reduction with bends in the range of bending angle of 8.5-14.3°. The custom GI taper transmission drops from a maximum value of 65% to less than 45% after 12.5°of bend for the under-filled beam condition ($0.055NA_{\text{eff}}$). Illuminating the taper input with an over-filled beam ($0.25NA_{\text{eff}}$) gives an overall fibre transmission that is less, as expected, 38% less than an under-filled beam at $0.05NA_{\text{eff}}$. The transmission drops more rapidly as bending angle is increased than with the under-filled beam. This is due to the over-filled beam generating more modes propagating along the fibre (Dennis, 2010) and even the fundamental mode may not transfer throughout the fibre. Some modes leak to the cladding. The over-filled beam is more sensitive to macrobending than the under-filled beam, which already has a smaller number of modes (primarily just the fundamental mode).

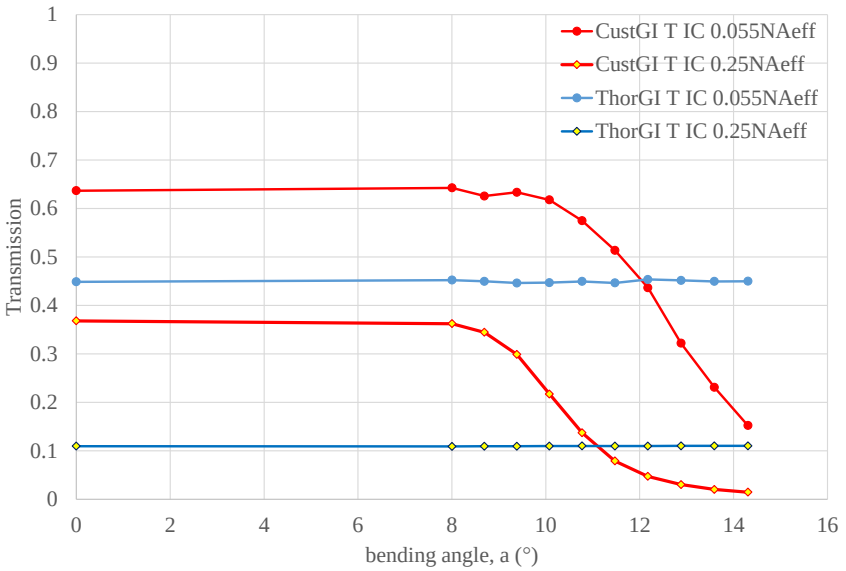

FIGURE 4.11: Result of transmission variation related to a bending of custom GI and Thorlabs GI tapered fibres. The test fibres have a 25 mm taper length, 5:1 tapered fibre and 20 mm waist. The source was incoherent light. Two NA_{eff}: 0.055 and 0.25 were chosen to present the bending impact on transmission and results of transmission were collected with the detector position at 0.12NAO condition.

For the custom fibre, the impact on transmission of macro bending is very clear but all transmission trends are relatively flat in Thorlabs GI taper. This contradicts other results (Makino et al., 2006). As the NA of the custom fibre (0.3) is bigger than the Thorlabs GI fibre NA (0.2), the loss should be less even though core diameter of both fibre type is the same size. Moreover, 0.3 NA 'silica' GI fibre is considered a relatively large NA fibre (Chu, 2006). Note that in the custom fibre the cladding size is 620 µm while Thorlabs's cladding diameter is 125 µm. Both fibres will experience the same strain for the same bending angle, however assuming that Young's modulus is the same for both fibres, the custom fibre's larger cross-section area will mean it experiences a force which is 24 times greater than the smaller diameter Thorlabs GI fibres. This large force will give rise to more modal variation in the larger diameter fibre. Note that for the spectrograph application, the fibre bending will be kept small so the bending impact will be kept.

From research reviews, there is no available product in the current market for core diameter$<$50µm graded-index fibre. The comparison between the step-index and graded-index with a small core diameter (10 µm) is performed with a 10 µm step-index fibre and a tapered graded-index fibre. Hence, another experiment was conducted in order to observe micro bending (Donlagic, 2009; Golnabi and Sharifian, 2013) impact the transmission. The samples were prepared in a similar way to the previous method but a weight was used to press a consistent periodic bending pattern

(teeth of comb) on an untapered part of the fibre. The fibre was bent periodically by 20 1-mm-width teeth with 1 mm gaps. The fibre was placed on top of a compliant surface so an estimate of the displacement could be made. The power output was measured before and after applying a fixed weight to the array of teeth at selected NA_{eff}. Three samples were tested: 25 mm Thorlabs graded-index tapered fibre, 10 μm step-index fibre and 50 μm graded-index fibre.

Table 4.3 and Figure 4.12 show the power difference in terms of percentage power change as a function of NA_{eff}. A higher percentage of power change indicates more change in mode interference or more modal noise. These results indicate that the modal noise in a 10 μm step-index untapered fibre is more than in a 50 μm graded-index untapered fibre and 5:1 tapered graded-index fibre for all NA_{eff}. The smaller size 10 μm SI fibre allows only a small number of modes to propagate through the fibre which tends to be dominated by the fundamental mode. The 50 μm GI fibre allows more modes to propagate than the 10 μm SI fibre by a factor of more than 10 according to the mode number equations in Olshansky (1976). The original mode number excited in the GI fibres is larger before bending compared to 10 μm SI. Therefore the modal noise changes are smaller in bigger core fibre (Makino et al., 2006). For a taper, the mode propagation is already restricted by the taper so micro bending in an untapered section after the taper has a small impact resulting in similar behaviour to 50 μm GI untapered fibre. The error bars for 50 μm GI untapered and tapered fibre overlap, so there is no significant difference in the modal noise between these two fibres. Note that the results at $NA_{\text{eff}} < 0.11$ are high in background light especially in SI fibre. Thus, the results are presented from $NA_{\text{eff}} > 0.10$.

TABLE 4.3: Table of percentage of power change (% Δ power) for the modal noise test in three fibre: 10 μm SI untapered, 50 μm GI untapered and 25 mm Thorlabs GI 5:1 tapered fibre. Incoherent light was the source. There were selected range of NA_{eff} 0.111, 0.167 and 0.25. NA of fibre defined the beam condition. Under-filled, filled and over-filled are defined as for the macro bending experimentation as set out in Table 4.2.

			% Δ power		
Fibre	NA^{+}/NA_{taper}	0.111 NA_{eff}	0.167 NA_{eff}	0.250 NA_{eff}	
10 μm SI	0.10	3.947	5.045	5.834	
			over-filled	over-filled	over-filled
50 μm GI	0.20	0.107	0.082	1.635	
			under-filled	under-filled	over-filled
25-mm Thor GI taper	0.04	0.524	0.303	0.718	
			over-filled	over-filled	over-filled

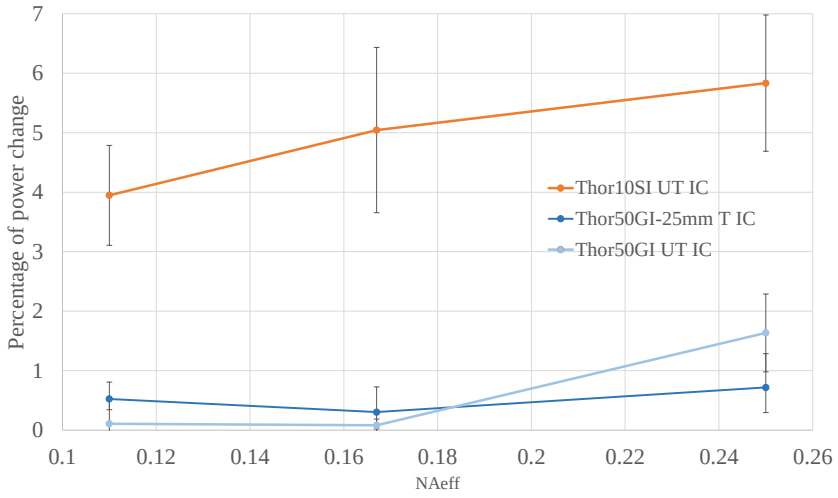

FIGURE 4.12: The percentage of difference in output power as a function of NA_{eff} is shown for periodic fibre bending. The source is incoherent light (IC). Test fibres are 10 µm step-index untapered (Thor10SI UT), 50 µm graded-index untapered (Thor50GI UT) and 25 mm Thorlabs graded-index tapered fibre (Thor50GI-25mm T). The results are shown at NA_{eff} = 0.111, 0.167 and 0.25.

4.4 Throughput and transmission

In this work, 'throughput' and 'transmission' were specifically used in a different context. Throughput is used when the output beam is measured after the combination of the optical setup and includes loss from the apparatus such as objective lenses or FC/PC fibre mating sleeves. Throughput is considered when the incoherent light source is gathered by a long 60-metre 50 µm GI untapered fibre loss is included i.e. throughput is a ratio of power measured between test fibre output (output power) and the fed-fibre 50 µm GI untapered fibre (input power). The 50 µm graded-index fibre is attached directly to the halogen lamp (Thorlabs: OSL2). There are two techniques applied to gather light from the fed-fibre 50 µm GI untapered fibre: 1. 'butt-coupling', which a fibre mating sleeve was used to connect 50 µm GI untapered fibre to test fibre and 2. 'a pair of objectives coupler', which applied a pair of objective lenses as the light collimator and focuser to the test fibre. This second method applied the incoherent light transmission test setup as in Figure 4.2. Meanwhile, the 'transmission' states for the ratio of output and input power measured in tested fibre without including loss from coupling optics such as objective lenses and fibre mating sleeves. For incoherent light setup shown in Figure 4.2, the input power position is after the second objective lens before the 3-axis translation stage. For the coherent light setup shown in Figure 4.3, the input power is located before the 3-axis translation stage and after the objective lens.

Table 4.4 shows throughput results for untapered and tapered fibre. Objective lens were pairing which are 4x and 4x, 4x and 10x or 10x and 10x. Note that there are collected data of a pair 4x and 4x and 10x and 10x for only some test fibres. Then the study continue to focus on testing with a pair of 4x and 10x. This is because results tendency suggested that 4x and 10x is the most optimal setup for transmission test. The output light was collected at 0.12NAO and 0.24NAO. As the 'butt coupling' method defined NA_{eff} by the fed fibre from the lamp, which is 0.2NA GI fibre in this case. So the input beam by butt coupling method is equivalent to 0.2NA. The results indicate that if compared to $0.2NA_{\text{eff}}$ results to the second method, the light loss is less in butt coupling setup. Moreover, the tapered fibres both custom and Thorlabs GI that were tapered from 50 µm GI fibre have higher throughput than 10 µmm SI untapered fibre.

TABLE 4.4: Table of relative throughput results. There are two methods of light coupling:1. butt-coupling 2. using the setup with a pair of objective lens. There are the pair of 4x and 10x, 4x and 4x, and 10x and 10x. T_{max} is maximum transmission at the 0.2NA according to butt-coupling NA. UT is untapered fibre and T is tapered fibre. Incoherent light was used as the source.

Fibre	coupling method	T_{max} at 0.12NAO	T_{max} at 0.24NAO
ESM	4x and 4x	-	< 0.010
ESM	10x and 10x	-	< 0.010
ESM	4x and 10x	-	< 0.010
ESM	Butt coupling	0.010	0.010
10 SI UT	4x and 4x	-	< 0.010
10 SI UT	10x and 10x	-	< 0.010
10 SI UT	4x and 10x	-	< 0.010
10 SI UT	Butt coupling	0.010	0.010
25 SI UT	Butt coupling	0.070	0.070
50 GI UT	4x and 4x	-	0.250
50 GI UT	10x and 10x	-	0.580
50 GI UT	4x and 10x	-	0.210
50 GI UT	Butt coupling	0.440	0.830
50 SI UT	4x and 4x	-	0.250
50 SI UT	10x and 10x	-	0.580
50 SI UT	4x and 10x	-	0.210
50 SI UT	Butt coupling	0.510	0.990
MFA-Thor SI T	10x and 10x	0.016	0.016
MFA-Thor SI T	4x and 10x	0.013	0.014
MFA-Thor SI T	Butt coupling	0.030	0.030
ThorSI-25mm T	10x and 10x	0.015	0.044
ThorSI-25mm T	4x and 10x	0.004	0.012
ThorSI-50mm T	10x and 10x	0.015	0.047
ThorSI-50mm T	4x and 10x	0.007	0.020
ThorGI-15mm T	4x and 10x	0.004	0.012
ThorGI-15mm T	Butt coupling	0.040	0.026
ThorGI-25mm T	4x and 10x	0.004	0.012
ThorGI-25mm T	Butt coupling	0.040	0.022
ThorGI-50mm T	10x and 10x	0.034	0.063
ThorGI-50mm T	4x and 10x	0.004	0.012
ThorGI-50mm T	Butt coupling	0.020	0.090
ThorGI-100mm T	4x and 10x	0.008	0.030
CustGI-25mm T	10x and 10x	0.081	0.243
CustGI-25mm T	4x and 10x	0.053	0.090
CustGI-25mm T	Butt coupling	0.200	0.370
CustGI-50mm T	4x and 10x	0.033	0.096
CustGI-100mm T	4x and 4x	0.030	0.044
CustGI-100mm T	10x and 10x	0.053	0.081
CustGI-100mm T	4x and 10x	0.036	0.058
CustGI-100mm T	Butt coupling	0.100	0.180
Spliced T	Butt coupling	0.004	0.004

4.5 Summary

In this chapter, transmission properties in untapered and tapered graded-index fibre with incoherent light illumination were studied including modal noise in both coherent and incoherent light. Results of measurement on how the incoherent light transmission of graded-index tapered fibre is affected by the numerical aperture of the input light are presented. Also, the exploration on the optimal coupling conditions for incoherent light into small to medium-size fibre cores (0.1-0.2 NA) was discussed. The methods that were used confirm the importance of matching light source NA with the acceptance NA of the test fibre. If this is not done losses will occur. With coherent light, the beam size coupling was easier to manipulate because of the highly collimated beam. However, incoherent light coupling into the fibre is difficult especially if the light source dimensions and NA are unmatched with the test fibre.

Then the study focused on 50 μm core diameter, graded-index fibre. Two types of graded-index fibre: Thorlabs GIF50E and a custom fibre manufactured by University of Bath were tested. The taper ratio was 5:1 and taper lengths were 15, 25, 50 and 100 mm. Simulations of step- and graded-index taper using COMSOL with the same dimensions as the test fibres were shown. The results indicate that as long as the fibre was tapered adiabatically, the transmission will improve with shorter length tapers. The experimental results agree with the simulations except for the step-index taper. This is believed that it is due to the taper core and cladding interface being disturbed by the tapering process. The effect of cladding light was also measured by comparing the light transmission through a tapered fibre before and after using index matching gel to suppress the cladding light. Comparing Thorlabs GI to custom GI transmission results, transmission is higher in custom fibre but so also is the presence of cladding light. Properly matching NA_{eff} with taper NA will give the optimum light output with the least cladding light.

In addition, the modal noise in multimode untapered and tapered fibre was investigated. Fibre modal noise was tested with both coherent and incoherent light. Also, the effect of misalignment of a coherent source into tapered GI fibre was discussed and there is an increase in the mode number as transmission decreases when the input beam is more misaligned. In addition, 'bending loss' were tested using two different methods. The first method created a variable bending angle in the test fibre. Results suggest the custom fibre with a larger diameter and manufacturer NA is more sensitive to bending than Thorlabs GI fibre, giving higher losses for the same bending angle $>12.5°$. In the second method, 'micro bending' by pressing a periodic bending pattern on top of the fibre with a weight was used. The test fibres were a 10 μm step-index fibre,

a 50 μm graded-index fibre and tapered grade-index fibre (Thorlabs:GIF50E). The indicator of modal noise in this micro bending test was the percentage of power change that occurs at the output before and then after the micro bending weight was applied. Results reveal the modal noise depends on the input beam NA for incoherent light illumination. The 50 μm graded-index untapered fibre has less modal noise in general than the 10 μm step-index untapered fibre. There is no significant modal noise difference between untapered and tapered Thorlabs GI fibre. Thus, the Thorlabs tapered fibre is a good candidate for beam converter for the astronomical instrument.

Furthermore, there is an introduction of the 'throughput' concept in this chapter, which will be used to identify the spectrograph performance later. The throughput is the ratio between the power measured at the output of the test fibre and original fed-fibre input. There are two proposed methods to deliver the coherent light source to the test fibre: 1. 'butt-coupling' and 2. 'a pair of objective lenses coupler'. As expected, the butt-coupling technique is the most optimal way to feed the light from the source to the spectrograph. The tapered fibre both custom and Thorlabs GI fibre have higher throughput than 10 μm SI untapered fibre.

As the EXOhSPEC wavelength range acceptable is 460-880 nm, the test of incoherent light already covered all of the interest ranges. This indicates that the light from taper can be expected to improve the performance of EXOhSPEC throughput if using GI taper instead of the conventional 10 μm SI untapered fibre. However, this only considers the transmission test without loss from the optics apparatus in the EXOhSPEC included.

Chapter 5

Application of tapered fibre on EXOhSPEC

5.1 Introduction

This chapter focuses on the application of tapered fibre to the fibre-fed spectrograph, which comprises the tapered fibre and EXOhSPEC spectrograph concept, a prototype of tapered fibre, and a performance test of untapered and tapered fibre used for feeding the light to EXOhSPEC. A concept of fibre-fed EXOhSPEC is explained in section 5.2. Two versions of prototypes of tapered fibre are shown in section 5.3. The novelty of the handmade technique of making trifurcated fibre is introduced by using commercial products in section 5.3 and the explanation on custom spliced taper Thorlabs product is presented in section 5.4. In section 5.5, tapered and untapered fibre is applied and tested with the fibre feeding of EXOhSPEC. The EXOhSPEC transmission and throughput concepts are explained and the coherent light results of EXOhSPEC transmission and throughput are included in section 5.5.1. Then the throughput is further investigated by incoherent light, which is a Tungsten lamp, by comparing with untapered and tapered fibre in section 5.5.2. Lastly, the spot image Full Width Half Max of ThAr spectral at 690 nm was investigated. This was obtained by EXOhSPEC using untapered 10 μm SI fibre and tapered fibre in section 5.5.3.

5.2 Tapered fibre and EXOhSPEC

Tapered fibres in this work were fabricated with an adiabatic tapering process by two machines from the University of Bath and Thorlabs company (a Thorlabs Vytran Automated glass processing workstation (GPX3400)) as already explained in Chapter 3 section 3.3.4.4. Tapered fibres studied have various tapered lengths: 15, 25, 50 and 100 mm. Since the main objective is to apply the tapered fibre to convert the beam NA from a telescope's fibre to EXOhSPEC from 0.2NA to 0.16NA, this work focuses on taper 50 µm 0.2NA multimode fibre with tapered ratio 5:1. This will allow the similar size of tapered end fibre to 10 µm step-index 0.1NA fibre. Figure 5.1 is a concept of using tapered fibre for fibre-fed EXOhSPEC.

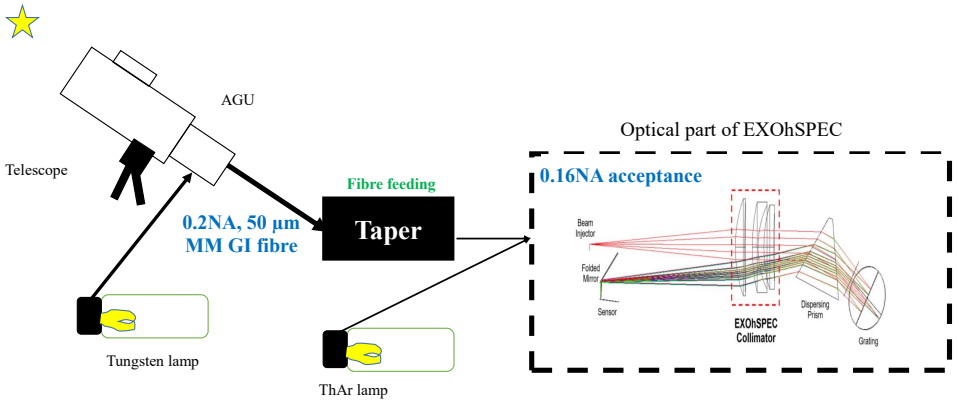

FIGURE 5.1: The concept of application of fibre-fed EXOhSPEC. The tapered fibre is linked between science fibre fed from the telescope (50 µm GI Thorlabs fibre). AGU is Acquisition and Guiding Unit used as the fibre injection unit for the telescope link to the spectrograph.

Research fibres are commercial step- and graded-index fibre from Thorlabs and custom graded-index fibre from Bath University. The custom graded-index fibre has an original 0.3NA with a relatively large cladding size compared to Thorlabs step- and graded-index fibre. Cladding diameter of custom GI fibre is 620 µm whilst Thorlabs fibre's cladding is 125 µm.

5.3 Tapered fibre prototype

For the application of the tapered fibre with the spectrograph, the prototypes were designed for specific use in this research on the EXOhSPEC fibre feeding. As the tapered fibre was fabricated from a bared fibre, i.e., fibre optics with only core and cladding layers without any protective layer. The procedure of enhancing the taper robustness by packaging such as connectorisation,

gluing, cabling extra protective layers is required. Then the taper will be ready for practical use for fibre link with the spectrograph. There are two prototypes: 1. handmade trifurcated fibre and 2. Thorlabs customised spliced tapered fibre.

5.3.1 Trifurcated fibre preparation method

The first prototype is a trifurcated fibre. Figure 5.2 shows the trifurcated fibre prototype of Thorlabs tapered fibre. Trifurcated fibre prototypes were made with jackets and FC/PC connectors. The prototype combines three different fibres which are 5:1 graded-index tapered fibre, 10 µm step-index fibre, and 50 µm graded-index fibre. Tapered fibre is for science light feeding to the spectrograph. Similarly, 10 µm step-index fibre was first used to collect the science light into the spectrograph and also is used as the reference for performance comparison with the tapered fibre. 10 µm core diameter size with 0.1NA is a requirement of the EXOhSPEC fibre link system. The GI tapered fibre is specifically designed to have the same size as 10 µm as the standard untapered fibre is for science fibre. Lastly, 50 µm GI untapered fibre is used for calibration light.

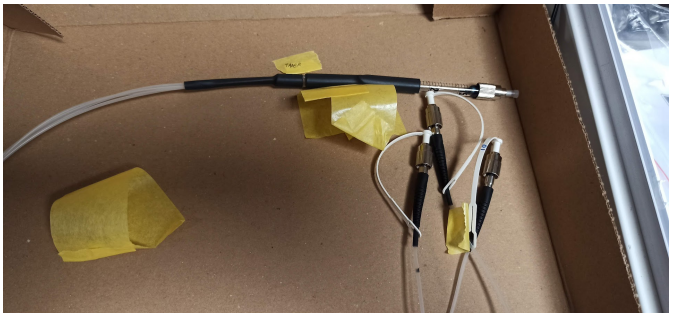

FIGURE 5.2: Prototype of handmade trifurcated fibre. This prototype consists of 10 µm step-index, 50 µm graded-index and 5:1 graded-index tapered fibre. Output end is the one combined fibre FC/PC connector. The tapered end is in the output end.

The first step is to prepare about 0.5-1 metre length of each fibre. Both ends were cleaved of the calibration fibres and one end of the taper to prepare for attaching FC/PC connectors. The trifurcated design has three separated fibre ends with 127 µm FC/PC connectors (Thorlabs: 30128C3) on the light input ends. All fibre ends were carefully inserted including the tapered end alongside each other into a single FC/PC connector (Thorlabs: 30250C1 for Thorlabs GI taper and 30640G3 for custom GI taper). The combined three fibre connector is the output end. Each fibre end was glued to the FC/PC connector with long pot life epoxy (Thorlabs: F112). After the epoxy was cured, the three fibres were inserted into a length of glass or copper tube $\sim$ 10 cm to support the fibres and used silicone sealant to seal at the end of the glass to fix the fibres in place. A heat shrink tube was used to support the sealant at the point of separated fibres.

The rest of the fibre's length was covered by small flexible plastic tubes and separated into three ends with connectors. Fibre ends were polished with Fiber Polishing/Lapping Film from crude (1500 µm) to fine (0.3 µm) grits.

As for exploring the design and aiming for testing the performance of transmission and using it as a fibre link to EXOhSPEC, some early prototypes are bifurcated fibre, which comprises 10 µm SI untapered and tapered fibre. The methodology of making bifurcated fibre is almost identical to the trifurcated fibre. The only difference is there were two fibres used instead of three fibres.

Note that both bi- and trifurcated fibre ends have a concerning issue from the epoxy curing. The contamination of epoxy was spotted after the prototype was made. This is due to the size of FC/PC connectors are not match with the three fibre ends (shown in Figure 5.3). This is believed that the void in fibre ends from unmatched-size connectors is the reason for uncured epoxy. However, this can easily be removed by polishing and cleaning. Figure 5.4 shows the coaxial and oblique illumination images of bifurcated fibre end before and after polishing and cleaning.

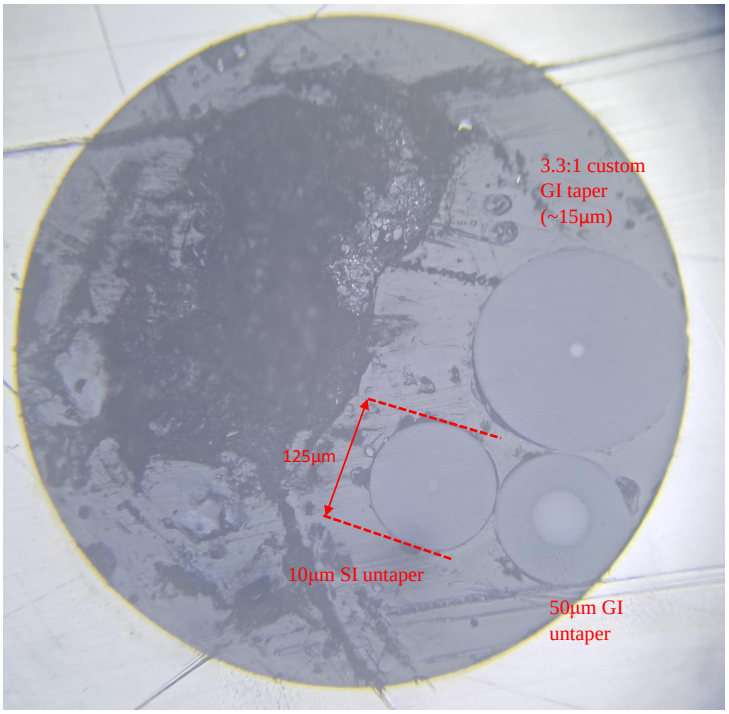

FIGURE 5.3: Image of trifurcated fibre end surface. This prototype consists of 10 µm step-index, 50 µm graded-index and 3.3:1 custom graded-index tapered fibre. Three fibre ends are located around the edge of the connector due to the unmatched size. The fibre ends were polished and cleaned.

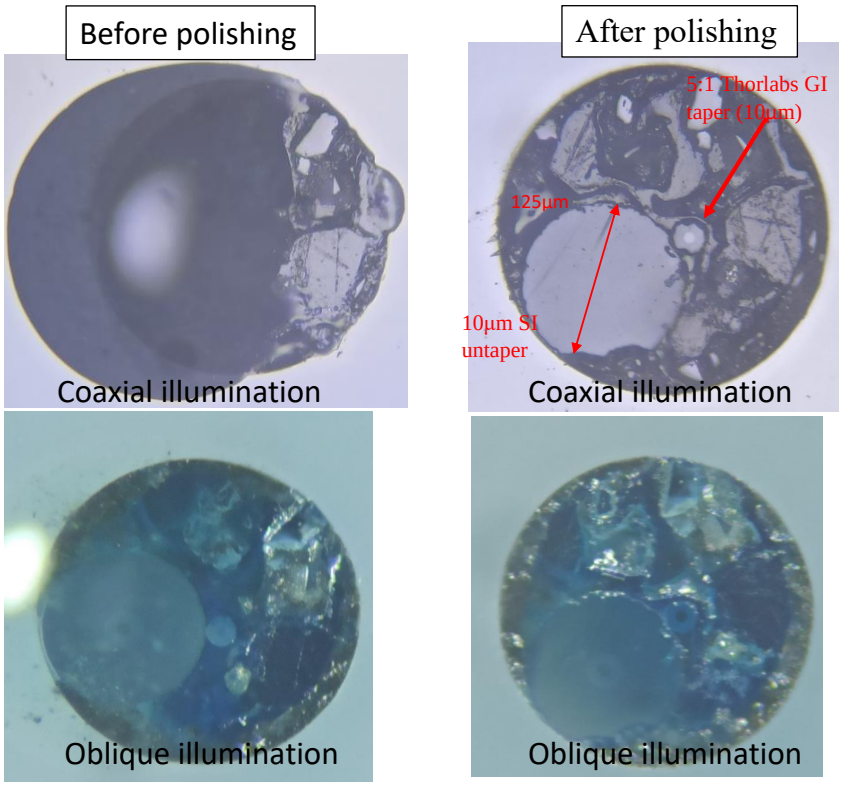

FIGURE 5.4: Image of bifurcated fibre end surface before and after polishing and cleaning. This prototype consists of 10 µm step-index and 5:1 Thorlabs graded-index tapered fibre. The Left and right columns are images of bifurcated fibre end before and after polishing, respectively. There are coaxial and oblique illumination images shown.

5.4 Spliced tapered fibre

A way to enhance the robustness of the tapered fibre was explored after facing some issues in handling the trifurcated fibre. The design was sensitive on bending and the cure of epoxy was not perfect as a result of epoxy contamination on the trifurcated end. Our research group then collaborated with Thorlabs Vytran Exerter UK to design a tapered fibre build-in packaging. Figure 5.5 shows the drawing of spliced taper designed and Figure 5.6 shows an image of spliced taper and final product. This taper was produced by a GPX3400 Glass Processor with an LDC400A cleaver. The prototypes have Thorlabs GI (GIF50E) tapered end spliced to 10 µm SI untapered fibre (FG010LDA). Taper length is 25 mm and the taper ratio is 5:1. The spliced parts are held firmly inside of the sturdy 3D plastic printed box. The adhesive is used to cure spliced taper and to suppress the cladding light in the same time. When compared to the hand-made version, this spliced taper is more robust. However, the light transmission is not improved. Results in Figure 5.7 show the comparison between spliced taper (denoted 'SP') to custom GI and Thorlabs GI taper.

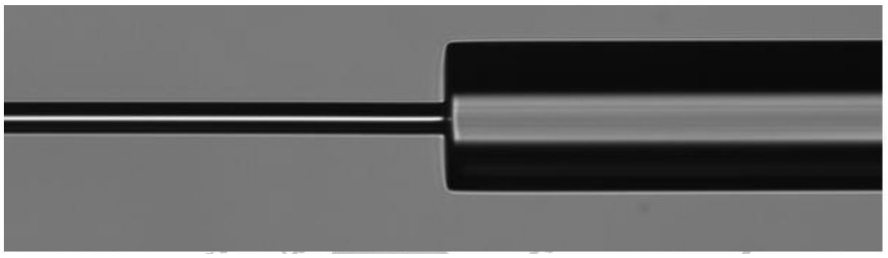

FIGURE 5.5: Image of the back view of spliced Thorlabs tapered GI fibre (GIF50E) with 10 µm SI MM fibre (FG010LDA).

FIGURE 5.6: Image of a prototype of spliced tapered fibre produced by Thorlabs

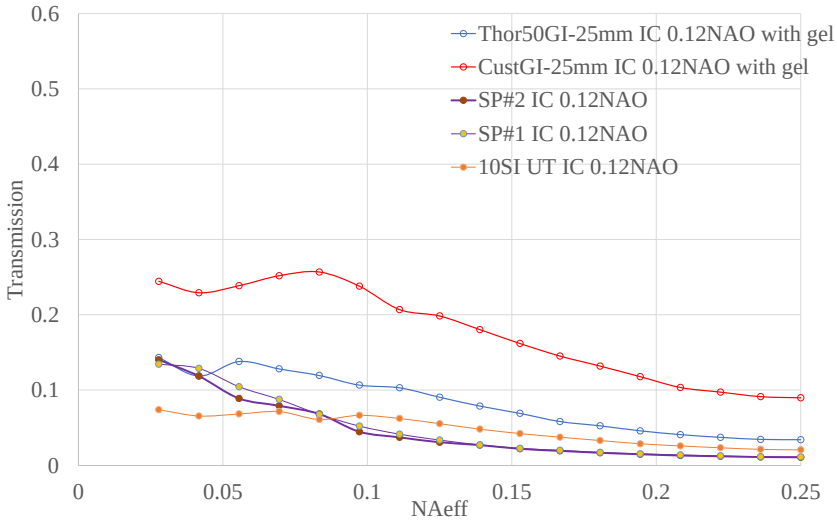

FIGURE 5.7: Results of transmission dependence on NA_{eff} of spliced taper prototypes #1 and #2 compared to Thorlabs GI and custom GI taper. Thorlabs GI and custom GI tapers cladding light is suppressed with refractive index matching gel.

5.5 EXOhSPEC and the fibre feeding

The objective of the fibre investigation is to apply the best tapered fibre from selected samples to the fibre-fed system of the high resolution spectrograph prototype EXOhSPEC. In order to achieve high resolution spectroscopy from a telescope, relatively large optics are required and most components are specifically manufactured. Furthermore, in order to also achieve the stability required for the detection of exoplanets, high stability of these large optical components

is necessary. Often the optics are placed in a vacuum and environmental control is necessary. For example, HARPS (Pepe et al., 2000) is a highly successful high resolution spectrograph but requires a mosaic of bespoke gratings and is placed in a large isolated room and vacuum chamber to limit it from the impact from humidity, temperature and background noise variations. Such requirements lead to the high cost of high resolution spectrographs. The concept of EXOhSPEC is to have a fibre feeding system which leads to a smaller beam size which enables all components to be smaller, largely 'commercial off-the-shelf'. There are a number of potential routes to a smaller beam size which have been pursued for this. There is a successful application of photonic lanterns for focal reduction which may enhance the fibre feeding of astronomical instrumentation (Jovanovic et al., 2012; Spaleniak et al., 2013; Birks et al., 2012, 2015). Also, the adaptive optics systems have been successfully deployed on a number of telescopes (Jovanovic et al., 2016). Given the promise of some literature results (Avila, 1988; Birks et al., 2012; Haynes et al., 2012) and the relative simplicity of tapering an optical fibre, this was further investigated as a route to a smaller beam size. Application of tapered fibre into the fibre feeding may lead to the improvement on the spectrograph throughput for the small size optics which require less opto-mechanics.

There are presently two EXOhSPEC prototypes, one at the University of Hertfordshire and one at the National Astronomical Research Institute of Thailand (NARIT). The overall design concept is described in Jones et al. (2021), including latest setup of UH EXOhSPEC. The optical design is described by Lhospice et al. (2019). The mechanical design of the collimator and its performance is modelled by Kawinkij et al. (2019) and the data reduction system for processing the raw data is presented by Errmann et al. (2020). Tapered fibre couplers based on this work have been tested at Thai National Telescope with the NARIT EXOhSPEC prototype.

5.5.1 EXOhSPEC fibre coupler transmission and throughput

The simple way to identify transmission of EXOhSPEC was measured by using 1. a 532 nm laser diode and 2. different fibre optics for 635 nm light feeding. This is called 'fibre coupler transmission' in this work. A power meter was used to measure power before the light entered the optics of EXOhSPEC and after the light passed through all optics at the position located before the CCD. Note that for 635 nm laser diode input to test fibre, the light was coupled into 50 μm GI fibre and then this fibre was 'butt-coupled' to the test fibre. The principal mode (brightest spot) was selected for the output power measurement. This is because the spectrum

obtained by the CCD is only the principal order. The 532 nm source setup is the imitation of the highly collimated input beam to the spectrograph i.e., small NA of beam input. Using selected fibres as the light feeding the NA of beam input can be varied from 0.1 to 0.39. Transmission of the EXOhSPEC system is the ratio of the output power of principal modes and input power from either 532 nm laser or test fibre.

For the observation, the throughput of EXOhSPEC is defined by including loss from the fibre feed from the telescope. In other words, the throughput is the ratio between output power after dispersed spectral from the optical apparatus of EXOhSPEC and the output of the fibre feed from the telescope. With the setup in the laboratory using 635 nm as mentioned earlier, the change of throughput based on changing optical fibre that is butt-coupled to a 50 μm GI fibre can be measured. Table 5.1 shows results of EXOhSPEC transmission and throughput from 532 nm and 635 nm coherent light.

Test fibre	Fibre coupler transmission	EXOhSPEC throughput
532 nm		
-	0.26	-
635 nm		
Thorlabs 50 μm GI taper 15 mm taper length	0.06	0.01
Thorlabs 50 μm GI taper 25 mm taper length	0.10	0.01
Thorlabs 62.5 μm GI taper 25 mm taper length	0.05	0.01
Custom GI taper 15 mm taper length	0.10	0.01
Spliced Thorlabs taper	0.26	$<$0.01
10 μm SI Thorlabs untaper	0.26	0.01
25 μm SI Thorlabs untaper	0.32	0.08
50 μm GI Thorlabs untaper	0.10	0.10
62.5 μm GI Thorlabs untaper	0.10	0.09
105 μm SI Thorlabs untaper	0.19	0.11
150 x 150 μm SI square-core Thorlabs untaper	0.11	0.11

TABLE 5.1: Result of transmission and throughput of the EXOhSPEC measurement from coherent light 532 and 635 nm coherent light.

5.5.2 Tungsten lamp results

The application of tapered trifurcated prototype is presented in this section. Thorlabs GI tapered and custom fibre was used for the fibre input to the UH EXOhSPEC. A tungsten lamp was used as a source in order to compare the photon count between 10 μm SI untapered fibre, Custom GI taper and Thorlabs GI taper. Note that the trifurcated fibre tested comprised 1. Taper fibre (either Thorlabs GI taper or Custom GI taper) 2. 10 μm SI untapered fibre and 3. 50 μm GI untapered fibre. The main interest in this research is a comparison of the performance between the 10 μm

SI untapered fibre and tapered fibre of choice, so the throughput test did not include 50 µm GI untapered fibre. Cross-section area from the spectrum was selected and the data was imported as pixel value or ADU (Analogue-to-Digital conversion Units) related to the pixel of the CCD (shown in Figure 5.8). The images were taken and normalized into the same scale exposure time of 0.35 seconds. Figure 5.9 shows tungsten spectral lines taken by UH EXOhSPEC. All results from 10 µm SI untapered fibre, Thorlabs spliced taper, Thorlabs GI tapered fibre and Custom GI tapered fibre were presented.

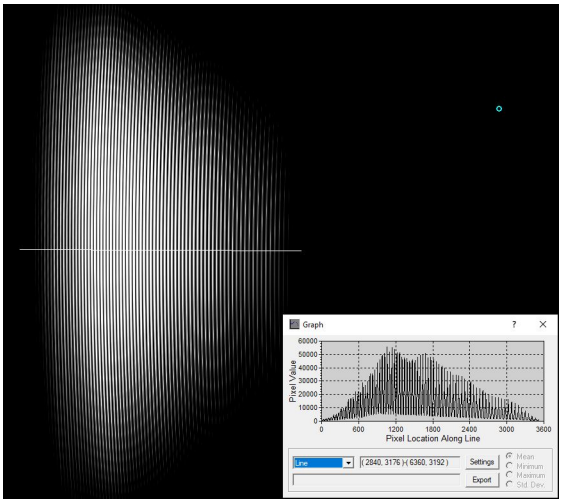

FIGURE 5.8: Example calibrated .fit file of Tungsten spectral lines obtained by EXOhSPEC using Custom GI taper. The cross-section selection is a horizontal line located in the middle of the spectral lines which was estimated that there are the most ADU counts. The line covered all the range of wavelengths.

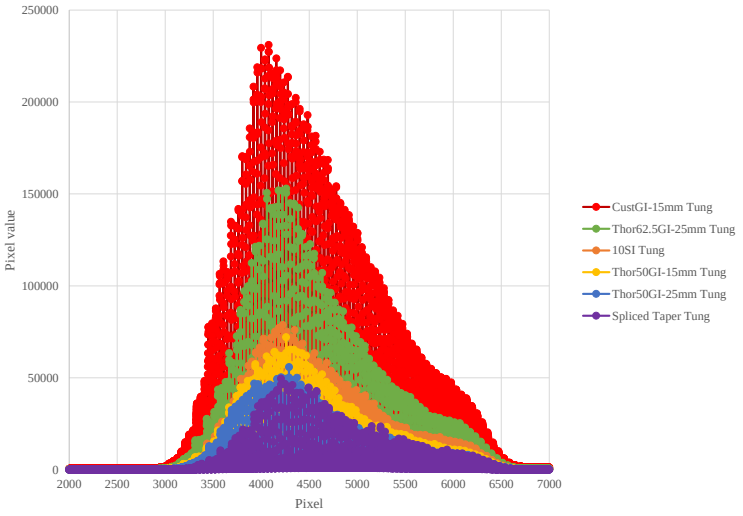

FIGURE 5.9: Tungsten spectrum obtained by EXOhSPEC using untapered and tapered fibre. Results show in pixel value versus pixel of 10 µm SI untapered fibre, Custom GI taper and Thorlabs GI taper.

The results were calibrated by subtraction of dark and bias. With this setup, the longer wavelength is located at a smaller number pixels at the CCD. A peak of pixel values is roughly 700 nm. A shorter wavelength is located at a bigger number of pixels after the peak on the right side of the graph. From the results, it is clear that a custom GI taper has better overall pixel values or more photons collected into the CCD chip than the others. Maximum of pixel values can reach a factor of 2 more compared to Thorlabs GI taper. Unexpectedly, the Thorlabs GI taper gives overall less pixel values compared to 10 μm SI untapered fibre. This contradicts to transmission related to NA_{eff} test at 0.12NAO that suggested the Thorlabs GI taper has less loss compared to the 10 μm SI untapered fibre. As the EXOhSPEC has NA acceptance of 0.16. The transmission results of 0.12NAO imitate the light propagation into the spectrograph. However, the spectral light detected in 10 μm SI untapered fibre is slightly better than Thorlabs GI taper, i.e., comparing at peak pixel value, the 10 μm SI untapered fibre value is more than Thorlabs taper in a factor of 1.16. Note that these two results, the transmission test and EXOhSPEC spectral throughput test, were under investigation in the different experimental setup and conditions. The transmission test does not include the loss from optical apparatus such as fibre feeding, prism, lens, and grating in the EXOhSPEC prototype and the transmission test was set for the most optimal light coupling into interest fibre/ taper. The Thorlabs spliced taper product has the least throughput. This was consistent with the Thorlabs taper since the product has spliced loss from taper to the 10 μm SI untapered fibre. In addition, the results of all test fibres indicate more loss in a shorter wavelength spectrum.

Moreover, coupling efficiency was investigated by changing of NA input by selecting different NA fibre for comparison of light output. The fibre that was changed was attached to the Tungsten source. Comparison fibres are from 50 μm GI untapered fibre with 0.2NA and 105 μm SI untapered fibre with 0.1NA. Figure 5.10 shows pixel values or Analogue-to-Digital conversion Units (ADUs) versus pixel comparison results of 105 μm SI and 50 μm GI fibre source coupling. A cross-section area of Tungsten spectral, which was obtained from the EXOhSPEC, was selected at the centre of spectral dispersion lines and covers all wavelengths. Results show more light loss using the 105 μm SI untapered fibre. The loss from coupling light from 50 μm GI untaper fibre to 10 μm SI untapered fibre is still the most optimal way. This is because the beam NA gather originally from the lamp with 50 μm GI fibre (0.2NA) is larger than the 105 μm (0.1NA). Though the light is lost by coupling to 0.1NA 10 μm fibre later on, the light collected from the first fibre is significantly more than directly collect to the 105 μm (0.1NA) single fibre.

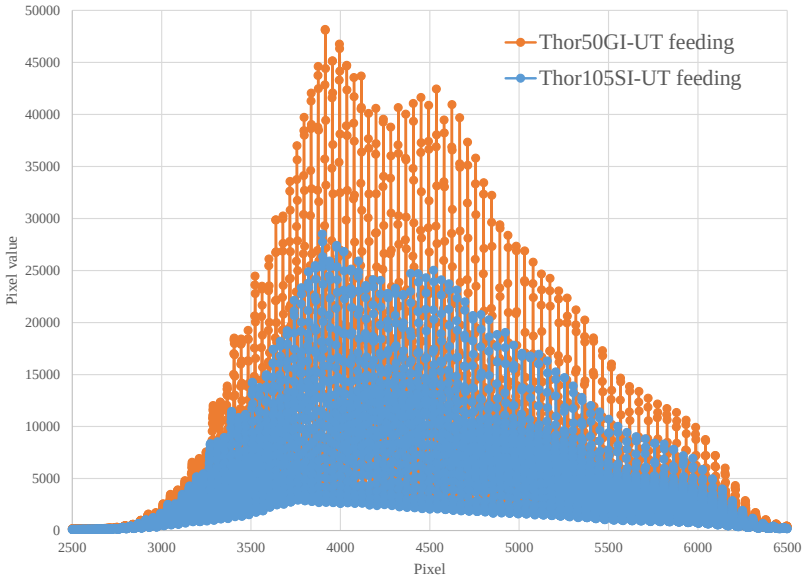

FIGURE 5.10: Tungsten spectral obtained by EXOhSPEC using 105 µm SI and 50 µm GI untapered as the fibre feeding from the tungsten lamp to science fibre to EXOhSPEC. Results present in pixel value versus pixel.

5.5.3 ThAr light results

The resolution of the spectrograph is usually defined by the ability to distinguish and identify between smallest closed spectral lines. This is also known as resolving power. The form of spectral resolution is commonly written as:

$$R = \frac{\lambda}{\Delta\lambda} \tag{5.1}$$

when R is the spectral resolution that can be quantified by the smallest distinction ($\Delta\lambda$) of spectral lines on a wavelength λ. It can be complicated in the design of the spectrograph in order to identify the resolving power. For example, EXOhSPEC resolution is defined by entrance pupil i.e., fibre core geometry, double passed lens, grating and dispersion prism. The resolution of EXOhSPEC is 70,000 (Jones et al., 2021).

As this work is aimed at simplifying the experimentation and avoiding using complicated methods for measuring the resolution, one of the ways is to measure 'Full Width Half Maximum (FWHM)' of ThAr spectral light obtained by the spectrograph. Thorium and Argon or ThAr discharge lamps are widely used as wavelength references. More than 11500 emission lines were catalogued at wavelength range 3000 to 11000 $\AA$ as reviewed by Lovis, C. and Pepe, F. (2007) and there was the further discovery of emission lines by HARPS of more than 8400 lines

at wavelength range 3785 to 6915 $\mathring{A}$ (Lovis, C. and Pepe, F., 2007). Considering light propagation with Gaussian profile and under the circumstance of no change of light dispersion on the CCD by changing the input fibre, the parameter 'Full Width Half Maximum (FWHM)' of the individual spot of ThAr light obtained by the spectrograph can be used to quantify the spectral resolution. By changing the fibre feed to the spectrograph, FWHM size comparison at the same spot wavelength is a fair comparison to quantify the spectral resolution. The narrower width of spot profile typically defines the higher resolution in the spectrograph. Only unsaturated images were taken from the linear response of the CCD.

For the experimentation, ThAr light was coupled into 50 µm Thorlabs GI fibre to imitate the fibre feeding from the telescope and then was butt-coupled to the test fibre. Then the light will be dispersed into a spectrum by a dispersion prism and an Echelle grating. After dispersion, spectrum is collected into a CCD of EXOhSPEC. The whole spectral wavelength range obtained by EXOhSPEC is from 460 to 880 nm (Jones et al., 2021). A 690 nm narrow bandpass (Thorlabs:FB690) was used to filter a 690 nm wavelength from ThAr. The FB690 filter central wavelength is $\pm$2 nm, FWHM is 10$\pm$2 nm and blocking wavelengths are 200-1200 nm. Three spots were selected for data analysis to simplify and minimize spectral spots samplings. Figure 5.11 shows the ThAr spectrum obtained by EXOhSPEC using 10 µm SI untapered fibre. The left image shows the whole spectral range without using a filter. The light dispersed to spectral lines and each spectral line has individual order from small to larger order numbers from left to right. Considering vertically, wavelengths are shorter at the top then they increase as further down on the image. Considering horizontally, wavelengths are shorter at the left then they increase as further right on the image The right image shows the ThAr spectral lines using 690 nm band pass filter. Three bright spots labelled as A, B and C were selected for FWHM comparison. The wavelength of each spot was obtained by HiFLEx pipeline (Errmann et al., 2020) as A=6937.66 $\mathring{A}$ (ArI), B=6943.61 $\mathring{A}$ (ThI) and C= 6965.43 $\mathring{A}$ (ArI). The reason for selecting these three spots is that they are not blended lines and are easy to use for comparison as the ADU count is relatively high.

The spectral spots FWHM obtained by the spectrograph were compared by using variety of fibres which are 10 µm untapered fibre, Thorlabs GI tapered fibre with 15 mm taper length and custom GI with 25 mm taper length tapered fibre. Maxlm DL 6 is used to record and analyse the spectral lines results including the export of FWHM data of each interested spot. In this work FWHM obtained is a physical line width.

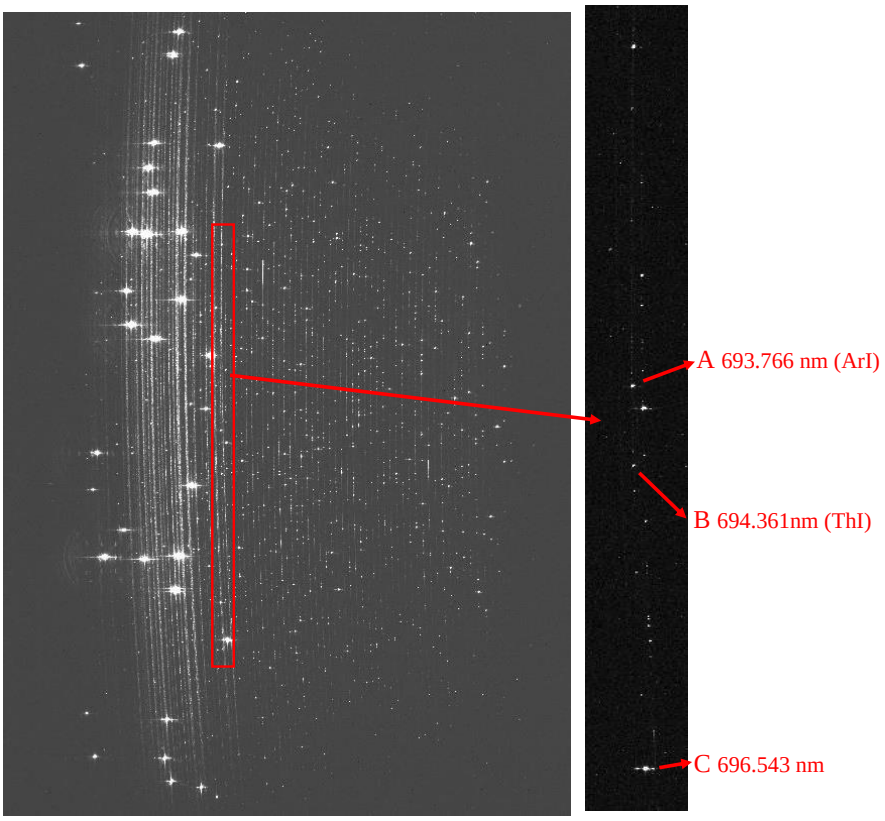

FIGURE 5.11: Calibrated image of spectral obtained by EXOhSPEC using 10 µm SI untapered fibre as fibre feeding. The left image shows the spectral lines from 460 to 880 nm wavelength range. Wavelengths are shorter when considering from bottom to top and from left to right. The right image is the 690 nm spectral line obtained by using 690 nm narrow bandpass filter. Labelled spots from A to C is for FWHM comparison in each test fibre that results discussed in Figure 5.12.

Figure 5.12 shows results of FWHM in µm for selected spots A to C at 690 nm wavelength. The FWHM error bar is 1σ from repeated measurement of focusing the spots at the CCD for 10 times by using 10 µm Thorlabs SI fibre. The repeated measurement was only done with the 10 µm SI UT fibre. Images exposure time was selected with the time period that allows optimum light collected but not saturated for each fibre. Exposure time for custom GI results is 5 seconds while 10 SI UT and Thorlabs GI taper exposure time are 8 seconds. Considering FWHM results in the first vertical axis, though the light throughput is better in custom GI taper (according to shorter exposure time before the image becomes saturated), the FWHM size of spots by custom GI taper are also the largest compared to the other two fibre results. This is due to the NA of custom GI taper is larger than the other two fibres and this allows more mode propagation in the custom GI fibre compared to SI UT or Thorlabs GI taper. As spots were sampled on different positions on the detector, the FWHM size of each spot depends on the position on the CCD. In other words, position on the CCD defines different wavelength of each spot. For example, if

considering at only one particular order for custom GI taper, the spots FWHM are reduced as the wavelength is increased. However, the spots' FWHM in Thorlabs taper and 10 µm SI untaper show a small significant difference in size but trends of size reducing are presented.

In addition, the physical line width i.e., FWHM multiplied by the dispersion of the spectrograph is presented in this graph. Dispersion in this work is defined as a ratio of wavelength difference to distance between a pair of spots. This is a parameter to show the distinguishability of each wavelength. For example, spot A and B are selected. Spot A and B have wavelength 6911.23 Åand 6937.66 Å. The distance between A and B in the vertical axis is 1472 pixels and CCD pixel size used in the test is 3.67 µm. So, the dispersion from spots A and B is 6937.66-6911.23 Å/ 1472 x 3.67 µm. = 4.89 Å/mm. As there are more than one pair of spots. Each spot is paired with the other and the dispersion value is obtained with the same method. The average value of dispersion is 4.7 Å/mm. The dispersion of the spectrograph is defined by the grating's groove density and dispersion prism. The graph represents a direct proportional relationship between FWHM and dispersion here. Moreover, there is a pattern of cladding light on the bright spots from the other wavelength spectrum using custom GI taper and Thorlabs GI taper. Though this may affect the cladding light contamination as it can increase FWHM as well.

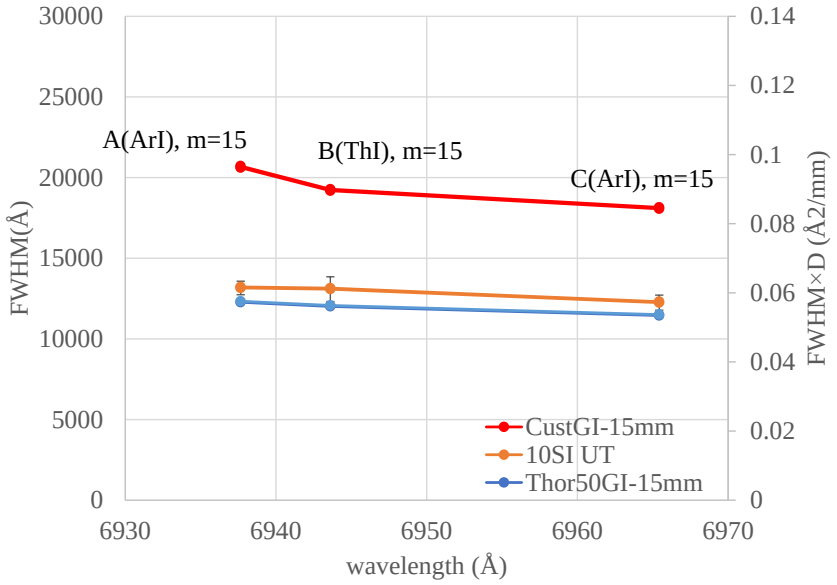

FIGURE 5.12: Full width half max (FWHM) and FWHM multiplied by dispersion of the ThAr spots in Angstrom at wavelength 690 nm obtained by EXOhSPEC with untapered and tapered fibre. FWHM (shown in the first vertical axis) is the physical size of each spot. Wavelengths of spot A, B and C are defined in Figure 5.11. m stands for order. The second vertical axis shows FWHM multiplied by the dispersion of the spectrograph (D). Test fibres are custom GI taper (CustGI-15mm) with 15 mm taper length, Thorlabs GI taper with 15 mm taper length (Thor50GI-15mm) and 10 µm Step-index untapered fibre (10SI UT).

5.6 Summary

This chapter focuses on the application of tapered fibre with the spectrograph. First, the technique to build connectorised trifurcated fibre from three bare fibres was presented. In this work, the prototype comprises tapered fibre, 10 μm SI untapered, and 50 μm GI untapered fibre. The process of building the prototype is extremely delicate. All processes need to be in a very clean environment due to dust contamination that can damage the fibre end surface while the epoxy cures as well as during the fibre end polishing process. Also, dust contamination into an epoxy layer while curing can cause voids and the fibre can fail to be fixed in the connector. It is difficult to contain 3 fibre end surfaces at the centre of the FC/PC connector. However, the shift from the centre in Thorlabs taper end is in the acceptable range.

In addition, the transmission of EXOhSPEC was measured. A 532 nm laser diode was used and EXOhSPEC transmission at the optimum light coupling condition is 26%. Then the trifurcated fibre prototype was used for evaluating the fibre link in EXOhSPEC. The light of fibre feed into spectrograph used untapered and tapered fibre with 1: Tungsten lamp and 2: ThAr lamp. The throughput of EXOhSPEC with incoherent light the Tungsten lamp, shows that the custom GI taper provided the most light throughput for the EXOhSPEC among taper and 10 μm SI fibre comparison fibres.

Moreover, the ThAr spectral lines were obtained by EXOhSPEC using the same fibre candidates for the test. Lines close to 690 nm wavelength were selected from the whole spectrum. Generally, if the irradiance of the light profile is not different, a narrower width usually indicates a higher resolution of the instrument. FWHM spots analysis obtained by Maxlm DL 6 presents that the FWHM of 10 μm SI untapered fibre and Thorlabs GI taper are not significantly different and custom GI taper has better light throughput. The cladding light also shows clearly in the spectral images of custom GI taper.

Chapter 6

Conclusions

The light transmission properties of untapered and tapered fibre were investigated. The main objective was to find the best candidate for fibre links to high-resolution spectrograph as throughput can improve with a single tapered fibre. The study was started with commercial fibre optics from Thorlabs and Chromis Fiberoptics. The test fibres were single mode and multimode fibre including some special type such as endlessly single mode, double-cladding fibre, square-core fibre and custom graded-index fibre. The range of core diameter of test fibres is from 10 to 150 μm. The transmission test setup was designed and the most optimal light coupling technique so called 'NA matching' was defined. This technique was applied for both coherent and incoherent light transmission tests. A variety of tapered fibres were tested. They are step-index and graded-index fibres produced from Thorlabs and custom GI fibre of Bath University. The light coupling into the fibre optics is critical to define the optimal light output. In this research, the light injection with an unmatched size of input NA beam was studied. Matching NA input with the taper by coupling the light from 50 μm (0.2NA) to 0.1NA fibre may optimize the overall throughput of light of EXOhSPEC. Especially the cladding light in the custom GI fibre may be suppressed optimally by this method.

The results of coherent light transmission tests show a severe light loss in step-index tapered fibre and overall better transmission in GI taper though COMSOL predictions suggested otherwise. Then this research focused mainly on graded-index tapered Thorlabs and custom GI tapers. Both coherent and incoherent light testing suggested that the overall transmission in custom GI taper is better than Thorlabs GI taper.

Although the custom GI taper has overall transmission better than the Thorlabs GI taper, the application for fibre-fed spectrographs still needs to be very carefully prepared. The sensitivity to modal noise is apparently more in the custom GI taper according to the evidence of tests in macro bending and also there is clearly cladding light impact on the taper for the shorter length as built. For both coherent light and incoherent light, if the light coupling is in optimum condition, and the NA of the input beam is matched to the tapered fibre NA, the best candidate for light gathering with small loss is obviously the custom GI taper.

6.1 The future

As the COMSOL predictions suggest that the light transmission in a SI tapered fibre should be generally better than GI tapered fibre that is fabricated from similar NA fibre, a test using different core doping SI fibre should be considered. For example, the Germanium doped SI fibre.

Cladding light is one of the most concerning issues in the fibre-fed spectrograph since the light has increased spot size and results in reduced resolution of the spectrograph. Even though using index matching gel in the test was effective, there is a challenge in applying the gel into the fibre sleeves and connectors of the prototype, especially the trifurcated fibre. Exploring the different chemical, material or methods to suppress cladding light such as coating taper transition surface, fabricating longer taper waist length i.e., 50 mm, applying index matching gel that is robust is another method to optimise the tapered fibre performance.

Epoxy curing in a build-in-house tapered fibre is the issue that causes the contamination on the fibre end surface. This can decrease the performance of fibre transmission as the epoxy curing performs best with temperatures more than 25°. Polishing and cleaning fibre end before use is required before using which is not a sustainable method because this can cause damage in the long-term use. The curing problem may be solved by using custom size of the FC/PC connector that fits with the tapered diameter. In another way around, using a bigger cladding fibre to tapered the size down to fit a standard FC/PC properly can be considered.

A narrowband incoherent light source (e.g. LED) for the testing on the tapered fibre can be useful information to include in the study since there were only results from incoherent and coherent light i.e. wide range wavelength and an individual wavelength. The small range of

wavelength tests can provide information on transmission and coupling at certain interesting ranges, particularly blue and red regions.

The application of a tapered fibre in an on-sky test with the 2.4-metre telescope with NARIT EXOhSPEC is the final test planned on the performance of the tapered fibre.

Bibliography

Alder, T., Stohr, A., Heinzelmann, R., et al., 2000. High-efficiency fiber-to-chip coupling using low-loss tapered single-mode fiber. *IEEE Photonics Technology Letters*, 12(8):1016.

Amitay, N., Presby, H., DiMarcello, F., et al., 1987. Optical fiber tapers–a novel approach to self-aligned beam expansion and single-mode hardware. *Journal of Lightwave Technology*, 5(1):70.

Arrue, J., Jiménez, F., Aldabaldetreku, G., et al., 2008. Analysis of the use of tapered graded-index polymer optical fibers for refractive-index sensors. *Opt. Express*, 16(21):16616.

Avila, G., 1988. Tests of optical fibres for astronomical instrumentation at ESO. In S.C. Barden, editor, *Fiber Optics in Astronomy*, volume 3 of *Astronomical Society of the Pacific Conference Series*, pages 63–73.

Avila, G., 1998. *Results on Fiber Characterization at ESO*, volume 152 of *Astronomical Society of the Pacific Conference Series*, page 44.

Barden, S.C., 1996. Fiber optics in astronomical instruments. *Opt. Photon. News*, 7(2):34.

Birks, T.A., Gris-Sánchez, I., Yerolatsitis, S., et al., 2015. The photonic lantern. *Adv. Opt. Photon.*, 7(2):107.

Birks, T.A. and Li, Y.W., 1992. The shape of fiber tapers. *Journal of Lightwave Technology*, 10(4):432.

Birks, T.A., Mangan, B.J., Díez, A., et al., 2012. "photonic lantern" spectral filters in multi-core fibre. *Opt. Express*, 20(13):13996.

Bland-Hawthorn, J. and Kern, P., 2009. Astrophotonics: a new era for astronomical instruments. *Opt. Express*, 17(3):1880.

Casperson, L. and Kirkwood, J., 1985. Beam propagation in tapered quadratic index waveguides: Numerical solutions. *Journal of Lightwave Technology*, 3(2):256.

Choochalerm, P., Martin, W.E., Jones, H.R., et al., 2021. Transmission properties of tapered optical fibres: Simulations and experimental measurements. *Optical Fiber Technology*, 66:102632.

Chu, P.L., 2006. Chapter 2 - recent development of a polymer optical fiber and its applications. In B.P. Pal, editor, *Guided Wave Optical Components and Devices*, pages 27–40. Academic Press, Burlington.

Content, R., Bland-Hawthorn, J., Ellis, S., et al., 2014. PRAXIS: low thermal emission high efficiency OH suppressed fibre spectrograph. In R. Navarro, C.R. Cunningham, and A.A. Barto, editors, *Advances in Optical and Mechanical Technologies for Telescopes and Instrumentation*. SPIE.

Dennis, T., 2010. Multimode fiber launch study: Estimating the impact on measurements of delay.

Donlagic, D., 2009. A low bending loss multimode fiber transmission system. *Opt. Express*, 17(24):22081.

Errmann, R., Cook, N., Anglada-Escudé, G., et al., 2020. HiFLEx—a highly flexible package to reduce cross-dispersed echelle spectra. *Publications of the Astronomical Society of the Pacific*, 132(1012):064504.

Gambling, W., 2000. The rise and rise of optical fibers. *IEEE Journal of Selected Topics in Quantum Electronics*, 6(6):1084.

Golnabi, H. and Sharifian, M., 2013. Investigation of bending and temperature effects in optical fibers. *Microwave and Optical Technology Letters*, 55(1):82.

Halverson, S., Roy, A., Mahadevan, S., et al., 2015. AN EFFICIENT, COMPACT, AND VERSATILE FIBER DOUBLE SCRAMBLER FOR HIGH PRECISION RADIAL VELOCITY INSTRUMENTS. *The Astrophysical Journal*, 806(1):61.

Haynes, D.M., Haynes, R., Olaya, J.C., et al., 2012. Optical fibre tapers: focal reduction and magnification. In *Modern Technologies in Space- and Ground-based Telescopes and Instrumentation II*, volume 8450 of *The proceeding of SPIE*, page 84503J.

Hecht, E., 2017. *Optics*. Pearson Education.

Hecht, J., 2020. The breakthrough birth of low-loss fiber optics. *Optics and Photonics News*, 31:26.

Hill, K.O., Tremblay, Y., and Kawasaki, B.S., 1980. Modal noise in multimode fiber links: theory and experiment. *Opt. Lett.*, 5(6):270.

Hudson, M.C., 1974. Calculation of the maximum optical coupling efficiency into multimode optical waveguides. *Appl. Opt.*, 13(5):1029.

Ishizuka, M., Kotani, T., Nishikawa, J., et al., 2018. Fiber Mode Scrambler for the Subaru Infrared Doppler Instrument (IRD). *PASP*, 130(6):065003.

Jones, H.R.A., Martin, W.E., Anglada-Escudé, G., et al., 2021. A small actively controlled high-resolution spectrograph based on off-the-shelf components. *Publications of the Astronomical Society of the Pacific*, 133(1020):025001.

Jovanovic, N., Schwab, C., Cvetojevic, N., et al., 2016. Enhancing stellar spectroscopy with extreme adaptive optics and photonics. *Publications of the Astronomical Society of the Pacific*, 128(970):121001.

Jovanovic, N., Spaleniak, I., Gross, S., et al., 2012. Integrated photonic building blocks for next-generation astronomical instrumentation i: the multimode waveguide. *Opt. Express*, 20(15):17029.

Kapron, F.P., Keck, D.B., and Maurer, R.D., 1970. Radiation losses in glass optical waveguides. *Apply Physics Letters*, 17(10):423.

Kawinkij, A., Prasit, A., Buisset, C., et al., 2019. EXOhSPEC collimator mechanical design. In T.B. Hull, D.W. Kim, and P. Hallibert, editors, *Astronomical Optics: Design, Manufacture, and Test of Space and Ground Systems II*, volume 11116, pages 443 – 452. International Society for Optics and Photonics, SPIE.

Keck, D., Maurer, R., and Schultz, P., 1973. On the ultimate lower limit of attenuation in glass optical waveguides. *Apply Physics Letters*, 22(7):307.

Kerttula, J., Filippov, V., Ustimchik, V., et al., 2012. Mode evolution in long tapered fibers with high tapering ratio. *Optics Express*, 20:25461.

Korposh, S., James, S.W., Lee, S.W., et al., 2019. Tapered optical fibre sensors: Current trends and future perspectives. *Sensors*, 19(10).

Kryukov, P.G., 2018. Lasers and fiber optics for astrophysics. *Physics-Uspekhi*, 61(11):1072.

Kumar, S., Kaushik, B.K., Singh, R., et al., 2019. Lspr-based cholesterol biosensor using a tapered optical fiber structure. *Biomed. Opt. Express*, 10(5):2150.

Lhospice, E., Buisset, C., Jones, H.R.A., et al., 2019. EXOhSPEC folded design optimization and performance estimation. In S.B. Shaklan, editor, *Techniques and Instrumentation for Detection of Exoplanets IX*, volume 11117, pages 312 – 326. International Society for Optics and Photonics, SPIE.

Li, Y.F. and Lit, J.W.Y., 1985. Transmission properties of a multimode optical-fiber taper. *J. Opt. Soc. Am. A*, 2(3):462.

Liu, X., Guo, J., Li, G., et al., 2019. Research on the influence of alignment error on coupling efficiency and beam quality for gaussian beam to multimode fiber. *Results in Physics*, 12:1044.

Lo Curto, G., Pepe, F., Avila, G., et al., 2015. HARPS Gets New Fibres After 12 Years of Operations. *The Messenger*, 162:9.

Lovis, C. and Pepe, F., 2007. A new list of thorium and argon spectral lines in the visible ***. *A&A*, 468(3):1115.

Makino, K., Ishigure, T., and Koike, Y., 2006. Waveguide parameter design of graded-index plastic optical fibers for bending-loss reduction. *Journal of lightwave technology*, 24(5):2108.

Marcel, J., Haynes, R., and Bland-Hawthorn, J., 2006. Application of fiber tapers in astronomy. In E. Atad-Ettedgui, J. Antebi, and D. Lemke, editors, *Optomechanical Technologies for Astronomy*, volume 6273, pages 1231–1240. International Society for Optics and Photonics, SPIE.

Marcuse, D., 1987. Mode conversion in optical fibers with monotonically increasing core radius. *Journal of Lightwave Technology*, 5(1):125.

Matsuura, M., Furukawa, R., Matsumoto, Y., et al., 2014. Evaluation of modal noise in graded-index silica and plastic optical fiber links for radio over multimode fiber systems. *Opt. Express*, 22(6):6562.

McMahon, D.H., 1975. Efficiency limitations imposed by thermodynamics on optical coupling in fiber-optic data links∗. *J. Opt. Soc. Am.*, 65(12):1479.

Mickelson, A.R. and Weierholt, A., 1983. Modal noise-limited signal-to-noise ratios in multimode optical fibers. *Appl. Opt.*, 22(19):3084.

Musa, B., Kamil, Y.M., Bakar, M.H.A., et al., 2016. Effects of taper parameters on free spectral range of non-adiabatic tapered optical fibers for sensing application. *Microwave and Optical Technology Letters*, 58(4):798.

Nelson, G.W., 1988. Introduction to Fiber Optics. In S.C. Barden, editor, *Fiber Optics in Astronomy*, volume 3 of *Astronomical Society of the Pacific Conference Series*, page 2.

Oliva, E., Rainer, M., Tozzi, A., et al., 2019. Experimental characterization of modal noise in multimode fibers for astronomical spectrometers. *A&A*, 632:A21.

Olshansky, R., 1976. Leaky modes in graded index optical fibers. *Appl. Opt.*, 15(11):2773.

Olshansky, R. and Keck, D.B., 1976. Pulse broadening in graded-index optical fibers. *Appl. Opt.*, 15(2):483.

Pepe, F., Mayor, M., Delabre, B., et al., 2000. HARPS: a new high-resolution spectrograph for the search of extrasolar planets. In M. Iye and A.F.M. Moorwood, editors, *Optical and IR Telescope Instrumentation and Detectors*, volume 4008, pages 582 – 592. International Society for Optics and Photonics, SPIE.

Petersburg, R.R., McCracken, T.M., Eggerman, D., et al., 2018. Modal noise mitigation through fiber agitation for fiber-fed radial velocity spectrographs. *The Astrophysical Journal*, 853(2):181.

Ramsey, L.W., 1988. Focal ratio degradation in optical fibers of astronomical interest. In S.C. Barden, editor, *Fiber Optics in Astronomy*, volume 3 of *Astronomical Society of the Pacific Conference Series*, pages 26–39.

Ravets, S., Hoffman, J.E., Kordell, P.R., et al., 2013. Intermodal energy transfer in a tapered optical fiber: optimizing transmission. *J. Opt. Soc. Am. A*, 30(11):2361.

Rawson, E.G., Goodman, J.W., and Norton, R.E., 1980. Analysis and measurement of the modal-noise probability distribution for a step-index optical fiber. *Opt. Lett.*, 5(8):357.

Self, S.A., 1983. Focusing of spherical gaussian beams. *Appl. Opt.*, 22(5):658.

Snyder, A.W. and Love, J.D., 1983. *Optical waveguide theory*. Chapman & Hall, London.

Snyder, A.W. and Pask, C., 1973. Incoherent illumination of an optical fiber. *J. Opt. Soc. Am.*, 63(7):806.

Snyder, A.W., Pask, C., and Mitchell, D.J., 1973. Light-acceptance property of an optical fiber. *J. Opt. Soc. Am.*, 63:59.

Spaleniak, I., Jovanovic, N., Gross, S., et al., 2013. Integrated photonic building blocks for next-generation astronomical instrumentation ii: the multimode to single mode transition. *Opt. Express*, 21(22):27197.

Stokes, L., 1994. Coupling light from incoherent sources to optical waveguides. *IEEE Circuits and Devices Magazine*, 10(1):46.

Stürmer, J., Stahl, O., Schwab, C., et al., 2014. CARMENES in SPIE 2014. Building a fibre link for CARMENES. In R. Navarro, C.R. Cunningham, and A.A. Barto, editors, *Advances in Optical and Mechanical Technologies for Telescopes and Instrumentation*, volume 9151, pages 1717 – 1728. International Society for Optics and Photonics, SPIE.

Sums, R. and Cozens, J., 1992. *Optical guided waves and devices*. McGRAW-HILL Book Company Europe, Shoppenhangers Road, Maidenhead, Berkshire, SL6 2QL, England.

Tian, Y., Wang, W., Wu, N., et al., 2011. Tapered optical fiber sensor for label-free detection of biomolecules. sensors. *Sensors (Basel)*, 11(4):3780–3790.

Tovar, A.A. and Casperson, L.W., 1994. Beam propagation in parabolically tapered graded-index waveguides. *Appl. Opt.*, 33(33):7733.

Tremblay, Y., Kawasaki, B.S., and Hill, K.O., 1981. Modal noise in optical fibers: open and closed speckle pattern regimes. *Appl. Opt.*, 20(9):1652.

Winzer, P.J., Neilson, D.T., and Chraplyvy, A.R., 2018. Fiber-optic transmission and networking: the previous 20 and the next 20 years. *Opt. Express*, 26(18):24190.

Yang, Y., Lee, J., Reichard, K., et al., 2005. Fabrication and implementation of a multi-to-single mode converter based on a tapered multimode fiber. *Optics Communications*, 249(1):129.

Yerolatsitis, S., Gris-Sánchez, I., and Birks, T.A., 2014. Adiabatically-tapered fiber mode multiplexers. *Opt. Express*, 22(1):608.

Yerolatsitis, S., Gris-Sánchez, I., and Birks, T.A., 2015. Tapered mode multiplexers for single mode to multi mode fibre mode transitions. In *2015 Optical Fiber Communications Conference and Exhibition (OFC)*, pages 1–3.